

HOT GAS DESULFURIZATION BY ZINC OXIDE-TITANIUM DIOXIDE REGENERABLE SORBENTS

Maria Flytzani-Stephanopoulos, Susan Lew, and Adel F. Sarofim
Department of Chemical Engineering
Massachusetts Institute of Technology
Cambridge, MA 02139

Keywords: high temperature desulfurization; zinc titanate; zinc oxide reduction

ABSTRACT

Comparative kinetic of reduction and sulfidation of zinc oxide and zinc titanate materials were carried out in a thermogravimetric apparatus over the temperature range of 600-1000°C (reduction) and 500-700°C (sulfidation). Both dry as well as wet (H₂O) reactant gas mixtures of H₂-N₂ were used in reduction. For sulfidation, gas mixtures of H₂-H₂S-N₂ were tested. Sulfidation reactivity and reduction stability were correlated with active sorbent crystal phase, e.g. ZnO, Zn₂TiO₄, ZnTiO₃, and Zn₂Ti₃O₈. TiO₂ addition into ZnO retarded reduction rate.

INTRODUCTION

The removal of H₂S to sufficiently low levels from coal-derived gas streams at elevated temperatures is crucial for the efficient and economic coal utilization in emerging advanced power generating systems such as the integrated gasification-combined cycle and the gasification-molten carbonate fuel cell. Previous studies (1,2) have investigated zinc oxide (ZnO) as a regenerable sorbent. The thermodynamic equilibrium for sulfidation of ZnO is quite favorable, yielding desulfurization down to a few ppm H₂S. However, a difficulty with all sorbents containing zinc oxide is some reduction to volatile elemental zinc at temperatures above 600°C. The instability of zinc oxide in a reducing atmosphere limits its operating temperature to approximately 600°C.

Recent sorbent developmental work has shown that mixtures of ZnO with TiO₂ in the form of compounds such as Zn₂TiO₄ or ZnTiO₃ can be used at higher desulfurization temperatures than pure ZnO without appreciable zinc loss by reduction and vaporization of zinc metal (3-5). The decrease in reduction was attributed to the formation of the mixed ZnO compounds.

In this study, the behavior of pure ZnO and several ZnO-TiO₂ sorbents with a molar ratio of ZnO to TiO₂ ranging from 2:3 to 9:1 was examined in both reduction with H₂-N₂ at 600-1000°C and sulfidation with H₂S-H₂-N₂ at 500-700°C. Detailed kinetic studies of a sorbent containing 2 ZnO:1 TiO₂ and of pure ZnO were conducted in reduction and sulfidation experiments. In addition, the effect of H₂O on the reduction behavior was studied. H₂O is usually a significant component of coal-derived gases. H₂O content varying from 50 vol% in a fixed bed Lurgi gasifier to 10 vol% in a fluidized bed KRW gasifier is typical (6).

EXPERIMENTAL

Model sorbent materials were prepared by the amorphous citrate technique (7) which involves the complexation of aqueous solutions of the metal salts in desired proportions with citric acid followed by rapid dehydration, pyrolysis and air calcination at various temperatures. The major advantage of this preparation technique is the production of bulk mixed oxides with good interdispersion and homogeneity. Additionally, mixed oxide particles produced by this technique are highly macroporous, and, thus, amenable to independent measurements of chemical kinetic rates and product layer diffusion (in the absence of pore diffusion). A typical material produced by this method is shown in Figure 1.

The sorbents were characterized by several bulk and surface analysis techniques. X-ray diffraction (XRD) identification of crystalline phases present in the mixed oxide sorbents was performed using a

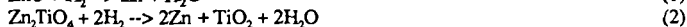
CuK α source by a Rigaku RU300 instrument. Specific surface area was measured with a Micromeritics Flow Sorb II 2300 BET apparatus. The pore volume and pore size distribution were determined by a Micromeritics Autopore 9200.

Reactions were performed in a Cahn 113-X thermogravimetric apparatus (TGA) equipped with a Cahn 2000 electrobalance, an electric furnace, a Micricon temperature controller, and a Bascom Turner data acquisition system. The balance section of the TGA is constantly purged with nitrogen gas flowing at a known flow rate. The reactant gas is introduced into the apparatus through a side-stream. A thin layer of sample (typically 2-4 mg and -115/+170 mesh size) was placed on a quartz pan suspended by a quartz hangdown wire.

RESULTS AND DISCUSSION

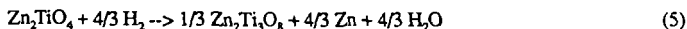
Sorbent Reduction

Reduction studies of ZnO neat and several ZnO-TiO₂ materials with various zinc to titanium ratios were carried out in the TGA. A few of the solids studied are listed in Table 1. Several different crystalline phases were identified in the mixed oxide sorbents, namely, ZnO, Zn₂TiO₄, Zn₂Ti₃O₈, and ZnTiO₃. The overall reduction reactions that can take place are:



The initial rate of reduction for samples with different composition of ZnO-TiO₂ is shown in Figure 2. The rates for two temperatures, 600°C and 700°C, in 10% H₂-90% N₂ are depicted. The initial rate is defined as the rate of Zn loss (mmol/s) normalized with the total surface area of the sample (cm²). Z2T (Table 1) which is composed of Zn₂TiO₄ corresponds to 66.7% ZnO in Figure 2. 0% ZnO is equivalent to 100% TiO₂. In agreement with previous studies (3-5), lower reduction rates are observed with zinc titanates. With as little as 10% TiO₂ (Z9T in Table 1), a noticeable decrease in the rate is observed. As shown in Figure 2, the reduction rate for the sample with 10% TiO₂ is approximately twice as slow as ZnO neat. For a sample with 25% TiO₂ (Z3T), the reduction rate is approximately 10 times slower than ZnO neat. This is true even though 33% of the zinc in Z3T is present as ZnO. The striking observation is that as the amount of TiO₂ increases above 25%, the reduction rate remains relatively unchanged. This is true regardless of the fact that the crystalline phases present vary with sorbent composition.

From XRD analyses of partially reduced Z2T3, only the phases of ZnTiO₃ and TiO₂ were found. Thus, reduction of ZnTiO₃ proceeds directly by reaction (4). The partially reduced sorbent Z2T is composed of a mixture of Zn₂TiO₄ and Zn₂Ti₃O₈. Thus, reduction of Zn₂TiO₄ proceeds by:



The Zn₂Ti₃O₈ formed is then reduced according to reaction (3). Zn₂Ti₃O₈ has a defect spinel structure. It is, thus, not surprising that abstraction of Zn atoms from Zn₂TiO₄, which is also a spinel, produces Zn₂Ti₃O₈. In both Z2T and Z2T3, reactions occur by the reduction of different initial crystalline phases and intermediates. The fact that the initial reduction rate is the same for both sorbents implies that the reduction kinetics are independent of the type of zinc titanate compound present.

Z2T was chosen for further studies of the reduction kinetics. Comparisons were made with ZnO. The reaction order with respect to H₂ concentration was determined at 700°C in a mixture of H₂ and N₂ gases. For Z2T, the reaction order is unity. However, for ZnO, it is 0.5. In Figure 3, an Arrhenius plot is shown using 10% H₂ and 90% N₂. In the temperature range of study (600-1000°C), the reduction rate of

ZnO is greater than Z2T. The apparent activation energy for Z2T reduction is 37 kcal/mol, while for ZnO, it is 24 kcal/mol. The activation energy (E) was determined by the rate equation:

$$r = k_0 e^{-E/RT} (C_{H_2})^n \quad (6)$$

The presence of H₂O drastically changed the reduction kinetics of ZnO. The reaction order for ZnO changed from 0.5 with 0% H₂O-H₂-N₂ to 1.0 in the presence of 3% H₂O-H₂-N₂. But, for Z2T, the reaction order was unaffected by the presence of H₂O. The reduction rate of ZnO decreased significantly when H₂O was present in the reactant stream. Figure 4 shows an Arrhenius plot for ZnO reduction in the presence of various amounts of H₂O. A large change in reduction rate was observed when the amount of H₂O was changed from 0% to 1%. With 3% H₂O, a much smaller drop in reduction rate took place compared to the change observed when the H₂O content was increased from 0% to 1%. At 8% H₂O, again only small changes in the reduction rate were observed.

In contrast to the effect of H₂O on ZnO reduction, a smaller decrease in reduction rate was observed for Z2T. In Figure 5, the Arrhenius plot for Z2T reduction in the presence of various amounts of water vapor is presented. The activation energy changed from 37 kcal/mol in the absence of H₂O to 44 kcal/mol in the presence of 3% H₂O. In the presence of 8% H₂O, as in the case of ZnO, only small additional changes in the reduction rate were observed. Figure 6 shows a comparison of the Arrhenius curves for ZnO and Z2T reduction in the presence of 3% water vapor. The activation energies (44 kcal/mol) for both sorbents were the same. ZnO reduction rate was 2-3 times faster than Z2T. Also, the reaction orders of ZnO and Z2T were both unity.

To explain the experimental data for both ZnO and Z2T reduction a kinetic model was developed. The inhibition of reduction by water vapor is presumably a result of competition by hydrogen and water vapor for active sites on the samples. This is in good agreement with an earlier study (8) carried out by Dent and Kokes who observed lower hydrogen adsorption on zinc oxide pre-adsorbed with H₂O. To explain the inhibition pattern observed in the present study, a two-site model similar to one found in the literature (9) is postulated. Two types of sites (Type A and Type B) on ZnO are involved in hydrogen adsorption. Other researchers (e.g. 8, 10-13) have also observed the presence of two hydrogen adsorption sites on zinc oxide at low temperatures (25-200°C). One is known to adsorb hydrogen very rapidly but is also poisoned by H₂O. The other site involves initially fast hydrogen adsorption followed by much slower absorption and is apparently not affected by H₂O. For this study, Type A sites are postulated to be very reactive and responsible for most of the reduction on ZnO. However, Type A sites also appear to be easily poisoned by H₂O. In the presence of H₂O, these sites are blocked and will not play a role in reduction. Type B sites are less reactive than Type A sites but are not as easily poisoned.

With a Langmuir-Hinshelwood model, the rate expressions for reduction are written as:

$$r_A = k_A C_{H_2} / (1 + K_{A,H_2}^{1/2} C_{H_2}^{1/2} + K_{A,H_2O}^{1/2} C_{H_2O}^{1/2})^2 \quad (7)$$

$$r_B = k_B C_{H_2} / (1 + K_{B,H_2}^{1/2} C_{H_2}^{1/2} + K_{B,H_2O}^{1/2} C_{H_2O}^{1/2})^2 \quad (8)$$

where $K_{A,H_2O} \gg K_{A,H_2}$, $K_{B,H_2}^{1/2} C_{H_2}^{1/2} \ll 1$, and $K_{B,H_2O} \ll K_{A,H_2O}$. The overall reaction rate is

$$r = r_A + r_B \quad (9)$$

In the absence of H₂O, the reduction rate for ZnO is:

$$r = r_A = k_A C_{H_2} / (1 + K_{A,H_2}^{1/2} C_{H_2}^{1/2})^2 \quad (10)$$

In the presence of H₂O, it becomes:

$$r = r_B = k_B C_{H_2} / (K_{B,H_2O}^{1/2} C_{H_2O}^{1/2})^2 \quad (11)$$

With Z2T, it is postulated that there are very few Type A sites. The reaction rate is due mainly to Type B sites. This is possible if similarities to the previous hydrogen adsorption studies (8,10-13) at low temperatures are drawn. The sites with rapid hydrogen adsorption are believed (10-11) to consist of clusters of adjacent Zn cations and at least one reactive O anion on a reconstructed polar face. If Ti cations are present in these sites, they may disrupt the interaction between ions necessary for active sites. It is not certain that similarities can be drawn to the previous studies since hydrogen adsorption on zinc oxide was conducted at considerably lower temperatures (25-200°C) than the temperatures (600-1000°C) in this present work. However, several similar characteristics are present, such as high reactivity and poisoning by H₂O.

Sorbent Sulfidation

Figure 7 presents the results of sulfidation experiments with different compositions of ZnO-TiO₂. The experiments were conducted with 2% H₂S-1% H₂-97% N₂ at 700°C. Comparative reduction experiments are also depicted in Figure 7. Similar to the results observed for reduction, the initial rate of sulfidation does not appear to be affected by the type of zinc titanate compounds (Zn₂TiO₄ and ZnTiO₃) or amount of TiO₂ (33-73%) present. The initial rate of sulfidation of ZnO is only about 1.5 times higher than zinc titanates. In contrast, the initial reduction rate of ZnO is about 10 times greater than that of zinc titanates.

More detailed sulfidation studies were conducted with Z2T and ZnO to determine kinetic parameters. The overall reactions considered are:



The reaction order with respect to hydrogen sulfide was unity for both ZnO and Z2T at 700°C. An Arrhenius plot for both sorbents is drawn in Figure 8. The activation energies for both sorbents are approximately the same (8-9 kcal/mol). Because of the similarity in reaction order and activation energy for ZnO and Z2T, the conclusion is made that sulfidation of Z2T (Zn₂TiO₄) proceeds by the same rate-controlling mechanism as ZnO. XRD analyses of partially sulfided (48 mole % converted) Z2T have identified a mixture of Zn₂TiO₄, Zn₂Ti₃O₈, α-ZnS, and β-ZnS. Thus, the similarity in kinetic parameters is not due to decomposition of Zn₂TiO₄ to ZnO and TiO₂. The low activation energy is suggestive of chemisorption of H₂S being the rate-controlling mechanism.

In Figure 8, the effect of various amounts of H₂ in the reactant gases is also shown. Hydrogen is added to the reactant gases because it is a major component of coal derived-gases and also because it can inhibit the decomposition of H₂S at these temperatures (500-700°C). The amount of hydrogen was varied from 0% to 10% H₂S. No significant change in the initial rate was observed for both ZnO and Z2T. This indicates that Type A hydrogen adsorption sites are different from hydrogen sulfide adsorption sites on ZnO. If the two types of sites were the same, the Langmuir-Hinshelwood expression for sulfidation would be:

$$r = k_{A,H_2S} C_{H_2S} / (1 + K_{A,H_2S} C_{H_2S} + K_{A,H_2}^{1/2} C_{H_2}^{1/2}) \quad (14)$$

Since the reaction order with respect to H₂S is unity, K_{A,H₂S} C_{H₂S} << 1, while K_{A,H₂}^{1/2} C_{H₂}^{1/2} is of order unity. Thus, increasing hydrogen concentration would decrease the sulfidation rate due to competitive adsorption of hydrogen. Since no change in rate was observed for ZnO sulfidation, it may be concluded that hydrogen sulfide adsorption sites are not the same as hydrogen adsorption sites. This can also explain why zinc titanate materials have such low reduction rates, without a similar decrease in sulfidation rates. Zinc titanate materials lack the highly reactive sites (Type A sites), which are crucial for reduction but not for sulfidation.

CONCLUSIONS

This study has demonstrated the advantages of ZnO-TiO₂ sorbents. As little as 25 wt % of TiO₂ (present as a zinc titanate compound) will give the same decrease in reduction rate as significantly more TiO₂ (60 wt%). In contrast to ZnO neat, a significantly lower reduction rate (approximately 10 times lower at 700°C) was observed in ZnO-TiO₂ materials in a H₂-N₂ reaction gas mixture. The presence of different zinc titanate compounds (i.e. Zn₂TiO₄, ZnTiO₃, or Zn₂Ti₃O₈) does not noticeably change the reduction rate. The presence of water vapor in the reactant gas will strongly inhibit ZnO reduction but will not have the same effect on ZnO-TiO₂ materials. ZnO reduction is only about 2-3 times faster than ZnO-TiO₂ in the presence of H₂O. It is postulated that the difference in reduction rate is due to the existence of highly reactive sites on ZnO which are poisoned by H₂O.

There is not a large difference in the initial rate of ZnO-TiO₂ sulfidation compared with ZnO sulfidation under identical reaction conditions. The initial sulfidation rate of ZnO is only about 1.5 times faster than for ZnO-TiO₂ sorbents. Because of similar kinetic parameters (i.e. activation energy and reaction order), similar sulfidation mechanisms are believed to be involved for both ZnO and ZnO-TiO₂. Again, no significant difference in sulfidation rate is observed with different zinc titanate compounds (i.e. Zn₂TiO₄ or ZnTiO₃).

REFERENCES

1. Grindley, T.; Steinfeld, G. Development and Testing of Regenerable Hot Coal Gas Desulfurization Sorbents. Final Report DOE/MC/16545-1125, October 1981; METC, Morgantown, WV.
2. Jalan, V.; Wu, D. High Temperature Desulfurization of Fuel Gases for Molten Carbonate Fuel Cell Power Plants. Paper presented at the National Fuel Cell Seminar, 1980, San Diego, CA.
3. Lew, S. High-Temperature Regenerative H₂S Removal by ZnO-TiO₂ Systems. M.S. Thesis, Massachusetts Institute of Technology, Cambridge, 1987.
4. Flytzani-Stephanopoulos, M.; Gavalas, G.R.; Jothimurugesan, K.; Lew, S.; Sharma, P.K.; Bagajewicz, M.J.; Patrick, V. Novel Sorbents for High-Temperature Regenerative Hot Coal Gas Desulfurization Sorbents. Final Report DOE/MC/22193-2582, October 1987; METC, Morgantown, WV.
5. Lew, S.; Jothimurugesan, K.; Flytzani-Stephanopoulos, M. High-Temperature H₂S Removal from Fuel Gases by Regenerable Zinc Oxide-Titanium Dioxide Sorbents. *I&EC Research*. **1989**, *28*, 535.
6. Halow, J.S. An Overview of the U.S DOE Coal Gasification Program. 21st Intersociety Energy Conversion Engineering Conference. 1986, 1, 170; San Diego, CA.
7. Marcilly, C.; Courty, P.; Delmon, B. Preparation of Highly Dispersed Mixed Oxides and Oxide Solid Solutions by Pyrolysis of Amorphous Organic Precursors. *J. Am. Ceram. Soc.* **1970**, *53*(1), 56.
8. Dent, A.L.; Kokes, R.J. Hydrogenation of Ethylene by Zinc Oxide. I. Role of Slow Hydrogen Chemisorption. *J. Phys. Chem.* **1969**, *73*, 3772.
9. Satterfield, C.N.; Modell, M.; Mayer, J.F. Interactions Between Catalytic Hydrodesulfurization of Thiophene and Hydrodenitrogenation of Pyridine. *AIChE J.* **1975**, *21*, 1100.
10. Dent, A.L.; Kokes, R.J. Hydrogenation of Ethylene by Zinc Oxide. II. Mechanism and Active Sites. *J. Phys. Chem.* **1969**, *73*, 3781.
11. Boccuzzi, F.; Borello, E.; Zecchina, A.; Bossi, A.; Camia, M. Infrared Study of ZnO Surface Properties I. Hydrogen and Deuterium Chemisorption at Room Temperature. *J. Catal.* **1978**, *51*, 150.
12. Griffin, G.L.; Yates, J.T. Combined Temperature-Programmed Desorption and Infrared Study of H₂ Chemisorption on ZnO. *J. Catal.* **1982**, *73*, 396.
13. Fubini, B.; Giamello, E.; Gatta, G.D.; Venturello, G. Adsorption of Hydrogen on Zinc Oxide. *J. Chem. Soc., Faraday Trans.* **1982**, *78*, 153.

Table 1. Physical and Chemical Properties of Sorbents^a

Sorbent Designation	Zn/Ti (atomic ratio)	surface area (m ² /g)	pore volume (cm ³ /g)	Crystalline Phases (wt %)				
				ZnO	Zn ₂ TiO ₄	ZnTiO ₃	Zn ₂ Ti ₃ O ₈	TiO ₂
ZnO	---	2.4	1.2	100	0	0	0	0
Z9T ^b	9/1	1.0	NA	72	28	0	0	0
Z3T	3/1	7.5	0.9	28	72	0	0	0
Z2T	2/1	4.1	0.7	0	100	0	0	0
Z3T2	3/2	2.2	0.7	0	82	18	0	0
ZT	1/1	1.6	0.6	0	0	45	55	0
Z2T3	2/3	1.3	0.3	0	0	83	0	17

^a calcined at 720°C; ^b calcined at 1000°C

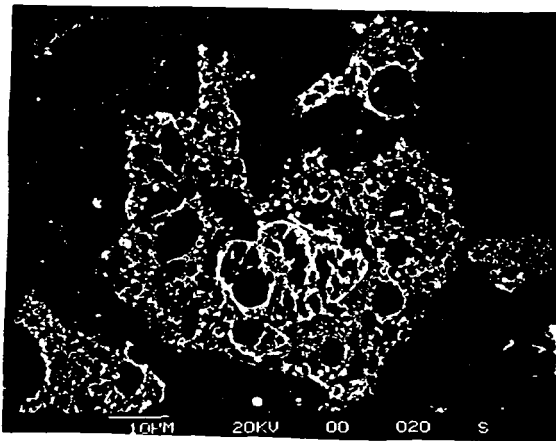


Figure 1. SEM micrograph showing the macroporous structure of a ZnO sorbent prepared by the amorphous citrate technique with pore volume=1.2 cm³/g and surface area=2.4 m²/g; sorbent cross-section shown.

Table 1. Physical and Chemical Properties of Sorbents^a

Sorbent Designation	Zn/Ti (atomic ratio)	surface area (m ² /g)	pore volume (cm ³ /g)	Crystalline Phases (wt %)				
				ZnO	Zn ₂ TiO ₄	ZnTiO ₃	Zn ₂ Ti ₃ O ₈	TiO ₂
ZnO	---	2.4	1.2	100	0	0	0	0
Z9T ^b	9/1	1.0	NA	72	28	0	0	0
Z3T	3/1	7.5	0.9	28	72	0	0	0
Z2T	2/1	4.1	0.7	0	100	0	0	0
Z3T2	3/2	2.2	0.7	0	82	18	0	0
ZT	1/1	1.6	0.6	0	0	45	55	0
Z2T3	2/3	1.3	0.3	0	0	83	0	17

^a calcined at 720°C; ^b calcined at 1000°C

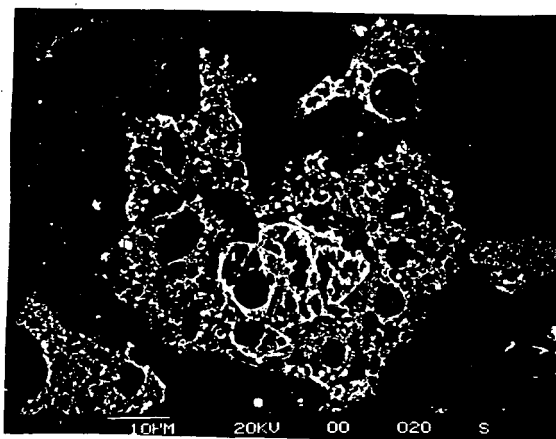


Figure 1. SEM micrograph showing the macroporous structure of a ZnO sorbent prepared by the amorphous citrate technique with pore volume=1.2 cm³/g and surface area=2.4 m²/g; sorbent cross-section shown.

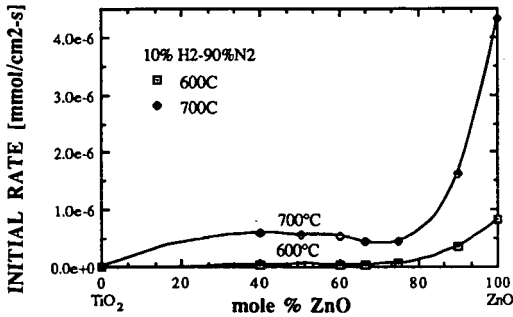


Figure 2. Comparison of initial rate of reduction of samples containing different amounts of ZnO and TiO₂.

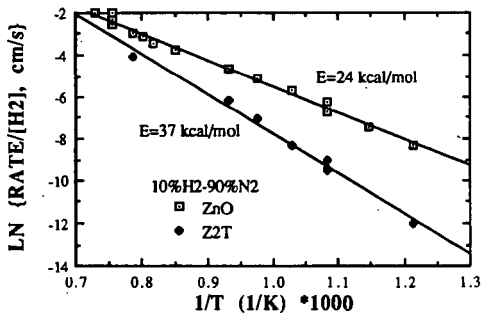


Figure 3. Arrhenius plot comparing reduction of ZnO with that of Z2T in 10%H₂-90%N₂ between 600-1000°C.

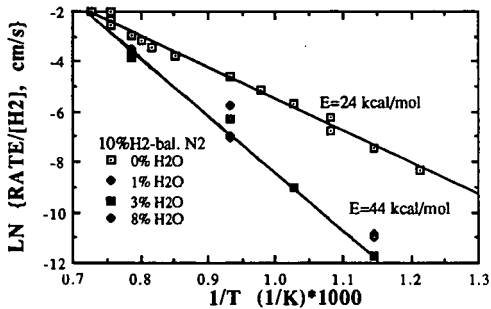


Figure 4. Arrhenius plot of ZnO reduction with various amounts of H₂O.

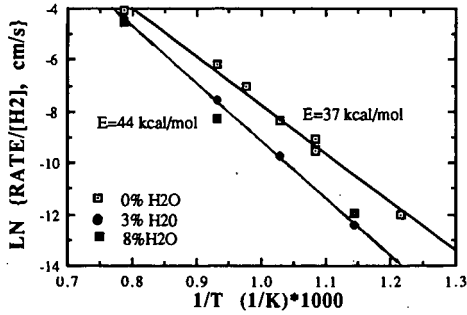


Figure 5. Arrhenius plot of Z2T reduction with various amounts of H₂O.

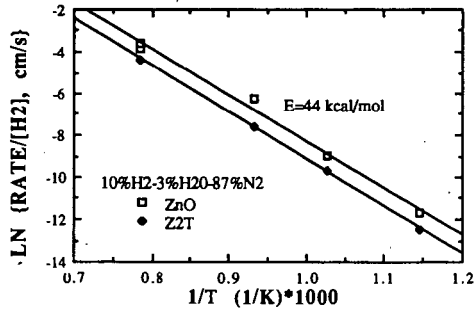


Figure 6. Comparison of ZnO and Z2T reduction in 10%H₂-3%H₂O-87%N₂.

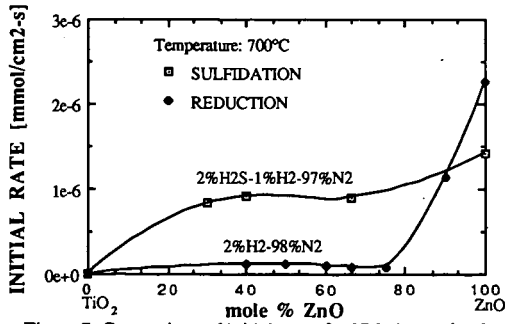


Figure 7. Comparison of initial rate of sulfidation and reduction of samples containing different amounts of ZnO and TiO₂.

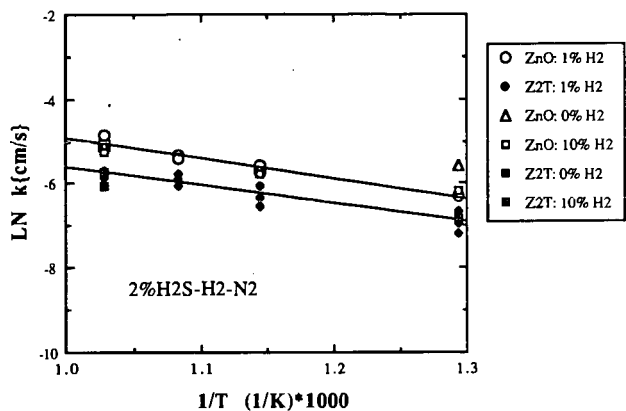


Figure 8. Arrhenius plot of ZnO and Z₂T sulfidation for various hydrogen concentrations. Rate= kC_{H_2S}

COPPER BASED SORBENT FOR HOT GAS CLEANUP

M. Desai, F. Brown, B. Chamberland, and V. Jalan,
ElectroChem, Inc, 400 W. Cummings Park, Woburn, MA 01801

Keywords: Hot Gas Cleanup, Desulfurization, Copper, Manganese Oxide

ABSTRACT

Coal-derived fuel gases contain significant levels of sulfur and other contaminants. Full realization of the tremendous commercial potential of coal gas fueled power plants and related technologies awaits the development of an inexpensive and reliable method for the removal of these contaminants. A family of copper manganese oxide sorbents was identified as a high temperature regenerable sulfur sorbent in the METC process. These compounds have demonstrated many advantages over other sorbents currently being studied, and there is potential for further improvement. The objectives of the development program include the study of sorbent properties such as physical characteristic, durability, temperature stability, life, rate of utilization, and development of design parameters. Copper manganese oxides provide excellent reactivity, high sulfur capacity, and complete chemical regenerability.

INTRODUCTION

For economically viable conversion of coal to electricity without significant loss of thermal energy, there is a need to reduce sulfur from coal gas stream at high temperatures, 500-800°C.¹ A capability for efficient removal of sulfur is essential for integration of coal gasifiers with synthesis gas catalytic conversion processes (methanol, methane, Fischer-Tropsch) and power plants such as gas turbine combined cycle and molten carbonate fuel cells. Over the past decade there have been extensive efforts by DOE/METC and its contractors to define appropriate high temperature regenerable desulfurizing agents,^{2,3} since there are both technical and economic advantages for the desulfurization of coal gas fuel and fossil fuel flue gases by hot dry scrubbing. Successful sorbents should provide efficient desulfurization and regeneration kinetics, a reduction to H₂S of 1 ppm level, and physical and chemical stability in both desulfurization and regeneration gas atmospheres at a temperature of 500°C and above.

Mixed metal oxides are recent experimental high temperature sulfure sorbents. They provide some outstanding properties for hot regenerative desulfurization of coal gases. Although quite promising results have been obtained for hot desulfurization of coal gases with these sorbent systems, they have limitations.

Zinc ferrite³⁻⁵ shows great potential and remains the sorbent of choice. Its sulfur capacity is relatively high and it is moderate in cost. The disadvantages are degradation due to thermal sintering, sulfate formation, and zinc volatilization. Copper zinc oxide⁶⁻⁹ has been investigated as a very low level H₂S sorbent. It was shown that copper in a mixed oxide state retains the thermodynamic properties of cuprous oxide and indeed reduced sulfur levels below 1 ppm at 650°C. This was subsequently verified by several other METC supported projects.¹⁰ Copper zinc oxide is expected to suffer from some of the same drawbacks as zinc ferrite. However, these led to many investigation of copper based mixed

oxides. Manganese oxide has been reported to be a potential candidate for high temperature desulfurization.¹¹⁻¹⁴ Its rate of reaction with hydrogen sulfide is four times faster than that of zinc oxide.¹² Air regeneration, unfortunately, leads to sulfate formation. It appears that $\text{Cu}_2\text{O-MnO}$ based sorbents will eliminate many of the deficiencies.

EXPERIMENTAL SECTION

Reactor System and Experimental Procedures

The reactor, used is an 18 inch long stainless steel tube with a 1 inch I.D. quartz liner. The first 10 inches of the reactor are filled with an inert porcelain packing to promote the heating of the inlet gases. Sorbents are placed on a stainless steel mesh retainer directly above this section. The reactor is mounted vertically inside an electric furnace and equipped with two K-type thermocouples which can be moved along the central axis. N_2 , H_2 , CO , CO_2 , and H_2S are individually metered through mass flow controllers and the desired concentration of water vapor is attained by injecting water via a metering pump. The experiments consisted of a sequence of alternate sulfidation and regeneration runs. The reactor temperature was held fixed in the range of 500-800°C for the duration of the experiments. Sulfided sorbents were regenerated with air and nitrogen at 500-750°C. The space velocity of gas used was in the range of 1000-2000 hr^{-1} during sulfidation and 600-800 hr^{-1} during regeneration.

Matheson-Kitagawa precision gas detection tubes were used to determine the concentrations of H_2S , CO_2 , and SO_2 in the inlet and effluent stream. Our previous experience shows that this technique is accurate and cost effective.^{2,6-9} Semi-quantitative methods were devised for the continuous monitoring of the effluent gas stream for H_2S during desulfurization and SO_2 during regeneration.

Sorbent Preparation

Several methods for synthesizing highly dispersed mixed oxides are described in the literature.¹⁵⁻¹⁶ The method selected for evaluation in this study is coprecipitation of inorganic salts. The development of technique for the production of low-cost finished sorbent is a long term objective of the program. The copper-manganese oxides were coprecipitated from aqueous nitrate solution by the addition of NaOH . The precipitate was recovered by filtration and washed with distilled water to remove soluble residues. The recovered mixed hydrous oxides were dried in air at 100°C. Sorbents with copper to manganese weight ratios of 90:10, 80:20, 75:25, 60:40, 54:46, 50:50, 40:60, 37:67, and 20:80, were prepared. Pure manganese oxide was also prepared by precipitation.

Sulfidation and Regeneration Studies

The H_2S concentration in the effluent rises rapidly when the sorbent has reached its sulfur capacity. This abrupt change is called the breakthrough; the elution profile is called an uptake curve. In the absence of transport and kinetic limitations, the uptake curve would be the step function $y = y^{\text{eq}}$ at $t < t^*$, $y = y^0$ at $t > t^*$ where y^{eq} and y^0 are the equilibrium and inlet mole fractions of hydrogen sulfide, respectively, and t^* is the theoretical time corresponding to complete sulfidation of the active

sorbent components. The results are presented in terms of the concentration of H_2S in the product gas versus the normalized time t/t^* . In the case of successive sulfidations, the uptake curve cycles are denoted 1, 2, etc. Regeneration was carried out in air at $650^\circ C$, and an overnight N_2 purge at $750^\circ C$ followed.

Results and Discussion

Sulfur loadings at 20 ppm and 100 ppm concentration in exit gas stream were estimated from the weight of sorbent, gas feed rate, and time to breakthrough. Figure 1 summarizes the effect of manganese content in the $Cu_xMn_yO_z$ system on the sulfur loading of the resulting sorbent. As expected, the performance of pure copper oxide is very poor. Incorporation of manganese oxide dramatically increases the sulfur loading capacity; this is attributed by the stabilization of cuprous oxide. Pure manganese oxide has a high sulfur capacity but lacks regenerability. Of interest is the decrease in sulfur capacity at the $CuMnO_2$ phase and a minimum at $CuMn_2O_4$ phase.¹⁷

Figure 2 shows the breakthrough curve of six sulfidation cycles of the sorbent with a copper to manganese atomic ratio of 1:1. The sulfur loading after the first cycle (19 weight percent at 20 ppm breakthrough) was in agreement with our previous results.¹⁷ The constant H_2S leakage rate of less than 30 ppm in the effluent was observed in subsequent cycles.

A single sulfidation test of freshly prepared sorbent $CuMnO_2$ was carried out in the 1 inch dia. reactor at 550, 600, 650, 700, 750, and $800^\circ C$. A constant space velocity of 2000 hr^{-1} , and simulated fuel gas mixture (feed gas) consisting of on dry basis 47% N_2 , 27% H_2 , 15% CO_2 , 10% CO and 1% H_2S was used. Sorbent loadings are presented in figure 3. It is clear that use of the $CuMnO_2$ sorbent at low temperatures ($550\text{--}600^\circ C$) gives longer breakthrough times than at higher temperatures. Sulfur loadings of the $CuMnO_2$ sorbent at $550^\circ C$ was 28% at 20 ppm breakthrough, with decreasing loadings at higher temperatures, to 1.6% at $800^\circ C$. An H_2S leakage rate of less than 20 ppm was obtained only for a short period of time (i.e. high loadings on the sorbent) only at temperatures of $650^\circ C$ and below, but leakage rates below 50 ppm were obtained over extended temperature range.

The primary conclusion from these tests is that a copper-manganese oxide sorbent with a Cu to Mn 1:1 atomic ratio will perform best at relatively low temperatures, preferably in the range of $550\text{--}600^\circ C$.

Figure 4 presents the results of copper-manganese oxide sorbent with a Cu to Mn 1:2 atomic ratio. The test conditions for the sulfidation cycles were same as mentioned above. The sulfur loadings were low, and short breakthrough times were observed for the tests performed at 550 and $600^\circ C$. The sulfur loadings improved as the sulfidation temperature increased. In all cases the breakthrough time for less than 40 ppm H_2S exit concentration were relatively short. A sulfur loading of 24% was observed at 50 ppm and $750^\circ C$. The sulfidation test at $800^\circ C$ showed a sulfur capacity reduced by half at 50 ppm breakthrough. The primary conclusion from tests is that a sorbent rich in manganese content performs better at relatively higher temperatures preferably in the range of $700\text{--}750^\circ C$, than sorbents with lower manganese content.

The results presented in figures 3 and 4 show that in both cases the sulfur loading decreased drastically at 800°C. These results suggest that it would be more advantageous to operate both sulfidation and regeneration cycles below 800°C to increase loadings and decrease loss of activity due to sintering or other processes that result in loss of mechanical integrity.

Additional sulfidation tests of a sorbent with copper to manganese stoichiometric ratio of 1:1 were carried out at 650°C and space velocity 2000 hr⁻¹, with various inlet H₂S concentrations, ranging from 500 ppm to 1%. Sorbent loadings under these conditions are shown as figure 5. The sulfur capacity was highest at 500 and 1000 ppm and decreased at 5000 ppm and 1% inlet H₂S concentrations. Duplicate test with 5000 ppm showed the same breakthrough time. The reason for the relatively low sulfur capacity at higher inlet H₂S concentrations is not clear. Since the sulfur loadings reported here are for relatively low H₂S exit concentrations (20-100 ppm) the sulfur loadings are not associated with equilibrium values. With high inlet H₂S concentrations a small amount of channeling through the reactor bed would explain the apparently anomalous behavior.

Figure 6 shows sulfur loadings of sulfidation tests of fresh sorbent copper manganese oxide with a Cu to Mn stoichiometric ratio of 1:1 at various inlet water concentrations ranging from 0 to 30%. The sulfur capacity decreases with an increase in the water content of feed gas. The mixed metal oxides reacts with H₂S producing metal sulfides and water. As the partial pressure of water increases in the feed gas, the reaction becomes more equilibrium limited, resulting in higher H₂S leakage in the effluent.

The CuMnO₂ sorbent prepared in 1/16" pellet form by the coprecipitation method was sulfided at 650°C for about 10 hours in the presence of a simulated coal gas mixture containing N₂ 47.07%, H₂ 27.3%, CO₂ 14.3%, CO 10.4%, and H₂S 0.93%. The sulfided sample was cooled to room temperature under N₂ and small portions of the sulfided sample were regenerated individually in air at various temperatures in the range of 650-950°C. Samples were also regenerated by thermal decomposition in a mixture of N₂ and steam at 850°C. These samples were analyzed by XRD.

The sulfided sample of copper manganese oxide sorbent regenerated in air at 650 and 700°C showed a spinel phase. The samples regenerated at 750, 850 and 950°C showed mixed phases containing both CuO and spinel. The sample regenerated by thermal decomposition at 850°C showed a mixture of MnO, Cu metal and trace amount of spinel. None of the samples regenerated at the above conditions showed any sulfate formation.

Another set of experiments was carried out using pure, single phase CuMnO₂. The sample was prepared from low surface area technical grade Cu₂O and Mn₂O₃ mixed in a 1:1 ratio and pelletized. A single tablet of pure CuMnO₂ was sulfided at 650°C for 2 hours. A half tablet from the sulfided sample was regenerated at 650/750°C in air/N₂. These samples were analyzed by XRD. The surface of the sulfided sample showed mostly MnS_{1-x}O_x, whereas the regenerated sample showed strong CuO. The presence of the MnS_{1-x}O_x phase indicates that sorption proceeds through a more complex mechanism than would be inferred from a simple description of the stoichiometry of the overall reaction.

Conclusion

Copper and manganese form stable oxide phases, that are easily sulfided and regenerated back to CuMnO_2 and CuMn_2O_4 . These results were verified by desulfurization/regeneration studies as well as chemical and XRD analysis of fresh, sulfided, and regenerated sorbents. Very advantageously, copper manganese sulfate exists only as a hydrated material, campigliaite, which is so unstable that it decomposed under the electron beam during microprobe studies.¹⁸⁻¹⁹ Unlike those of zinc, copper and manganese compounds are stable and do not volatilize at temperatures of interest.

Sorbents with Cu to Mn 1:2 atomic ratio have the highest sulfur capacity at higher temperature, while the sorbent with Cu to Mn 1:1 atomic ratio have the highest sulfur capacity at lower temperature. Loading capacity is influenced by water content, as expected, but the results are not too sensitive to water content in the 20-30% H_2O range at 650°C.

We have demonstrated that copper manganese oxides are attractive candidates for high temperature regenerable sulfur sorbents. The absence of sulfate formation, very low thermal sintering below 650°C, provide incentive to pursue further development of this process.

Acknowledgment

We wish to gratefully acknowledge the support of this work by the Morgantown Energy Technology Center (METC) of the U.S. Department of Energy under Contract No. DE-AC02-87ER80494, and the many helpful discussion with Dr. Mark Williams and Mr. Suresh Jain, of METC.

References

- (1) Jalan, V., "High-Temperature Desulfurization of Coal Gases By Regenerative Sorption," Proceedings of the 1981 International Gas Research Conference, Los Angeles, California, pp. 291-303 (1981).
- (2) Jalan, V., "High-Temperature Desulfurization of Coal Gases," Acid and Sour Gas Treating Processes, S. A. Newman, ed., Houston, Texas (1985).
- (3) Grindley, T. and G. Steinfeld, "Desulfurization of Hot Coal Gas by Zinc Ferrite", Chapter 16 in Acid and Sour Gas Treating Processes, Edited by S. A. Newman, Gulf Publishing Company, Houston, Texas, pp. 419-465 (1985).
- (4) Grindley, T. and G. Steinfeld, "Development and Testing of Regenerable Hot Coal Gas Desulfurization Sorbents," U. S. Department of Energy Report DOE/MC16545-1124 (1981).
- (5) Grindley, T., "The Effect of Temperature and Pressure in the Regeneration of Zinc Ferrite Sorbents," presented at the Sixth Annual Contractor's Meeting on Contaminant Control in Hot Coal Derived Gas Streams (June 4-5, 1986).
- (6) Jalan, V., C. Brooks, C. Georgakis, and M. Desai, "Metal Oxide Absorbents for H_2S Control," Proceedings of the Second Annual

Meeting on Contaminant Control in Hot Coal Derived Gas Streams, DOE CONF-820208 (1982).

(7) Jalan, V., "Studies Involving High Temperature Desulfurization/Regeneration Reactions of Metal Oxides for Fuel Cell Development," Final Report DOE/MC/16021-1486 (1983).

(8) Jalan, V., M. Desai, C. Brooks, and R. Waterhouse, "Metal/Metal Oxides as High Temperature Desulfurization Sorbent," Proceedings of the Third Annual Meeting on Contaminant Control in Hot Coal Derived Gas Streams, DOE/METC DE 84000216 (1983).

(9) Jalan, V. and J. Young, "High Temperature Sorbent Method for Removal of Sulfur Containing Gases from Gaseous Mixtures," U.S. Patent No. 4,442,078, (April 10, 1984).

(10) Krishnan, G. N., G. T. Tong, R. H. Lamoreaux, R. D. Brittain, and B. J. Wood, "An Experimental and Theoretical Investigation into Sulfur Formation in the Regeneration of Zinc Ferrite Sorbents," Final Report DE-AC21-83MC20092 (1985).

(11) Westmoreland, P. R. and D. P. Harrison, "Evaluation of Candidate Solids for High Temperature Desulfurization of Low BTU Gases," Environmental Science & Technology, 10, pp. 659-661 (1976).

(12) Westmoreland, P. R., J. B. Gibson, and D. P. Harrison, "Comparative Kinetics of High-Temperature Reaction Between H₂S and Selected Metal Oxides," Environmental Science & Technology, 11, pp. 488-491 (1977).

(13) Olsson, R. G. and E. T. Turkdogan, "Desulfurization of Hot Reducing Gas," U.S. Patent 4,180,549, (December 25, 1979).

(14) Erickson, D. C., "Regenerable Manganese Oxide Hot Gas Desulfurization Process," U.S. Patent 4,283,374, (August 11, 1981).

(15) Longo, J., H. Horowitz, and L. Clavenna, "A Low Temperature Route to Complex Oxides," Advances in Chemistry Series No. 186, p. 139, American Chemical Society, Washington, D.C. (1980).

(16) Marcilly, C., P. Courty, and B. Delmon, J. Am. Cer. Soc., 53 p. 56 (1970).

(17) Jalan, V. and M. Desai, "Copper-Based Sorbents For Hot Gas Cleanup," Proceedings of the Eighth Annual Gasification and Gas Stream Cleanup Systems Contractors Review Meeting, DOE/METC DE 884010253 (1988).

(18) Menchetti, S., Sabelli, Am. Mineral., 67, 385 (1982).

(19) Sabelli, C., Am. Mineral., 67, p. 388 (1982).

FIG. 1 SULFUR LOADING OF COPPER BASED SORBENTS

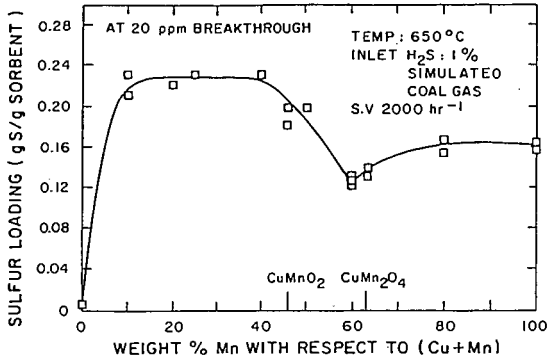


FIG. 2 H₂S BREAKTHROUGH CURVES FOR CuMnO₂

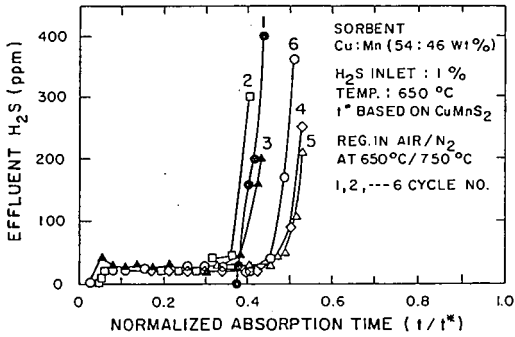


FIG. 3 SULFUR CAPACITY VS. SULFIDATION TEMP. (CuMnO₂ 1/16" PELLETS)

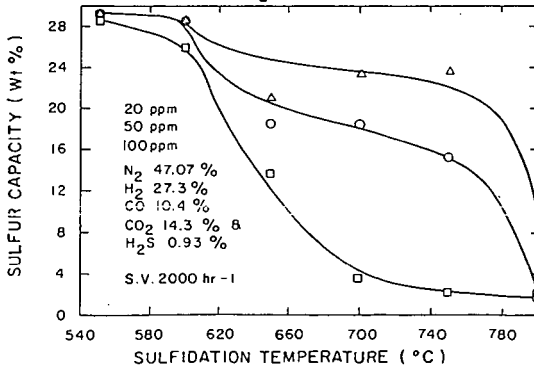


FIG. 4 SULFUR CAPACITY VS. SULFIDATION TEMP.
(CuMnO_2 1/16" PELLETS)

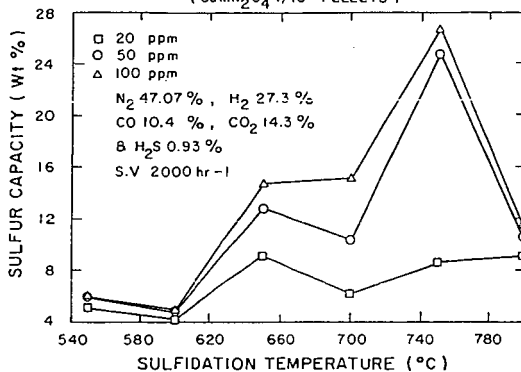


FIG. 5 SULFUR CAPACITY VS. INLET H_2S CONC.
(CuMnO_2 1/16" PELLETS)

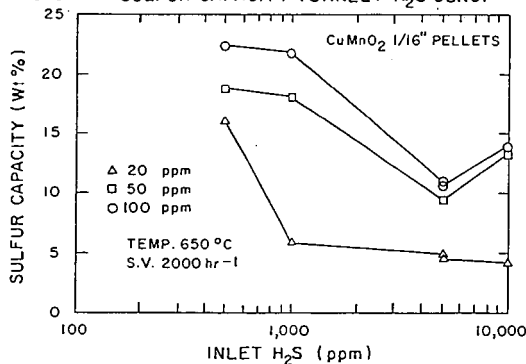
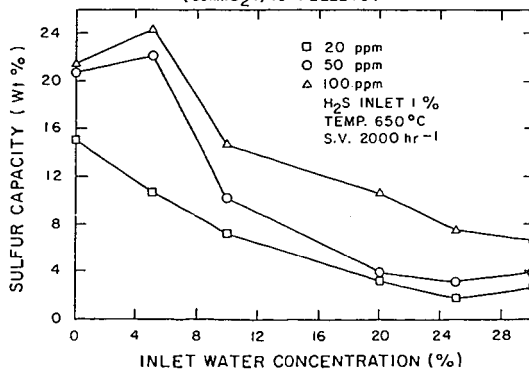


FIG. 6 SULFUR CAPACITY VS. INLET WATER CONC.
(CuMnO_2 1/16" PELLETS)



**SEM MICROANALYSIS TECHNIQUES IN DEMONSTRATION OF
SULFUR CAPTURE BY SLAG AND SORBENTS DURING
GASIFICATION OF COAL IN A TEXACO GASIFIER**

Tristan A. Laurion, Mitri S. Najjar, Ronald J. McKeon
Texaco Research Center
P.O. Box 509, Beacon, New York, 12508

Keywords: SEM Coal Slag Microanalysis, Sulfur Capture by Coal
Slag, In-Situ Desulfurization in Coal Gasification

ABSTRACT

In Texaco's Coal Gasification Process, a significant portion of desulfurization of the product gas (synthesis gas, "syngas") may be achieved by slag capture in the gasification step when various sorbents are added to the coal slurry. For example, when iron oxide is added to the coal slurry, sulfur is captured primarily in a discrete iron oxysulfide phase and to a lesser degree in the glassy silicates phase. Evidence confirming the success of the sorbents approach was gathered through high-temperature, high-pressure bench scale microreactor experiments as well as those with a pilot unit gasifier at Texaco's Montebello, CA research facility. The roles of optical and scanning electron microscopy (SEM) in discerning and analyzing the phases and obtaining approximate phase quantitation are presented.

INTRODUCTION

One of the most promising approaches for utilizing coal in an environmentally safe manner that has been recently demonstrated is the generation of electric power via partial oxidation of coal in an integrated gasification-combined cycle (IGCC) plant. To minimize emission of sulfur compounds, these processes typically separate the reaction step (when coal is converted to raw syngas under reducing conditions at high temperatures) from the acid gas removal step (where physical solvents are generally used to scrub hydrogen sulfide and carbonyl sulfide from the crude syngas). Currently, this approach requires cooling of the hot syngas to the low temperatures commonly needed for physical solvents and subsequent reheating of this cleaned syngas prior to its introduction into the gas turbine. Consequently, these heating and cooling cycles require significant capital investments as well as operating costs.

A potentially more efficient alternative is to combine coal gasification with the sulfur removal step in the same reaction vessel. However, the solubility of sulfur in coal slags is quite low (typically between 0.01 and 0.05 weight percent). One possible approach to enhance sulfur solubility in coal slags is the addition of sulfur-capturing sorbents along with the coal feed to the gasifier. The ideal sorbent should be an inexpensive

additive that chemically reacts with the sulfur compounds in the gas phase (primarily hydrogen sulfide with smaller amounts of carbonyl sulfide) to form a disposable sulfide or oxysulfide that is encapsulated into the resultant slag, but this additive should not cause any complications for slag removal from the gasifier.

Although iron-based compounds have been employed as sorbents, most studies have been done at the lower temperatures encountered in a fluidized bed combustion or an external desulfurization process. In-situ desulfurization has not yet been demonstrated on a commercial scale with any gasification process.

To rapidly screen iron oxide as a sorbent for sulfur capture prior to its being tested in the pilot gasification unit, tests were performed in an experimental bench scale unit^{1,2} to estimate the solubility of sulfur in a given coal slag with and without added iron as a solvent. Typical experimental SEM/EDX microanalysis data from bench-scale drop tube furnace runs with coal slag using iron oxide as an additive under simulated Texaco coal gasifier syngas compositions are presented for comparison with SEM/EDX data on slags generated from the pilot gasifier unit.

EXPERIMENTAL

SLAG SAMPLES PREPARATION

The solidified slag droplets from the drop tube furnace runs and the gasifier slag particles were prepared for polarized light microscopy studies and SEM/EDX microanalysis by encapsulating them in epoxy binder and polishing the 1-inch dia. specimen to reveal the typical particle cross sections for analysis. For SEM/EDX microanalysis the polished specimens were affixed to SEM mounts and carbon coated to render the surface conductive, thereby minimizing charge buildup by the electron beam.

SCANNING ELECTRON MICROSCOPE

Amray 1645 SEM equipped with: 1) lanthanum hexaboride (LaB6) electron emitter source, 2) imaging detectors for secondary as well as backscattered electrons and 3) interfaced with the EDX X-ray equipment for normalized elemental analysis for sodium (Z=11) and elements of higher atomic number, element mapping and digital image acquisition. The analysis regime used 20 KV acceleration voltage, as well as a working distance of 24 or 35mm and zero tilt for the specimen.

ENERGY DISPERSIVE X-RAY ANALYSIS SYSTEM

Tracor Northern TN-5500 EDX Microanalysis System equipped with a Si(Li) semiconductor detector, LSI 11/73 CPU with 3 MByte working memory and 30 MByte mass storage capacity to record and process multielement spectra, acquire and store digital element

distribution maps and digital images. Following element mapping performed for as many as 14 elements simultaneously, the XPHASE routine was used to obtain 4-element correlations (16 combinations) pertinent to estimating phase areas. For more recent samples, an upgrade to the system also permitted estimation of the oxysulfide phase by using the distribution of contrast levels (0-255) in the 512 x 512 pixel image (Figure 4).

The EDX spectra leading to numerical elemental analyses were obtained by electron beam excitation of specific phases. Features of size 10 μm or less were generally analyzed at 5000x and minimum partial field or in spot mode to obtain spectra from a small region of approx. 2 μm dia. The spectra stored to disk were processed to numerical results using EDX standardless software routines and ZAF interelement correction procedures. Polished mineral standards purchased from Biorad Polaron were used to estimate element biases in the normalized results. For this report, silicon results were approximately 10 percent high (relative) when measured with aluminosilicates. Iron disulfide proved to be 0.7 percent high in sulfur and 8 percent low for iron as suggested by the spectra typical of Figure 2.

RESULTS OVERVIEW

SEM/EDX microanalysis techniques have contributed considerably to evaluating the success of both the bench scale desulfurization experiments and the pilot unit gasifier runs.

In the bench-scale drop furnace equilibrium type experiments the slag product available for analysis was limited to about 100 mg. In spite of this constraint, the high magnification/analysis capability allowed intimate insight into the manner in which the sulfur containing gases combined with the sorbent-slag melt to form the expected iron oxysulfides. In this connection the EDX standardless analysis methods were sufficient to give reasonable confirmation that the slag capture product was one in which the Fe/S atom ratio was close to unity (Figures 1, 2). This capability also documented the occasional reduction of the iron oxide to metallic iron where gas partial pressures and temperature conditions favored it (Figure 1 and Table I).

When applied to slag materials from pilot unit gasifier runs, the SEM/EDX microanalysis technique was able to document that sulfur capture takes place not only in the sulfide phase but also in the silicates phase as may be seen from the Table I comparison of gasifier experiments with and without sorbent on both medium-sulfur and high-sulfur coals. Although not documented here, SEM microanalysis methods are also useful for: 1) identifying phases that inhibit slag flow, 2) judging the amount of sorbent to be added to the coal prior to gasification, and 3) evaluating gasifier parameters such as temperature and slag droplet residence time.

Even without detailed microanalysis, the simple low magnification backscattered electron detector image of coal slag particle arrays immediately informs the viewer on the extent of sulfur capture. Without the use of the iron oxide sorbent only occasional miniscule iron sulfide phases are observed. When sorbent is used the iron oxysulfide phase is very visible during SEM exploration of the sample as well as in the BSED images (Fig. 3). Multielement mapping correlations and stored image analysis (Figure 4 and Table I) give numerical expression to the estimate of sulfur capture. Our recent upgrade that allows stored image analysis also permits analysis of up to 100 operator selected points per study field; this gives us the potential to determine particle-to-particle variations in both the silicate and iron oxysulfide phases. Post-SEM evaluations of the analysis files easily allow grouping and averaging of the results for a given phase.

ACKNOWLEDGEMENTS

The authors gratefully acknowledge financial support for this work under the five-year Texaco/Department of Energy Cooperative Program (Contract No. DE-FC21-87MC23277) administered by the Morgantown Energy Technology Center, Morgantown, WV. We are indebted to Ms. Melanie Behrens and Mr. Thomas Scalzo for the dedicated and consistent SEM work on a large number of samples of the bench scale type and gasifier slag particles. We appreciate discussion of results with Messrs. Dick Jung, Enrique DePaz and Thomas Decker and their coordinating various analysis reports with the gasifier team at Texaco's Montebello Research Laboratory.

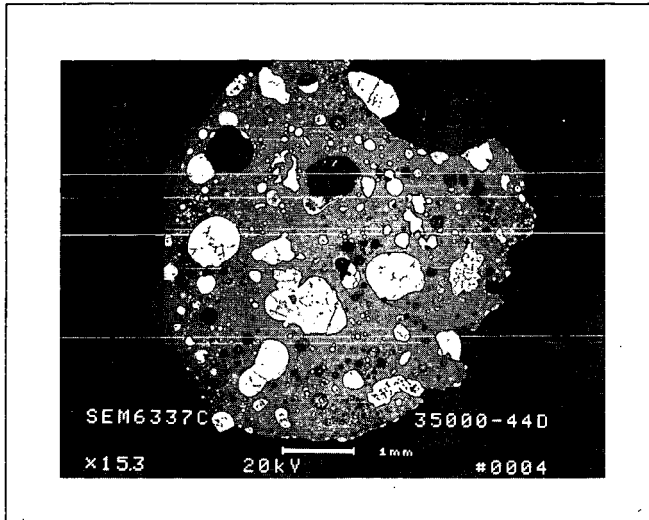
REFERENCES

1. A. M. Robin, C. M. Wu, and M. S. Najjar, "Integration and Testing of Hot Desulfurization and Entrained Flow Gasification For Power Generation Systems", Proceedings of the Eighth Annual Gasification and Gas Stream Cleanup Systems Contractors Review Meeting, DOE/METC-88/6092, May, 1988.
2. M. S. Najjar, D. Y. Jung, A. M. Robin, Poster Presentation, "Theoretical Calculations and Bench-Scale Test Results of Sulfur Capture in Coal Slags Under Partial Oxidation Conditions", Third International Conference on Processing and Utilization of High-Sulfur Coals, Iowa State University, 11/15/89.

TABLE I.
 --- COAL SLAG CHARACTERIZATION ---
 USING SEM/EDX MICROANALYSIS

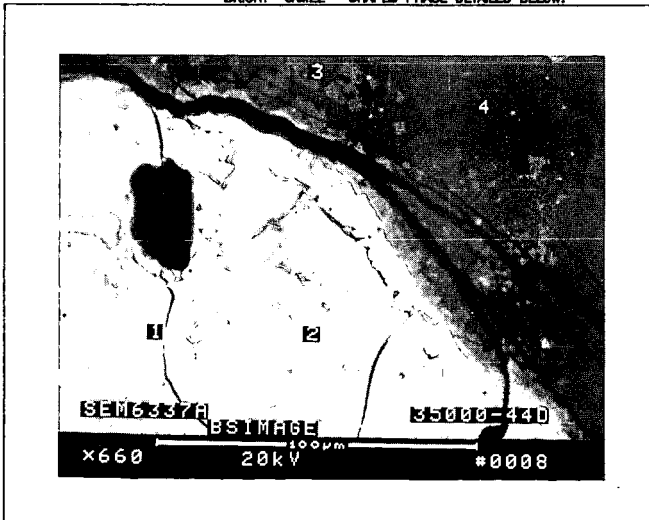
EXPERIMENT	SORBENT	COAL	SLAG PHASE	KEY ELEMENTS BY EDX (WT%)			KEY WT OR (ATCM)RATIO		PHASE AREA(%)
				SI	S	FE			
Drop Tube Furnace 35000-44D	Iron	Med S	Metallic Fe	0.5	0.2	97.9	---	---	12
			Silicate	47.7	0.4	6.0	Fe/Si	0.17	87
			Oxysulfide	1.8	30.7	62.6	Fe/S	(1.17)	21
Gasifier 88-MRL-67	None	Med S	Silicate	39.1	0.4	28.4	Fe/Si	0.73	Major
			Oxysulfide	1.7	26.7	68.5	Fe/S	(1.42)	Trace
Gasifier 88-MRL-70	Iron Oxide	Med S	Silicate	15.7	4.4	85.8	Fe/Si	4.17	Major
			Oxysulfide	3.2	15.4	78.2	Fe/S	(2.83)	HiMinor
Gasifier 89-MRL-58	None	HighS	Silicate	37.8	0.9	32.3	Fe/Si	0.85	98.7
			Oxysulfide	0.4	35.8	80.9	Fe/S	(0.98)	1.3
Gasifier 89-MRL-63	Iron Oxide	HighS	Silicate	24.5	3.5	51.8	Fe/Si	2.11	89.5
			Oxysulfide	0.8	27.2	68.9	Fe/S	(1.45)	30.5

FIGURE 1
DROP TUBE FURNACE SLAG



SEM 6337C

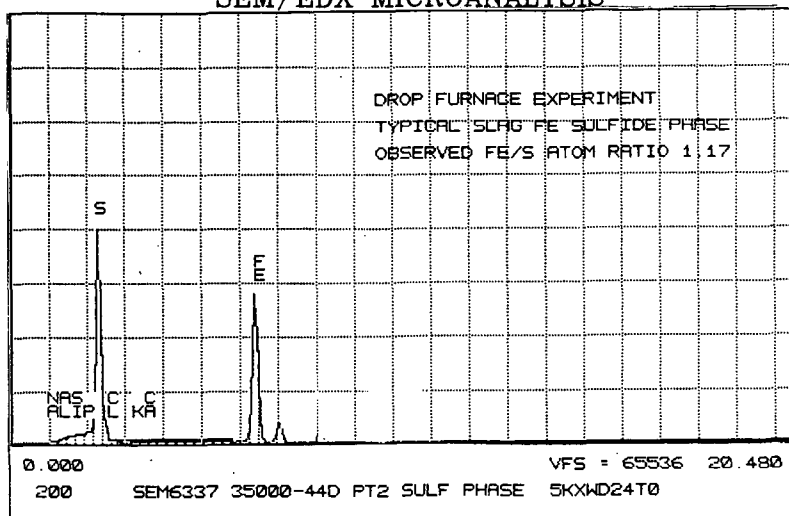
BACKSCATTERED ELECTRON IMAGE OF OVERALL PARTICLE FROM DROP TUBE FURNACE EQUILIBRIUM OF MED-SULFUR COAL SLAG AND SULFUR CONTAINING GASES. SUBJECTED TO SEM/EDX MULTIELEMENT ANALYSIS & MAPPING SUMMARIZED IN TABLE I. BRIGHT "CAMEL"-SHAPED PHASE DETAILED BELOW.



SEM 6337A

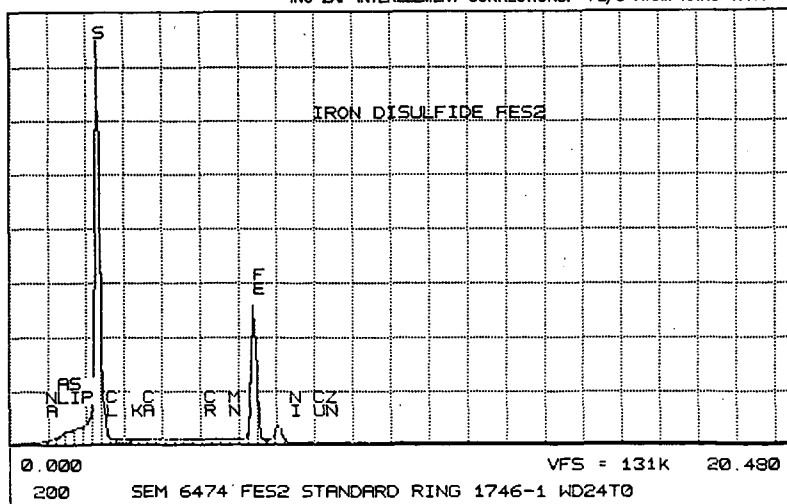
P1 - METALLIC FE. P2 - SULFIDE PHASE FE/S WT RATIO 2.04, AND FE/S ATOM RATIO 1.17. P3 - AL-FE PHASE FE/AL RATIO 0.86. P4 - SILICATE MATRIX FE/SI WT RATIO 0.17.

FIGURE 2
SEM/EDX MICROANALYSIS



EDX SPECTRUM
OXY SULFIDE PHASE

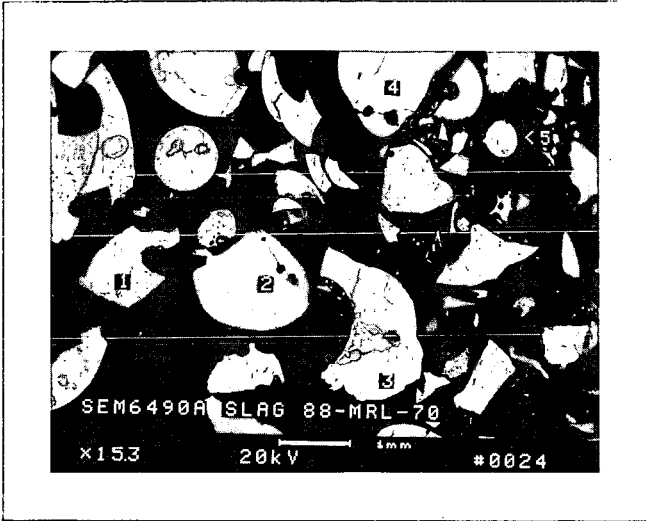
OBTAINED FROM PHASE AT POINT 2 IN SEM 6337A (FIGURE 1).
EXHIBITING SULFUR AND IRON, SPECTRUM WAS CONVERTED TO
NUMERICAL VALUES BY STANDARDLESS QUANT METHODS EMPLOY-
ING ZAF INTERELEMENT CORRECTIONS. FE/S ATOM RATIO 1.17.



EDX SPECTRUM
IRON DISULFIDE

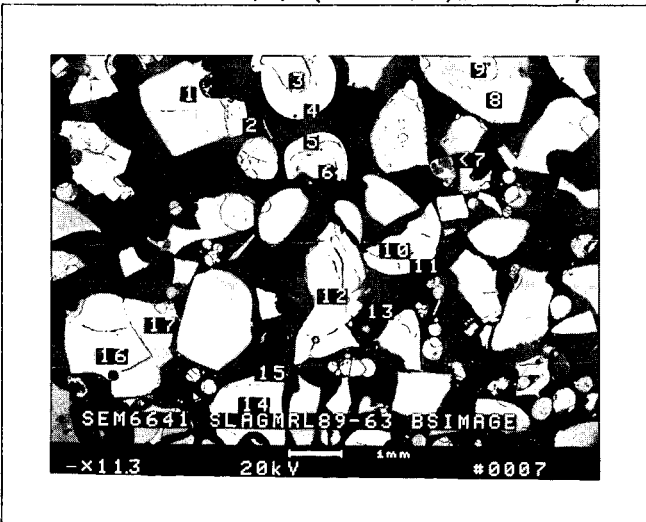
FES2 MINERAL (POLISHED IN POLARON ANNULAR STD 1746-1).
THEORETICAL FE/S ATOM RATIO OF 0.50. CONVERSION OF
SPECTRUM GIVES OBSERVED FE/S ATOM RATIO 0.46.

FIGURE 3
 SLAGS FR COAL GASIFICATION W/IRON OXIDE



SEM 6490A, SLAG
 MED-SULFUR COAL

PARTICLES FROM GASIFICATION OF MED-SULFUR COAL. PARTICLES 1, 3, 5 HAVE OXY-SULFIDE PHASES; OXY-SULFIDE PHASE FOR #1 GIVES OBS. FE/S ATOM RATIO 2.8 (TABLE 1). PHASES 2, 4 ARE TYPICAL OF SILICATES AND CONTAIN AL, SI, S, CA, FE (PHASE 2 GIVES FE/SI WT RATIO 4.17).

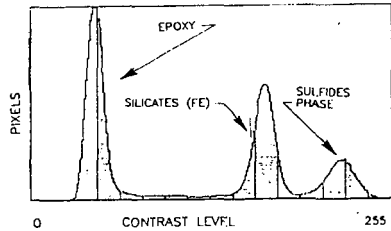
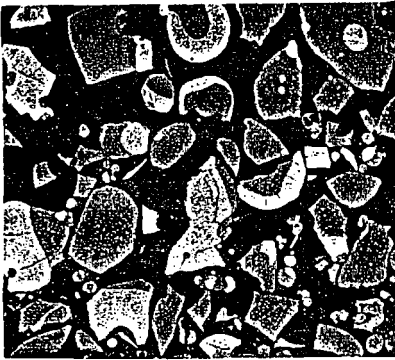


SEM 6641 SLAG
 HIGH-SULFUR COAL

AVERAGING ANALYSES FOR 8 OXY-SULFIDE PHASES GIVES FE/S RATIO OF 1.45 (TABLE 1). OXY-SULFIDE PHASE ESTIMATED BY ELEMENT MAPPING IS 31.9%. BY STORED IMAGE ANALYSIS 30.8% (TBL 1, FIG. 4).

FIGURE 4.

PHASE QUANTITATION BY STORED IMAGE ANALYSIS
USING SEGMENTED CONTRAST



DISTRIBUTION FOR PIXELS IN STORED IMAGE

PHASE/FEATURE	-- IMAGE PIXELS (512 X 512 ARRAY) --	
	CONTRAST LEVEL	OBSERVED% NORMALIZED%
EPOXY	0- 79	46.7
AL-SI (LOW-FE)	80-139	3.3
AL-SI-S-CA-FE	140-189	33.8
FE-S OXYSULFIDE	190-255	16.3

A NOVEL SUPPORTED SORBENT FOR HOT GAS DESULFURIZATION

Aysel T. Atimtay
Lee D. Gasper-Galvin
James A. Poston
Morgantown Energy Technology Center
Morgantown, WV 26505

Keywords: Desulfurization, Supported Sorbents, Hot Gas Cleanup

INTRODUCTION

Integrated gasification combined cycle (IGCC) system is one of the most promising power systems for producing electrical energy from coal due to the noticeable improvement in thermal efficiency that it can provide. This advanced power generating system involves the direct contact of hot coal-derived gases with turbine blades. In order to protect the turbines and related equipment from corrosion and abrasion, it is necessary to clean the coal gas. Economical as well as environmental requirements for advanced power generating systems mandate the high-temperature removal of corrosive and abrasive compounds from coal gases such as sulfur and nitrogen containing compounds, trace metals, alkali, residual hydrocarbons, and particulates. Sulfur-containing compounds account for most of the acidic species formed during coal gasification. Hydrogen sulfide, which is the most abundant sulfur-containing compound in coal gas, can react readily with the oxides of alkali earth and transition metals (1).

Westmoreland, et al. (2) reported the results of a thermodynamic screening of the high temperature desulfurization potential of 28 single metal oxides by using the free energy minimization method. Also, kinetic limits for ZnO, MnO, CaO, and V₂O₅ were reported by Westmoreland, et al. (3) for desulfurization reactions. ZnO showed a very favorable thermodynamic equilibrium with H₂S (4) and iron oxide showed easy regenerability with air. Results regarding structural changes in the pure ZnO sorbent at high temperatures were reported by Ranade and Harrison (5). They showed that sintering actually causes the particle to shrink radially, thus for the same number of particles the surface area available for reaction is smaller. Also, zinc metal produced by reduction of ZnO in coal-gas volatilizes above 1290°F (699°C).

Favorable properties of zinc oxide and iron oxide towards absorbing H₂S were combined at the in-house research program of Department of Energy's Morgantown Energy Technology Center. The combined metal oxide sorbent, zinc ferrite, was shown to reduce H₂S levels in gasifier gases to less than 10 ppmv (6). However, zinc ferrite has a temperature limitation. The maximum operating temperature for zinc ferrite is about 1200°F (649°C). Focht, et al. (7) showed that the sorbent lost its pore volume during reduction, and subsequent loss of reactivity was observed during sulfidation. The sorbent also showed a substantial amount of decrepitation above 1200°F (649°C).

Improvements in the original formulation have been attempted in an effort to overcome the limitations of zinc ferrite. An inorganic binder, bentonite, was added to zinc ferrite. Thus, a sorbent with comparable reactivity and capacity to the original sorbent, but with a higher temperature limit than the original zinc ferrite was obtained. This sorbent can withstand temperatures up to 1275°F (691°C), which is not very satisfactory for high temperature fluidized and entrained bed gasifiers.

The need for developing a sorbent having better properties (durability and reactivity) than the original or modified zinc ferrite led researchers to try

other metal oxides. Various combination of metal oxides, such as Zn, Cu, Al, Ti, Fe, Co, Mo, and V were tried at Massachusetts Institute of Technology (MIT) and Jet Propulsion Laboratory (JPL) in an effort to develop a durable and high capacity sorbent for removal of H₂S from hot coal-derived gases (8). Basically, the sorbents tested were divided into two groups: 1. Zinc-based sorbents, 2. Copper-based sorbents. Zinc-based sorbents included zinc ferrite (ZF), zinc-copper ferrite (ZCF), and zinc titanate (ZT). Copper-based sorbents included copper aluminate (CA) and copper-iron aluminate (CFA). Research results (8) showed that zinc-based sorbents were more promising than copper-based sorbents in the temperature range of 1000° - 1350° F (538° - 732°C). One of the most promising sorbents among the zinc-based sorbents was zinc titanate (maximum operating temperature of 1340°F (727°C)). It was found that the TiO₂ phase helps to stabilize the ZnO phase, and volatilization of Zn at temperatures higher than 1290°F (699°C) has been reduced (about 1 wt % Zn is lost in 1000 hours of operation). However, TiO₂ does not absorb H₂S effectively. Therefore, the capacity of zinc titanate is lower than that of zinc ferrite due to dilution effect.

Extrudates of regenerable mixed metal oxide sorbents (copper-modified zinc ferrite, zinc titanate, copper aluminate and copper-iron aluminate) were tested in a high temperature-high pressure (HTHP) fixed bed reactor by Research Triangle Institute (RTI) (9). Reductions in H₂S concentration from >10,000 ppmv to < 1 to 50 ppmv were achieved. The copper-modified zinc ferrite sorbent reduced the H₂S concentration to less than 1 ppmv at up to 1100°F (593°C) with 20 % steam in the gas. The zinc ferrite sorbent was also tested in the same reactor. Zinc titanate outperformed the other mixed metal oxide sorbents in structural strength and capacity at steam levels as low as 5 % and temperatures as high as 1350°F (732°C). However, entrained and fluidized bed gasifiers which are presently being developed have outlet temperatures as high as 1500°F (816°C) to 1800°F (982°C). Furthermore, for continuous desulfurization of a full scale gasification stream, a fluidized bed sorbent system instead of a fixed bed would improve the process efficiency considerably by providing a means for continuous solids regeneration. Zinc ferrite sinters at temperatures higher than 1200°F (649°C). It does not have sufficient attrition resistance to withstand a fluidized bed environment. Zinc titanate can withstand temperatures up to 1350°F (732°C), and has medium strength, but the utilization is low, i.e. 35 - 45 %. Therefore, novel sorbents are still being sought which will show improved resistance to higher temperatures and attrition. Recently, copper manganese sorbents (bulk) are under study by ElectroChem Inc. (10).

The objective of this research is to develop a novel regenerable sorbent which will show improved resistance to higher temperatures and attrition. The potential advantages of supported sorbents, as compared to bulk sorbents, are higher surface area, less resistance for diffusional transport, and higher temperature and attrition resistance. The sorbent investigated in this study is copper and manganese oxides supported on SP-115 zeolite. Results of sulfidation and regeneration experiments conducted using a simulated coal gas mixture at temperatures of 1000° - 1600°F (538° - 871°C) will be reported.

EXPERIMENTAL SECTION

Sorbent Preparation

The sorbents investigated in this study were prepared by a coprecipitation process. SP-115 zeolite (1/8" extrudates, Union Carbide) was used as the support. SP-115 had the following characteristics : SiO₂ > 99 % by weight, surface area = 482 m²/g, crush strength = 6.6 kg/cm, pore diameter = 5.4 Å. The coprecipitation process included : 1) Impregnation of the zeolite with a solution of cupric acetate and manganese acetate in a rotary vacuum evaporator, 2) Dehydration of the sorbent in a vacuum oven at 158°F (70°C) and 0.1 inch Hg, 3) Calcination of the sorbent in a muffle furnace at 1382°F (750°C) for 7 hours. Three samples were

prepared with this process (SP1C5M5, SP2C5M5, and SP2C9M1). The atomic absorption spectrophotometer analysis showed that Cu and Mn loadings on the sorbent SP1C5M5 were 1.82 % and 1.64 % by weight, respectively. SP2C5M5 had 4.39 % by wt. Cu and 6.11 % by wt. Mn. The corresponding values for SP2C9M1 were 5.15 % and 5.73 % by weight, respectively. The uncertainty in the atomic absorption analysis is $\pm 1\%$.

Experimental

A schematic diagram of the experimental system is shown in Figure 1. The system consisted of a gas mixing system, a fixed bed reactor, a condenser and a water knock-out pot, a gas sampling system, and a tail-gas cleanup system. Gases were supplied from gas cylinders and the flow rates were monitored through mass flow controllers. After the gases were mixed in a manifold, they were fed into the fixed bed reactor. This gas mixture simulated the partially quenched exit gas of an air-blown KRW fluidized bed coal gasifier which had the following molar composition: 42.5 % N_2 , 11 % CO_2 , 12.5 % CO , 13.8 % H_2 , 1 % CH_4 , and 0.2 % H_2S . 19 % H_2O in the gas mixture was provided by adding a predetermined amount of water into the gas stream before it entered the reactor via a high pressure pump.

The reactor which consisted of a zirconia tube, with 0.875-inch inside diameter and 12-inch length, was placed vertically in an electric furnace equipped with graphite heating elements. The furnace was water cooled. The graphite heating elements were located in a helium atmosphere to protect them from oxidation. The temperatures of the gas at the inlet and the center of the reactor were measured by K-type thermocouples located along the central axis. The reactor was designed to withstand a pressure of 15 psig and a temperature of 3000°F (1649°C). The sorbent sample was placed in the center of the reactor and the bed height was 2 inches. The gas lines between the reactor outlet and the condenser inlet were heated via heating tapes and heavily insulated to prevent the condensation of steam in the gas lines. The exit gas from the reactor was filtered, cooled down in the condenser, and sampled for gas analysis. The tail gas was sent through the absorbers to remove the sulfurous gases before it was discharged to the atmosphere.

The experiments consisted of a sequence of sulfidation and regeneration runs. The reactor temperature was held constant during the sulfidation and regeneration experiments. Reactor pressure was maintained at 5 ± 3 psig. Three temperatures were tested: 1000, 1250, and 1600° F (538°, 677°, and 871°C). The space velocities for the sulfidation and the regeneration runs were 2000 and 600 hr^{-1} , respectively. Regeneration of the sulfided sorbent was conducted with air only and with a 50 % air/50 % steam mixture. Breakthrough during sulfidation runs was defined as 200 ppmv H_2S in the effluent gas. After the sulfidation run was stopped, the reactor was purged with nitrogen for at least 15 minutes. Regeneration was carried out at the reaction temperature. The regeneration cycle was stopped when the SO_2 concentration of the effluent gas was below 500 ppmv. The sorbents were subjected to five sulfidation/regeneration cycles to establish sulfur sorption capacity and regenerability.

Selected sorbent samples were analyzed for total weight, metal and sulfur content, crush strength, surface area, average pore diameter, pore volume, and pore size distribution both before and after reaction. Gas grab samples obtained during experimentation were analyzed by gas chromatography. Also Gas-tech precision gas detection tubes were used to determine the H_2S and SO_2 concentrations in the inlet and outlet gas streams.

RESULTS AND DISCUSSION

The effect of temperature on sorbent capacity is shown in Figure 2. The H_2S breakthrough curves indicate that the breakthrough times were 37, 45, and 45 minutes at 1000°F (538°C), 1250°F (677°C), and 1600°F (871°C), respectively. The

sorbent has greater capacity at 1250°F (677°C) and 1600°F (871°C) than at 1000°F (538°C). However, the prebreakthrough H₂S levels are lower at 1000°F (538°C) and 1250°F (677°C) than at 1600°F (871°C). Although the prebreakthrough H₂S level is lower at 1000°F (538°C), the sorbent has more total capacity at the higher temperatures.

Two runs were conducted at 1250°F (677°C) with different samples from the same batch of SP1C5M5 sorbent, to establish the extent of reproducibility of the experimental method. Twelve detector tube readings of H₂S were taken, 5 min apart, for each run. The average difference between readings for the two runs was 30 ppmv. Thus, the experimental method appears to be reasonably reproducible.

Sorbent regenerability was tested at 1250°F (677°C). Two and one-half cycles were conducted with only air as the regenerant gas, and five cycles were studied using a 50 mole % steam/50 mole % air mixture for regeneration. Two criterion were used to assess the regenerability of the sorbent: (1) a comparison of the H₂S breakthrough curves, and (2) a comparison of the SO₂ outlet curves during the sulfidations.

When the sorbent was regenerated with air, the second and third sulfidation breakthrough curves were somewhat similar. However, the prebreakthrough average H₂S outlet concentration was approximately 50 ppmv less for the third sulfidation than for the second sulfidation. Figure 3 shows the H₂S breakthrough curves after the sorbent was regenerated with steam/air. The curve for the first sulfidation was not shown, as the reactor bypass was accidentally left open during the run. The third through sixth sulfidations, conducted with steam/air regeneration, gave similar breakthrough curves. Thus, the steam/air regeneration appears to give better regenerability than air regeneration.

Outlet SO₂ concentrations were compared for the second and third sulfidations (set I) using air regeneration, with the second, third, and fourth sulfidations (set II) using steam/air regeneration. After 15 min on-stream, set I showed outlet SO₂ concentrations between 500 and 600 ppmv. After the same period, set II yielded SO₂ concentrations ranging between 30 and 450 ppmv. These results indicate that more sulfate was formed during air regeneration than during steam/air regeneration. This is not unexpected, since the presence of steam reduces the overall oxidative properties of the regenerant stream. In general, if SO₂ is released in large quantities when reducing gases are introduced after oxidative regeneration, this indicates that sulfates have been formed during the regeneration. The release of such sulfurous gases must be avoided during sulfidation. It has been suggested in studies on zinc ferrite that a clean reducing gas could be used for reductive regeneration of the sorbent after oxidative regeneration, and prior to sulfidation. However, the economics for carrying out a reductive regeneration step are poor, due to the capital cost of additional vessels and the introduction of complications into the overall operation of the system (11).

Although no carbonyl sulfide was fed to the reactor in the simulated gas mixture, appreciable concentrations were detected in the outlet gas during sulfidation. The COS concentration was usually greater than 50 ppmv, and often as high as 100-250 ppmv in the outlet gas. It is well known that certain zeolites can catalyze the COS formation reactions. CO and CO₂ can react with H₂S according to the following reactions (12):



At temperatures between 440°F (227°C) and 1340°F (727°C), the thermodynamics of reaction [2] are more favorable than those of reaction [1]. Figure 4 shows that COS production became a minimum after about 30-40 min on-stream, and then

increased. The initial decrease in COS may have been due to reduced availability of CO, because of the competing reactions in which CO reduces copper oxides. The later increase in COS formation may have been caused by the kinetic effect of gradual heating of the sorbent bed with time on-stream. The effect of increased temperature on COS formation can be seen in Figure 5. It appears that 1250°F (677°C) is a more favorable temperature for COS formation than either 1000°F (538°C) or 1500°F (816°C). The figure also suggests that COS production may increase with the number of cycles; other data which were collected support this conclusion.

The effect of a single loading of the metal acetate solution versus a double loading of the metals is shown in Figure 6. As expected, the double-coated sorbent, SP2C5M5, has a breakthrough time that is nearly double that of the single-coated SP1C5M5. Thus, the capacity of the sorbent extrudates can be increased via multiple loadings of the metal salts.

Sorbents SP2C5M5 and SP2C9M1 were also compared for their ability to remove H₂S from the simulated coal gas mixture. The second and third sulfidations of each sorbent are shown in Figure 7. The SP2C9M1 sorbent appears to have greater capacity than SP2C5M5 for H₂S removal.

The surface area of the sorbent was determined before and after the reaction by using the Langmuir adsorption method, with a maximum error of $\pm 1.5\%$. The fresh SP-115 zeolite without metal coating had an average surface area of 482 m²/g. The unreacted SP1C5M5 had an average surface area of 434 m²/g, with a metal loading of 1.82 wt % Cu and 1.64 wt % Mn. This suggests that the presence of the metal has caused some pore blockage. After single sulfidations at 1000°F (538°C), 1250°F (677°C), and 1600°F (871°C), the surface area decreased to 379, 370, and 237 m²/g, respectively. The loss of surface area under reaction conditions may be due to coalescence of pores of the zeolite, or to a certain extent, silicic acid formation by reaction of the zeolite with high-temperature steam.

For a 5-cycle set of experiments on sorbent SP2C5M5, the utilization of sorbent at breakthrough for each of the first through fifth sulfidations was, respectively, 20%, 7%, 7%, 13%, and 12%. These percent utilizations were calculated using the following assumptions: (1) the H₂S breakthrough point was 200 ppmv H₂S in the outlet gas, (2) the metal composition of the sorbent was 4.39 wt % Cu and 6.11 wt % Mn, as determined by atomic absorption analysis, (3) the concentration of H₂S in the inlet gas was 2000 ppmv, and (4) the sulfided metals in the sorbent were present only in the form of Cu₂S + MnS. The decrease in sorbent utilization after the first sulfidation was due to incomplete regeneration. The increase between 7% and 12-13% may have been due to random variations. It is possible that the relatively low utilization of the sorbent was caused by ineffective coating of the zeolite pores, i.e., the metals were deposited in several atomic layers on the outer surface of the extrudate, rather than inside the pores. Or, even if the pores were effectively coated, there may have been significant resistances to diffusion of H₂S into the pores.

Six different samples of the bed material from the 5-cycle set performed with SP2C5M5 at 1250°F (677°C) and the 3-cycle set run with SP2C9M1 at 1250°F were analyzed using atomic absorption. There was no conclusive evidence for loss of Cu or Mn greater than a few percent. Thus, these metals do not appear to undergo appreciable volatilization under these conditions of sulfidation and regeneration.

The crush strength of the sorbent extrudates is an important consideration for practical operation. Crush strength was determined by taking the average of the force per unit length of extrudate required to crush 15 extrudates; the range of error for these tests is $\pm 20\text{-}35\%$, within the first standard deviation. The fresh SP-115 zeolite without metal coating had an average crush strength of 6.58 kg/cm. The crush strength for fresh SP2C5M5 and SP2C9M1 were 29.6 and 11.1 kg/cm, respectively. The metal coating makes the extrudates much stronger; particularly

the Mn appears to promote increased resistance to crushing. The average crush strength of 6 samples from the SP2C5M5 bed, after 5 cycles, decreased by only 6%. The average crush strength of 5 samples from the SP2C9M1 bed, after 3 cycles, increased by 3%. Therefore, the crush strength of the zeolite was increased by the metal loading, and essentially unchanged by reaction.

CONCLUSIONS

For the temperature range of 1000°-1600°F (538°-871°C), the SP-115 zeolite-supported Cu/Mn oxides sorbent had more total capacity at 1250°F (677°C) and 1600°F (871°C) than at 1000°F (538°C). Regeneration with a 50 mole % steam/50 mole % air mixture was preferred over air regeneration, due to decreased sulfate formation in the presence of steam. Further studies would be required to optimize regeneration conditions, so that minimal sulfate is formed during oxidative regeneration. Appreciable amounts of COS were formed at 1250°F (677°C), probably due to reactions catalyzed by the zeolite; however, at 1500°F (816°C) the production of COS greatly decreased. The sorbent containing Cu:Mn molar ratios of 9:1 had greater capacity for H₂S than those containing equimolar ratios of the metals. Sorbent utilization with repeated sulfidation/regeneration cycles was low (<13% for SP2C5M5). Surface area of the sorbent decreased with metal loading and with reaction temperatures between 1250°F (677°C) and 1600°F (871°C). It is uncertain whether the zeolite pores had been effectively coated or plugged by the metal acetate solutions during preparation. There was little or no volatilization of the metals at 1250°F (677°C). The SP-115 zeolite will require further testing to determine whether it can withstand the highest temperatures (1250°-1600°F) (677°-871°C) for multiple cycles.

REFERENCES

1. T. Kyotani, H. Kawashima, A. Tomita, A. Palmer, and E. Furimsky, " Removal of H₂S From Hot Gas in the Presence of Cu-Containing Sorbents," *Fuel*, 68, pp.74, 1989.
2. P. R. Westmoreland and D. P. Harrison, " Evaluation of Candidate Solids for High-Temperature Desulfurization of Low-Btu Gases," *Env.Sci.Tech.*, 10, pp. 659, 1976.
3. P. R. Westmoreland, J. B. Gibson, and D. P. Harrison, " Comparative Kinetics of High Temperature Reaction Between H₂S and Selected Metal Oxides," *Env.Sci.Tech.*, 11, pp. 488, 1977.
4. T. R. Rao and R. Kumar, " An Experimental Study of Oxidation of Zinc Sulfide Pellets," *Chem.Eng.Sci.*, 37, pp.987, 1982.
5. P. V. Ranade and D. P. Harrison, " The Variable Property Grain Model Applied to the Zinc Oxide-Hydrogen Sulfide Reaction," *Chem.Eng.Sci.*, 36, pp. 1079, 1981.
6. T. Grindley and G. Steinfeld, " Development and Testing of Regenerable Hot Coal-Gas Desulfurization Sorbent," Report DOE/METC/16545-1125, 1981.
7. G. D. Focht, et al., " Structural Property Changes in Metal Oxide Hot Coal Gas Desulfurization Sorbents," Report DOE/MC/21166-2163 (DOE 86016041), 1986.
8. M. Flytzani-Stephanopoulos, et al., "Detailed Studies of Novel Regenerable Sorbents for High-Temperature Coal-Gas Desulfurization," Proceedings of the Seventh Annual Gasification and Gas Stream Cleanup Systems Contractors Review Meeting, DOE/METC-87/6079, Vol. 2, pp. 726, 1987.
9. S. K. Gangwal, et al., " Bench-Scale Testing of Novel High-Temperature Desulfurization Sorbents," Proceedings of the Eighth Annual Gasification and Gas

Stream Cleanup Systems Contractors Review Meeting, DOE/METC-88/6092, Vol. 1, pp. 103, 1988.

10. V. Jalan and M. Desai, "Copper-Based Sorbents For Hot Gas Cleanup," Proceedings of the Eighth Annual Gasification and Gas Stream Cleanup Systems Contractors Review Meeting, DOE/METC-88/6092, Vol. 1, pp. 45, 1988.
11. L. Bissett, "Aspects of Fixed Bed Gasification/Fixed Bed Zinc Ferrite Integration," Ninth Annual Gasification and Gas Stream Cleanup Systems Contractors Review Meeting, DOE/METC/PETC, June 27-29, 1989, Morgantown, WV.
12. Chemistry of Hot Gas Cleanup in Coal Gasification and Combustion, Morgantown Energy Research Center, MERC/SP-78/2, 1978.

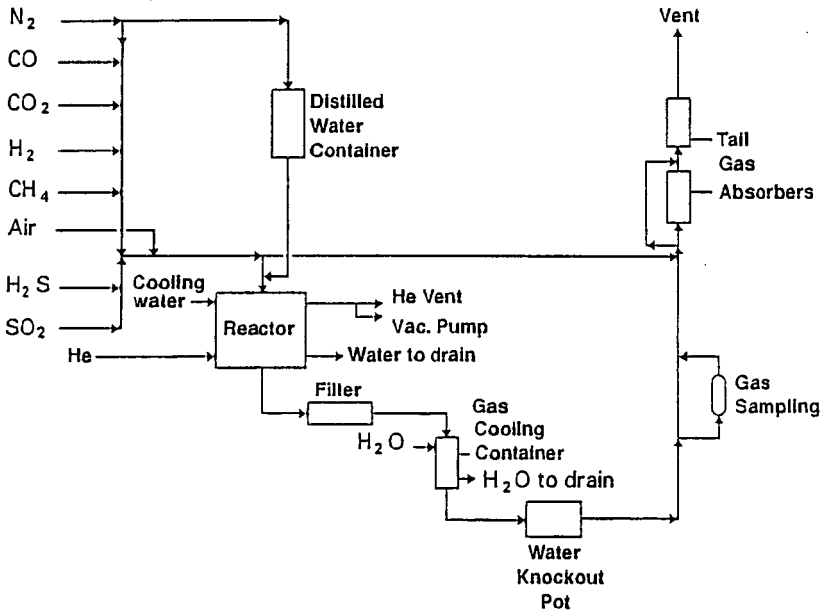


Fig. 1 Flow diagram of fixed bed reactor system

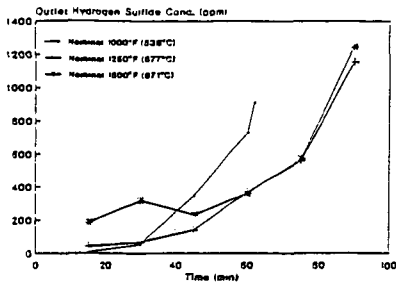


Fig. 2 Hydrogen sulfide breakthrough curves for single sulfidations of SPIC5M5 sorbent: The effect of temperature

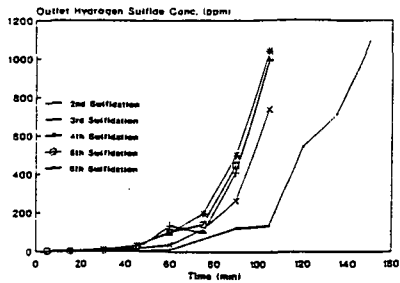


Fig. 3 Hydrogen sulfide breakthrough curves for multiple sulfidations of SP2C5M5 sorbent at nominal 1250°F (677°C) with 50 mole % steam/50 mole % air used for regeneration: Regenerability

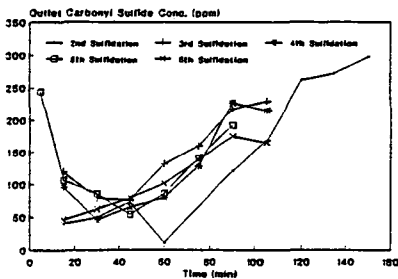


Fig. 4 Outlet concentrations of carbonyl sulfide for multiple sulfidations of SP2C5M5 sorbent at nominal 1250°C (677°C) with 50 mole % steam/50 mole % air used for regeneration: The effect of cycle number (after steam/air regeneration) on carbonyl sulfide formation

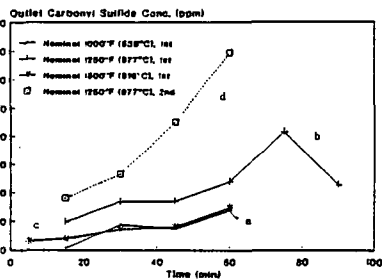


Fig. 5 Outlet concentrations of carbonyl sulfide for sorbent SPIC5M5 for (a-c) single sulfidations, and (d) a second sulfidation after air regeneration: The effect of temperature and cycle number (after air regeneration) on carbonyl sulfide formation

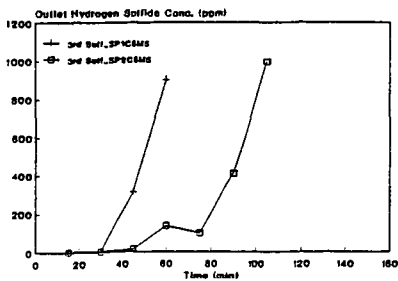


Fig. 6 Hydrogen sulfide breakthrough curves for the third sulfidation of sorbents SPIC5M5 and SP2C5M5 at nominal 1250°F (677°C): The effect of the number of metal loadings

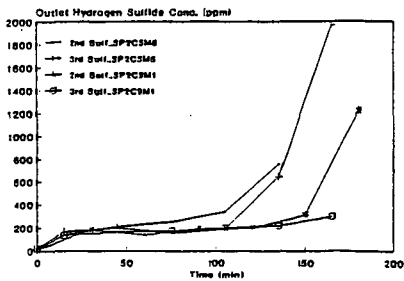


Fig. 7 Hydrogen sulfide breakthrough curves for the second and third sulfidations of sorbents SP2C5M5 and SP2C9M1 at nominal 1250°F (677°C): The effect of nominal molar ratios of Cu:Mn of 3:5 versus 9:1

SYNGAS DESULFURIZATION OVER METAL ZEOLITES

Clyde S. Brooks
RECYCLE METALS
Glastonbury, Connecticut 06033

Metal oxides supported on zeolites have been demonstrated as effective regenerable desulfurization agents for high temperature removal of hydrogen sulfide from fossil fuels. Desulfurization occurs by sulfide formation with Fe or Zn on the surface of the zeolite lattice with the hydrogen sulfide of the fuel gas. Regeneration by air oxidation of the supported metal sulfide displaces the sulfur as sulfur oxides. Both sulfidation and oxidation show efficient kinetics within a temperature range of 500-600C, which is above the range of physical adsorption and below where metal vaporization or support instability prove limitations. Zinc faujasite Y is of particular interest because of demonstrated ability to reduce the sulfur concentration to several PPM in the temperature range 500 to 650 C.

INTRODUCTION

The potential for increased efficiency of gas cleanup and improved economics provides the incentive for development of high temperature desulfurization of fossil fuels (coal gas or syngas). Numerous processes are available for low temperature desulfurization. However, advantages in processing, notably energy conservation and capital savings, make high temperature desulfurization attractive.

Attention is given here to the use of metal zeolites as regenerable desulfurization agents. Consideration is given to the merits of high temperature desulfurization, the rationale of agent selection and bench scale evaluations have been conducted of the desulfurization-regeneration performance of iron and zinc zeolites.

THE MERITS OF HOT DESULFURIZATION

Two assessments that show the energy and capital cost advantages of high temperature desulfurization of several available coal gasification alternatives are summarized here:

One comparison (1) has been made for low and high temperature gas cleanup of a 1000 MW coal gasification combined cycle power plant for two possible gas turbine inlet temperatures (1070 C and 1320 C) for 4 gasification options: 1) air blown Lurgi (fixed bed), 2) oxygen blown Lurgi (fixed bed), 3) oxygen blown bituminous gasifier cleaner (slagging fixed bed) and 4) an air blown Foster Wheeler (entrained bed). The high temperature hot gas cleanup (HGC) used was the Morgantown Energy Technology Center (METC) iron oxide fixed bed desulfurization process. The low temperature gas cleanup (LGC) used was the Benefield process. The HGC alternative provided advantages in thermal efficiency, capital cost, electricity cost and purification system component costs. Savings of 34% in capital requirements and 30% in cost of electricity were obtained with HGC.

In a second assessment (2) 4 gasifier configurations were evaluated, 3 employing entrained flow, by Texaco, Shell-Koppers and by Foster Wheeler/Bituminous Coal Research (FW/BCR) and Institute of Gas Technology (IGT) fluid bed using 24 variations of air and gas blown gasification with 3 temperatures for desulfurization. Low temperature (150C) desulfurization was with a Selexol liquid scrubber. Intermediate temperature (540C) desulfurization was with the METC iron oxide fixed bed. High temperature (820C) desulfurization used a Conoco half-calcined dolomite in a fluidized bed. All processes met EPA emission standards. The medium and high temperature processes provided advantages in thermal efficiency, plant capital and overall electricity cost. The greatest advantage provided was reduced capital cost.

SELECTION OF DESULFURIZATION AGENTS -PRIOR WORK

The elements considered for desulfurization agents have been selected largely on an empirical basis from essentially every group of the periodic table. Westmoreland and Harrison (3) made a systematic examination of candidates for the hot desulfurization of low BTU coal gases. In their approach they made use of the free energy minimization method of Van Zeggeren and Story and selected 11 of 28 elements as potential candidates for fuel gas desulfurization within a temperature range of 400-1200C. These candidates were Fe, Zn, Mo, Mn, V, Ca, Sr, Ba, Co, Cu and W. Based on thermodynamic considerations they selected MnO, CuO, V_2O_3 and ZnO for kinetic studies. A second systematic selection of sulfur removal agents based on thermodynamics has been made for fuel cell applications (4). Attainable equilibrium H_2S concentrations for coal gas at 650C was the selection criterion. Of 42 agents examined, 12 candidates Fe, Co, Cd, Mo, Pb, W, Zn, V, Mn, Ba, Sr and Cu were evaluated with Cu/CuO, ZnO, and V_2O_3 examined experimentally.

A comprehensive review of hot gas (>430C) cleanup processes applicable to sulfur removal, as H_2S from coal gases was prepared by Onursal (5) in 1979. Comment on desulfurization work with an updating since 1979 is appropriate. First comments will be made of results obtained with the single component systems Fe, Cu and Zn:

Early work with iron oxides on the Appleby-Frodingham process (6,7) demonstrated excessive sorbent degradation and was abandoned. The MERC iron oxide/silica (fly ash) sorbent (8,9) achieved 200-800 ppm H_2S in coal gases in the temperature range 400-750C with regeneration at 950C in air or steam.

Zinc oxide has been widely used for removal of low concentrations of H_2S at low to mid temperatures but only as a nonregenerable system. Supported ZnO has been evaluated at Giner Inc. (10,11) and by Institute Francais Du Petrole (IFP) (12) and H_2S levels down to 1 ppm were obtained at bench scale. Evaluations of the IFP ZnO at METC (12) confirmed the low H_2S concentrations but indicated low sulfur loadings relative to unsupported ZnO.

Several studies have involved copper sorbents (13,14,15,16,17). Copper supported on silica (16) has been used to desulfurize H_2S/H_2 mixtures over the temperature range 300-1000C with ultimate application intended for coke oven, producer, and water gases and hydrocarbon vapors. Studies have been conducted by Kennecott Copper Co. (13,17) for Lurgi fuel gases containing H_2 , CO and 1-1.5% H_2S in the temperature range 480-510C. Sulfur removal efficiencies of 80% (to 1500 ppm H_2S) were obtained. Sorbents were regenerated at 816C using solid-solid reaction with CuO but with limited success.

Most desulfurization studies have been conducted with mixed metal oxides. About the earliest significant study was made at Johns Hopkins University (14) for mixed oxides of Cu, Fe, U, Cr, Sn, Mn, V, Mo, Sb, Bi as binary and ternary combinations with various binders such as clay, pumice, alundum and lime. Regeneration of the sulfided sorbents was by air oxidation, but sustained performance was not obtained. Nachod (15) used mixed oxides of Cu, Zn and Pb supported on aluminosilicates to remove sulfur from petroleum distillates and gases with H_2S and organic sulfur compounds in the temperature range 90-550C. Regeneration was with air/steam at 370-540C, but the supports were lacking in stability.

Investigations at METC extending earlier work with Fe oxides (6-9) have shown that sulfur levels of 2-10 ppm in the temperature range 550-750C can be achieved for a zinc ferrite sorbent with simulated Lurgi fixed-bed gasifier off-gas. To date this zinc ferrite of METC has been advanced to the highest stage of development, pilot plant, of any sorbent.

However, investigations by Battelle, IGT, MIT, Giner, Research Triangle and Electrochem, largely under DOE funding, continue to evaluate promising alternatives for high temperature regenerable desulfurization of coal gases. Work at Battelle (18) has been conducted with molten carbonates supported on Ca-Li aluminate. Dual adsorbent beds with mixed oxides of ZnO, Fe_2O_3 , CuO in

one bed and CoTiO₃ in a second bed have been evaluated at ICT (19). Work with oxides of Cu and Zn has been done at Giner (20) and work with oxides of Cu and Mn pursued at Electrochem (21). A number of mixed oxides of ZnO, CuO, TiO₂, and MoO₃, notably co-precipitated with alumina have been investigated at MIT (22). Additional studies with mixed oxides of ZnO/CuO/Fe₂O₃; ZnO/TiO₂; CuO/Fe₂O₃/Al₂O₃ and CuO/Al₂O₃ have been conducted by the Research Triangle (23).

SELECTION OF ADSORBENT COMPONENTS

Iron and zinc were selected as the desulfurization agents for evaluation based on consideration of the results of prior work and the prospects for favorable sulfidation kinetics, low equilibrium sulfur concentration at high temperature and good oxidation regeneration kinetics. Most prior desulfurization work has been conducted and continues with co-precipitated metal oxides. In this study a zeolite support was chosen to provide a hydrothermally stable substrate favorable for maintenance of a highly dispersed desulfurization agent for many sulfidation/oxidation duty cycles. A synthetic mordenite (Zeolon 900) was initially evaluated but the availability of rare-earth stabilized faujasite Y zeolite (Linde SK 500) led to making it the support of choice.

EXPERIMENTAL PROCEDURES

The metals of interest Fe and Zn were ion exchanged with the zeolite pellets by equilibration at 25-60C with 3 Molar aq. solutions of nitrate salts of the metals. Ion exchanged zeolites were separated from the exchange solutions, dried at 150C and air calcined at 500C. The properties of the sorbents are given in Table 1.

The desulfurization performance tests were conducted in a stainless steel fixed bed reactor with 2-12 gr. of adsorbent (20-40 mesh). Corrosion resistant alloys must be used if the reactor is to have bare metal walls to avoid wall effects. The safest practice is to use a quartz liner in the reaction zone. Gas compositions consisted of dry and wet (10-20 Mol % H₂O) H₂ with 200-8000 ppm H₂S. Reaction conditions consisted of 1-2 atmos. gas pressure, a 450-650C temperature range and a space velocity range of 500-10000 hr⁻¹. Tests were conducted to breakthrough concentrations of 20 ppm H₂S. Sulfur concentration in the exit gas was determined with Kitagawa tubes and at intervals of 30-60 min. by absorption in CdSO₄ aq. solution and thiosulfate titration.

The sulfided adsorbents were regenerated with air or simulated fuel cell exhaust gas (11 Mol % O₂) at 450-650C with periodic measurement of SO₂ in the exit gas by Kitagawa tube and absorption in aq. NaOH.

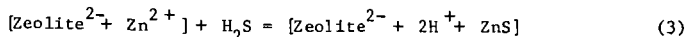
Post test adsorbents were characterized by sulfur analysis and for selected systems metal analysis, X-Ray diffraction analysis and BET surface area determinations.

REACTION MECHANISMS

The sulfidation reactions postulated for the supported metals as separate interstitial entities with H₂S at temperature in the range 450-650C in a reducing atmosphere are assumed to be:



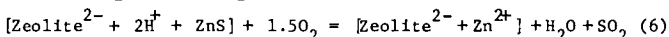
The mechanism proposed for the exchanged cations is that they are present predominantly as integral components of the zeolite lattice surface so that the sulfidation reaction can be visualized:



Limited thermal stability precludes sulfide stoichiometries with sulfur to metal ratios higher than indicated in reactions (1)-(3).

Reactions (1)-(2) would lead to significant inhibition of sulfidation by an appreciable water partial pressure. Since coal gases will contain 10-20 Mole % H₂O depending upon whether the gas is air or O₂ blown this is an important consideration. While the water partial pressure of 10 Mole % might raise the H₂S equilibrium concentration from 1-2 to 10 ppm at 650C there would be an advantage in minimizing the volatility of Zn.

The oxidation regeneration reactions for the sulfided metals are considered to be:



The expectation is that at the elevated temperature of oxidation most of the sulfur will be evolved as SO₂/SO₃ with minimal sulfate formation if extended exposure to excess oxygen is avoided. The decomposition temperatures of the sulfates, if formed, are relatively high being 500-630C for FeSO₄ and 600-840C for ZnSO₄ (24).

DESULFURIZATION PERFORMANCE

In Table 2 a comparison is made for 4 adsorbents, Fe and Zn mordenite, a Zn impregnated alumina and a rare earth loaded Zn faujasite Y. After 5 sulfidation/regeneration duty cycles at 540C the Zn faujasite Y demonstrated a decided advantage in sulfur loading at breakthrough at 20 ppm with a H₂S concentration less than 10 ppm prior to breakthrough combined with maintenance of a high BET area of 360 M²/Gr. Typical results with wet (15 Mole %) H₂ with 1000 ppm H₂S at 500C over Zn faujasite Y (Fig. 1) show sustained performance for 4 duty cycles with less than 10 ppm H₂S.

If the objective is to obtain a low sulfur concentration prior to breakthrough Zn zeolite is decidedly superior to Fe zeolite (Fig. 2). For this test with a sulfur concentration of 7900 ppm, typical of coal gas, for wet (10 Mole %) H₂ residual sulfur concentrations before breakthrough appreciably less than equilibrium H₂S values are obtained for either Fe or Zn.

The role of the rare earths present on the SK 500 faujasite Y used as support for the Fe and Zn in the desulfurization process has not been determined but published results (25,26) indicate La has potential as a sulfidation adsorbent but would require a temperature above 650C for oxidation regeneration. The present study indicates the rare earths play a minor role in sulfidation but a major role in contributing to thermal stability. Zinc has been proposed (27) for improving the thermal stability of zeolites.

OXIDATION REGENERATION

Oxidation-regeneration at 650C of sulfided Fe and Zn faujasite Y adsorbents with simulated fuel cell exhaust gas (11 Mole % O₂) is essentially complete within 60 minutes (Fig. 3). The extent of residual sulfur retention after regeneration is shown in Table 2.

To complete thermal decomposition of residual ZnSO₄ a temperature approaching 800C is necessary for a gas with less than about 15 Mole % O₂. By using a N₂ purge between completion of the oxidation-regeneration cycle and the next fuel gas desulfurization cycle combined with utilization of the exothermic heat from the oxidation reaction permits completion of regeneration of the adsorbent at a temperature between 800C and 650C the temperature desired in the bed for the next desulfurization cycle.

The thermal stability of the Zn faujasite Y is promising in view of the high BET surface area observed for the regenerated adsorbent (Table 2). An

important consideration is that the Zn zeolite should not experience temperatures much above 650C in a reducing atmosphere to minimize losses by volatilization. In the interval between oxidation-regeneration and the next desulfurization cycle the adsorbent exposure to temperatures above 650C is in an oxidized state minimizing volatilization.

CONCLUSIONS

Bench scale evaluations have demonstrated the performance of metal zeolites for high temperature regenerable desulfurization of fossil fuels containing H₂S. Metal zeolites, notably with zinc, provide regenerable sulfur removal capability and achieve low residual sulfur concentrations and a good potential for repetitive sulfidation/oxidation duty cycles. Zinc faujasite Y, in particular, provides a superior desulfurization agent with the active metal in a high state of dispersion on a hydrothermally stable support. Alternation of sulfidation and oxidation typical of desulfurization-regeneration duty cycles favors maintenance of the initial high state of dispersion for the active desulfurization agent, Fe or Zn, notably if the metal is retained in close proximity to the surface of the zeolite lattice.

Potential applications for these metal zeolite desulfurization agents consists of:

1) Providing sulfur removal for low to intermediate BTU coal gases for combined cycle power plants to minimize sulfur emissions and the protection of gas turbine or fuel cell power plants.

2) Protecting sulfur sensitive catalysts used for processing fossil fuels, notable coal syngas.

REFERENCES

1. Jones, C.H. and Donohue, J.M., Stone and Webster Eng. Corp., New York EPRI-AF-416, 151 (1977).
2. Robson, F.L. and Blecher, W.A., United Technologies Corp., Hartford, DOE/METC 12050-149 (1981).
3. Westmoreland, P.R. and Harrison, D.P., Environ. Sci. & Tech. 10, 659 (1976).
4. Jalan, V., Conf. Proceed. 1981 Int. Gas Res., Los Angeles, CA., 291 (1981).
5. Onursal, A.B., Hot Gas Cleanup Process, EPS-600-7-79-169, (1979).
6. Reeve, L., J. Inst. of Fuel, Vol. 319 (1958).
7. Bureau, A.C. and Olden, J.J.F., The Chemical Engineer, (1967).
8. Shultz, F.G. and Berber, J.S., J. Air Pollution Control Assoc., 20,93 (1970).
9. Oldaker E.C., etal, Removal of Hydrogen Sulfide from Hot Low BTU Gas with Iron Oxide-Fly Ash Sorbents, MERC/TPR-75-1, (1975).
10. Jalan, V., Brooks, C.S., Georgakis, C. and Desai, M., Metal Oxide Adsorbents for Hydrogen Sulfide Control, Second Annual Contractors Meeting on Contaminant Control in Hot Coal Gas, Proceedings, 350, NTIS, DOE/METC-82-47, (1982).
11. Jalan, V., Studies Involving High Temperature Desulfurization/Regeneration Reactions of Metal Oxides for Fuel Cell Development, Giner Inc. NTIS, DOE/METC/16021-1486 (1983).
12. Steinfield G. and Grindley, T., Development and Testing of Regenerable

- Hot Coal Gas Desulfurization Sorbents, 332, ref. 10.
13. Agarwal, J.C., Metal Oxide Hot Gas Desulfurization Process, AIChE Conf. Philadelphia, PA, (1980).
 14. Huff, W.J. and Logan, L., AGA Proceed., 18, 359 (1965).
 15. Nachod, F.C., U.S. Patent 2,442,982, (1948).
 16. Lewis, W.K., U.S. Patent 3,079,223, (1963).
 17. Meyer, J.P. and Edwards, M.S., ORNL Rept. TM-6072, (1978).
 18. Lyke, S.E. and Sealock, L.J. (Battelle Pacific NW Labs) Proceed. 3rd Annual Contaminant Control in Hot Coal Derived Gas Streams, Merkel, K.E., Ed., DOE/METC 84-6, NTIS DE84000216,173 (1983).
 19. Anderson, G.L., (IGT), Annual Gasification and Gas Stream Cleanup Systems Contractors Review Meeting, Vol. 2, Chate, M.R., Markel, K.E., Jarr, L.A. and Bossart, S.J., Eds. Morgantown, W.VA, DOE/METC87/6079-DE87006496, 642 (1987).
 20. Jalan, V., Studies Involving High Temperature Desulfurization/Regeneration Reactions of Metal Oxides for Fuel Cells, (Giner Inc.) DOE Rpts. 31-109-39-5804, ANL-K-83-12 and NTIS DE3008714 and DE83008715 (1981).
 21. Jalan, V., 9th Annual Gasification and Gas Stream Cleanup Systems Contractors Review Meeting, METC, Morgantown, W.VA B4, (1989).
 22. Flytzani-Stephanopoulos, M., See ref. 19, 726 (1987).
 23. Harkins, S.M. and Gangwal, S.K., (Research Triangle), see ref. 19, 749 (1987).
 24. Mu, J. and Perlmutter, D.D., Ind. Eng. Chem. Process Des. & Dev., 20, 640 (1981).
 25. Wheelock, K.S. and Aldridge, C.L., U.S. Patent 3,974,256, (1976).
 26. Wheelock, K.S. and Say, R.S., U.S. Patent 4,002,720, (1977).
 27. Wilson, R.C., U.S. Patent 3,804,780, (1974).

Table 1. Sulfur Removal Capacity for Zinc Zeolites

Zeolite	Cation Exchange Capacity CEC MEQ/Gr.	Metal Loading Equiv. to CEC Wt. %	Theoretical Sulfur Loading as ZnS Wt. %	High Temp. Stability Deg. C.
Syn. Mordenite	2.5	8.2	4.0	650
Faujasite Y	4.0	13.2	6.4	650-980

Table 2. A Comparison of Desulfurization Adsorbents

Adsorbent	Metal	Wt. %	Sulfur Loading Wt. %	Percentage of Theoretical Sulfur Loading	Residual Sulfur Wt. %	BET Area Sq.M./Gr.
Faujasite Y (Linde SK 500)	Zn	13.2	4.8	75	1.41	360
ZnO on Alumina (Harshaw AL-0104T)	Zn	11.7	2.4	-	0.71	119
Syn.Mordenite (Norton Zeolon 900)	Zn	10.9	2.4	60	0.51	129
Syn. Mordenite (Norton Zeolon 900)	Fe	14.0	3.7	-	0.33	-

Notes:

- 1) Five tests were conducted with 10.3 cu.cm. of adsorbent bed with 1000 ppm H_2S in H_2 at 540C and at 2 Atmos. in the space velocity (GHSV) range 4000-9000 hr^{-1} to a breakthrough of 20 ppm H_2S .
- 2) Oxidation regenerations were conducted with simulated fuel cell cathode exhaust gas with 11% O_2 , 7% CO_2 and 72% N_2 .
- 3) Water partial pressure was 15 Mole % for desulfurization and regeneration.
- 4) ZnO was mounted on alumina by solution impregnation.

Fig.1 SULFUR REMOVAL FROM WET (15 MOLE PERCENT H_2O) HYDROGEN WITH 1000 PPMV H_2S OVER SUPPORTED ZINC FAUJASITE Y AT 500° C

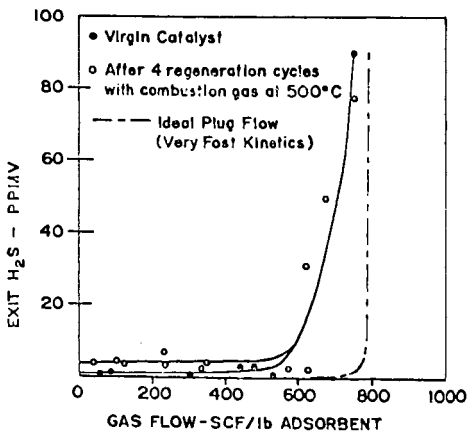


Fig.2 SULFUR REMOVAL FROM WET
 (10 MOLE PERCENT H₂O) HYDROGEN
 WITH H₂S (7900 PPMV) AT 650°C
 1500 HR⁻¹ SPACE VELOCITY

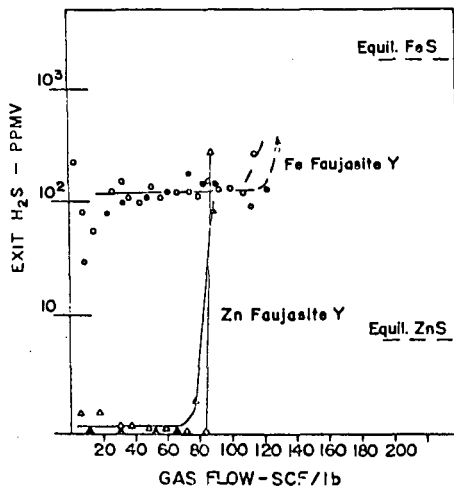
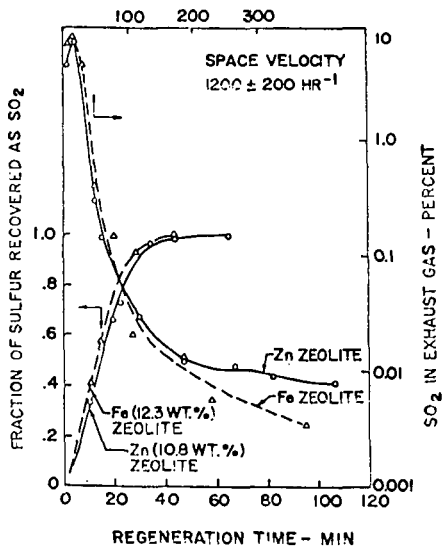


Fig.3 AIR REGENERATION AT 650°C OF
 SULFIDED IRON AND ZINC FAUJASITE Y



ENHANCED DURABILITY OF HIGH-TEMPERATURE DESULFURIZATION SORBENTS FOR MOVING-BED APPLICATIONS

R.E. Ayala¹, E. Gal², S.K. Gangwal³, and S. Jain⁴

¹GE Corporate Research and Development, Schenectady, New York 12301.

²GE Environmental Systems, Lebanon, Pennsylvania, 17042.

³Research Triangle Institute, Research Triangle Park, North Carolina 27709.

⁴U.S. Dept. of Energy, METC, Morgantown, West Virginia 26505.

Keywords: coal gas cleanup, high-temperature desulfurization, zinc ferrite.

1. - INTRODUCTION

Sulfur removal will be mandatory for all power generation coal gas applications in order to comply with future environmental standards. Two promising technologies that are currently being optimized for coal-based power generation are the integrated gasification combined cycle (IGCC) and the gasifier/molten carbonate fuel cell (MCFC) systems. Methods to remove hydrogen sulfide from the product gas at elevated temperatures will provide the highest possible thermal efficiency for these systems. A high-temperature desulfurization system also eliminates the need for costly heat exchanger systems to cool coal-derived gas to the required by low-temperature scrubbing processes, reheating of the clean coal-derived gases before they are injected into a combustor/turbine component, and treatment of the condensate formed during gas cooling.

A major part of the research on high-temperature desulfurization of coal-derived gases has been directed to the use of mixed-metal oxide sorbents, such as zinc ferrite, because of their ability to capture a large fraction of sulfur species in the coal gas and to be regenerated in multiple cycles of absorption and regeneration. However, quantitative evaluations of their performance during multicycle operation have shown that a gradual physical and chemical deterioration of the sorbent takes place. The sorbent's mechanical strength and its chemical reactivity for sulfur capture are strongly affected by the gasifier operating conditions.

Zinc ferrite is currently the leading candidate to serve as a sulfur removal agent in the IGCC systems. It has been demonstrated that this material can remove hydrogen sulfide from a reducing gas to levels of 10 ppmv or less at reasonable rates of reaction. GE has developed a patented moving-bed coal gas desulfurization system that has been shown to achieve a reduction in complexity and cost in a simplified IGCC system relative to conventional IGCC configurations (Cook et al., 1988). In moving-bed systems with long-term cyclic operation, the movement of pelletized sorbent requires that the sorbent have a higher degree of attrition resistance than in fixed-bed operations. In moving-bed and fixed-bed systems, chemical reactivity and physical strength of the sorbent are both important. For a constant sorbent quality, these two properties tend to vary inversely.

The moving-bed configuration offers many advantages over the fixed-bed cleanup system by minimizing sulfate formation during regeneration, minimizing accumulation of fines during sulfidation, utilization of full sorbent capacity, provision of continuous steady-state operation, and production of a high concentration sulfur dioxide tail gas stream. In this paper, results of new zinc ferrite formulations having enhanced mechanical strength over the Baseline formulation for the moving-bed application will be discussed.

2. - EXPERIMENTAL PROCEDURE

2.1 - Materials

The objective of sorbent preparation is to fabricate various zinc ferrite formulations with enhanced chemical and mechanical properties relative to the DOE-selected Baseline formulation, known as T-2465. This Baseline formulation is a cylindrical extrudate that contains 2% bentonite binder.

Several zinc ferrite formulations were prepared by United Catalysts, Inc. (UCI) and their properties are presented in Table 1. All formulations were fabricated as ellipsoidal, or "rounded" pellets with an average 0.64 cm major axis and aspect ratio between 1.1 and 1.3. Fabrication parameters selected for this study were: iron oxide type (catalyst and pigment grade), binder type (bentonite, calcium aluminate, Portland cement, titanium dioxide), binder content (up to 17% total binder), and calcination temperature (1550 and 1750 °F). The same composition of T-2465 was fabricated as a rounded pellet and labeled L-3404 in Table 1. T-2465M is a formulation fabricated as a 20,000 lb. batch following a double rounding procedure to densify the material even further.

Several guidelines were followed to assess sorbent performance and identify superior formulations for moving-bed systems. Among the guidelines, a formulation had to meet:

- Mechanical strength requirements:
 - Crush strength greater than 20 lb/pellet for the fresh material.
 - Attrition resistance greater than that of the DOE-selected Baseline formulation (ASTM procedure D4058-81) as a fresh material.
 - Attrition resistance greater than 94% (ASTM procedure D4058-81) at high temperatures (e.g., 1000 °F) as a fresh material.
- Single-pellet chemical reactivity requirements:
 - TGA fractional conversion greater than 0.5 (i.e., 50% conversion) in 2 hrs. at standard conditions (1022 °F, 1 atm., 3% H₂S).
 - TGA conversion greater than 70% of theoretical for fresh zinc ferrite.
- Pellet physical morphology requirements:
 - Specific pore volume in the range 0.2 to 0.3 cm³/g.
 - Mean pore diameter greater than 1000 Å.

Only three of the formulations that met these minimum requirements were selected for bench-scale reactor testing.

2.2 - Physical /Mechanical Characterization

The pore volume distributions of selected fresh and used sorbents were measured by a mercury porosimeter (Micromeritics Model 9220) with a mercury penetration capability of 60,000 psia. A number of measurements including pore volume, mean pore diameter (diameter at 50% intrusion), pellet density, and cumulative and differential pore volume distributions were made.

Formulations fabricated by UCI were tested for crush strength (i.e., dead weight load) and for attrition resistance at ambient temperature and at 1000 °F. Attrition resistance is defined as 100% minus attrition rate according to ASTM method D4058-81.

2.3 - Chemical Characterization

A thermogravimetric analyzer (Cahn 1000) capable of continuously measuring sorbent weight changes with an accuracy of 10 µg in reactive (or inert) gas environments as a function of temperature and time, was used to measure the chemical reactivity of the sorbents. The equipment and zinc ferrite reaction chemistry (which can be used to predict maximum weight changes) is described elsewhere (Wood et al., 1989). Typically, a 1.5-cycle reactivity test was conducted consisting of two sulfidations at 550 °C with an interim regeneration at 675 °C. Prior to each sulfidation, a 30-minute reduction was conducted at 550 °C. The gas compositions used for reduction, sulfidation, and regeneration are shown in Table 2. The sulfiding gas was typical of the GE air-blown fixed-bed gasifier except for H₂S. The abnormally high level

of H₂S, as opposed to a normal 0.5% in the sulfiding gas, was to enable a 1.5-cycle test to be performed in a normal 8-hour day.

Formulations meeting the minimum requirements described in Section 2.1 were tested in a packed-bed, bench-scale reactor unit. A schematic diagram of the bench-scale reactor unit is presented in Figure 1. The bench-unit consists of three main parts: gas-handling system, reactor system, and gas-analysis instrumentation. Compressed gases from cylinders were mixed in the gas-mixing manifold to simulate compositions typical of an air-blown, fixed-bed gasifier gas and the regeneration gases of a moving-bed, hot gas cleanup system. Three reactor vessels were operated in parallel at a space velocity of 2000 hr⁻¹ each. In this way, three different formulations could be tested under identical conditions of flow rate and gas composition. The three sorbent formulations selected for testing in the reactor system were: T-2465M, L-3407, and L-3404 (the Baseline sorbent). Each reactor vessel had a 2.5 in. (6.35 cm.) internal diameter and a sorbent bed 8 in. (20.3 cm.) long.

Sulfidation was carried out at 1000 °F (538 °C) with an artificially high H₂S concentration (1% v/v), to accelerate the testing over 10 cycles. Gas composition was the same as that in the sulfiding gas in Table 2, except for the H₂S and N₂ concentrations. The reaction was stopped when the effluent H₂S concentration, or breakthrough concentration, reached 200 ppmv. Regeneration was carried out at 1000 °F first using 1 to 4% oxygen from air (balance nitrogen), while maintaining the maximum bed temperature below 1250 °F, until oxygen breakthrough was approximately equal to the inlet concentration, and then the gas mixture switched to pure air with the temperature gradually increased to 1400 °F (760 °C) to promote thermal decomposition of sulfate. This procedure was intended to mimic the moving bed regeneration process conditions.

3. - RESULTS

3.1 - TGA

Sorbents L-3404 (1550 °F), L-3406 (1550 °F), L-3407 (1550 °F, 1750 °F), L-3409 (1550 °F), T-2465M (1550 °F), and L-3467B (1750 °F) were selected for chemical reactivity screening by TGA. The choice was somewhat arbitrary because of similarity of the various properties and because all sorbents met the required pore volume and mean pore diameter criteria. First cycle sulfidation capacities (as a fraction of maximum theoretical capacities) after 2 hours of sulfidation are compared for these sorbents in Table 3. For all sorbents we have assumed bentonite to be inert, ZnO to convert to ZnS via $ZnO + H_2S \rightarrow ZnS + H_2O$, Fe₂O₃ to convert to FeS via $Fe_2O_3 + 2H_2S + H_2 \rightarrow 2FeS + 3H_2O$ and CaAl₂O₄ to convert to CaS via $CaAl_2O_4 + H_2S \rightarrow CaS + Al_2O_3 + H_2O$. These reactions were used to obtain the maximum potential weight gain while fractional conversion over 2 hours was calculated by dividing the actual weight gain by the maximum potential weight gain.

All sorbents met the criteria for 70% conversion over unlimited time (defined as 8 hours maximum). However, the sorbents L-3409 and L-3467B failed to meet the 50% utilization criteria over 2 hours. Among the other sorbents, L-3406 with the pigment grade iron oxide was good in attrition resistance but was relatively unreactive. This sorbent, although not selected initially for bench-scale testing, may be used at a later date. L-3404 and its denser twin T-2465M were selected based on TGA studies. Among the L-3407 formulations, the significantly higher reactivity of the 1750 °F sorbent cannot be explained readily. In any event, since the attrition properties of the two L-3407 sorbents were not significantly different, L-3407 (1750 °F) was recommended for further bench-scale testing.

3.2 - Mechanical Characterization

Crush strength, attrition resistance, and mercury porosimetry measurements were conducted on fresh sorbents, on samples tested on the TGA, and on samples extracted from the bench-scale unit after multiple absorption-regeneration cycles.

The results of crush strength and attrition resistance of fresh sorbents at ambient temperature and at 1000 °F are given in Table 1 and in Figure 2. Several sorbents in Table 1 exhibited low and nearly equivalent

(ranging from 94.0 to 96.0%) attrition resistance. The baseline formulation L-3404 exhibited a lower attrition resistance of 91% whereas T-2465M, prepared using the same chemical composition as L-3404 but in a different pilot-scale equipment, exhibited a higher attrition resistance of 95.4%. The difference is believed to be caused by the lower pore volume (or higher density) of T-2465M, which may be attributable to the scale of equipment and/or repeatability of formulation procedures. Attrition resistance at 1000 °F is slightly higher compared to ambient conditions for all cases studied, a favorable result for the intended moving-bed process. Three formulations were selected for bench-scale testing: L-3407, T-2465M, and L-3404. This selection was based mainly on the high attrition resistance exhibited by these three formulations.

Mercury porosimetry results for fresh sorbents and for those extracted from the TGA following 1.5 cycles are presented in Table 4. Only a few results are presented here for the sorbents selected for the bench unit. The pore volume of the sorbents correlated with fractional sulfidation. Pore volume of sulfided sorbent decreased and that of regenerated sorbent following sulfidation increased as shown in Table 4. The lower restoration of pore volume of regenerated L-3407 versus L-3404 is attributed to incomplete regeneration of the calcium aluminate binder.

The same mechanical characterization methods were conducted on samples extracted from the bench-scale unit after ten cycles of absorption and nine cycles of regeneration (i.e., sulfided sorbent), and after ten cycles of absorption and ten cycles of regeneration (i.e., regenerated sorbent). The tenth regeneration was concluded with the usual oxidative regeneration temperature increase up to approximately 1400 °F. Samples were taken from three locations in the reactor bed: gas inlet, midsection, and gas outlet as shown in Table 5. In contrast to the TGA results, there appeared to be no correlation of the pore volume of the sulfided and regenerated L-3407 sorbent and the degree of fractional sulfidation. The reasons for this are believed to be the extensive thermal cycling of the sorbent in the bench-scale unit, incomplete regeneration of calcium aluminate binder in the sorbent, and residual sulfate in the sorbent (as confirmed by TGA test of the regenerated sorbent). The pore volumes and mean pore diameters in Table 5 are quite good and suggest no pore plugging.

Attrition resistance and crush strength of the corresponding L-3407 samples extracted from the bench-scale reactor unit are also included in Table 5. In both cases crush strength of sulfided and oxidatively regenerated samples is similar to that of the fresh material. However, the attrition resistance decreased significantly from 96% for the fresh sorbent to 65-85% for the cycled sorbents. The sorbent in the gas inlet side, where the sorbent was exposed to the H₂S environment for a longer period, was weaker than the sorbent in the gas outlet side.

3.3 – Bench-scale Reactor System

Breakthrough H₂S concentrations are presented in Figure 3 for the three selected sorbent formulations. H₂S concentrations prior to breakthrough were measured in the range of 5 to 15 ppmv, depending on formulation, and were near equilibrium values for H₂S at the test conditions.

According to the unreacted-core model for chemical reactivity in porous media, a sorbent having a lower mean pore diameter should exhibit a higher diffusional resistance for gas reactants and a lower reactivity. As expected, the time required for the 200 ppmv breakthrough to occur was inversely related to the amount of binder present and the mean pore diameter (MPD) of the three sorbents tested following the trend:

L-3407	< T-2465M	< L-3404
(15% binder, 2126 Å MPD)	(2% binder, 2197 Å MPD)	(2% binder, 2648 Å MPD)

The large difference in reactivity between L-3407 and the other two sorbents is a result of both its higher binder content and its lower mean pore diameter. The difference in reactivity between the T-2465M and

L-3404, both containing 2% binder, is a result of differences in mean pore diameter, with T-2465M exhibiting a lower value. It is evident that the mean pore diameter, closely describing the pore volume distribution, is an important parameter for the prediction of bed reactivity when differences in other sorbent properties are not significant.

As shown in the upper x-axis scale of Figure 3, the dimensionless time provides a measure of the overall sorbent bed utilization (in terms of sulfur capture) relative to that at the calculated bed saturation time (from H₂S flow rate and mass of zinc ferrite in the bed). At the 200 ppmv H₂S breakthrough time, bed utilization between 5%-11% for L-3407 and between 20%-28% for T-2465M can be calculated. The sorbent utilization for the formulations tested is expected to be higher for commercial systems where much larger reactor beds are employed and the smaller ratio of pellet diameter to reactor diameter minimizes potential gas bypassing or channeling.

Zinc ferrite sorbents with higher bed utilization, typically 40%, have been manufactured in the past but at the expense of being weaker or softer and, hence, less suitable for long-term operation in moving-bed systems. L-3404, the Baseline formulation, has the same chemical composition of previous DOE-tested sorbents, differing in the fabrication procedure (rounding versus cylindrical extrusion).

4. - CONCLUSIONS

Based on the proposed program screening procedure, three formulations, L-3407, T-2465M, and L-3404 were selected as potential candidates for bench-scale testing and determination of enhanced formulations suitable for moving-bed applications. All formulations tested met the criteria for 70% conversion over unlimited time and suitable pellet morphology (i.e., pore volume and mean pore diameter). However, several formulations failed the criteria for 50% conversion in 2 hrs., attrition resistance, and crush strength. Pore volumes measured by mercury porosimetry correlated well with degree of sulfidation for fresh samples in TGA tests but not for cycled samples extracted from the bench-scale unit. It is speculated that the discrepancy is due to extensive thermal cycling, incomplete regeneration of calcium aluminate binder, and residual sulfate in the sorbent. Attrition resistance was somewhat higher for all fresh formulations at 1000 °F than at ambient temperature.

Bench-scale tests showed that prebreakthrough H₂S concentrations in the effluent gas are low enough for use of the sorbents in high-temperature desulfurization of coal gas, with differences in breakthrough times explained by differences in binder content and mean pore diameter of the materials. Sorbent bed capacities were below 30% of theoretical at the 200 ppmv breakthrough level and were lower than those measured in the past for weaker formulations. A significant decrease in attrition resistance was measured in the L-3407 sorbent, from 96 to 65%, while the observed crush strength was similar to that of fresh material after 10 cycles of bench-scale testing. Thus far, the three rounded formulations (L-3407, T-2465M, and L-3404) tested in the bench-scale unit appear promising for future moving-bed applications. All three rounded formulations have shown enhanced mechanical properties over the DOE-selected T-2465 Baseline formulation while maintaining adequate chemical reactivity for the moving-bed system.

5. - REFERENCES

Cook, C.S., Gal, E., Furman, A.H., and Ayala, R.E., "Integrated Operation of a Pressurized Fixed-Bed Gasifier and Hot Gas Desulfurization System," Proceedings, *Eight Annual Gasification and Gas Stream Cleanup Systems Contractor's Meeting*, DOE/METC-88/6092, p. 11-20.

Woods, M.C., Leese, K.E., Gangwal, S.K., Harrison, D.P., and Jothimurugesan, K., "Reaction Kinetics and Simulation Models for Novel High-Temperature Desulfurization Sorbents," DOE/MC/24160-2671 (DE89000950), February 1989.

Table 1 - Properties of Zinc Ferrite Formulations*

Formul.	Oxide Content (%)	Binder Content (%)	Calcination Temp. (°F)	Density (lb/ft ³)	Crush Strength (lb/pellet)	Attrition Resistance (%)	Poro Vol. (cm ³ /g)	Mean Pore Diam. (Å)
L-3404	33.1 ZnO	2.0 Bentonite	1550	85.0	21	91.0	0.25	2185
	64.9 UCI Fe ₂ O ₃		1750	89.5	21	90.0	0.25	3040
L-3405	32.1 ZnO	5.0 Bentonite	1550	86.0	16	94.0	0.25	2060
	62.9 UCI Fe ₂ O ₃		1750	85.0	18.5	94.5	0.20	2330
L-3406	33.1 ZnO	2.0 Bentonite	1550	88.0	28.5	96.0	0.19	2190
	64.9 Mobay Fe ₂ O ₃		1750	90.5	27.0	95.5	0.24	2330
L-3407	28.7 ZnO	3.0 Bentonite	1550	86.5	29.0	95.0	0.24	1095
	56.3 UCI Fe ₂ O ₃		1750	86.5	20.0	96.0	0.31	3180
L-3407A	28.7 ZnO	3.0 Bentonite	1550	76.0	17.0	93.0	0.3	2185
	56.3 UCI Fe ₂ O ₃		1750	75.0	19.0	95.0	0.25	3180
L-3408	28.7 ZnO	3.0 Bentonite	1550	74.2	19.5	88.0	0.25	3180
	56.3 UCI Fe ₂ O ₃		1750	78.4	14.0	91.0	0.31	3040
L-3409	27.0 ZnO	3.0 Bentonite	1550	90.5	42	92.0	0.23	1165
	53.0 UCI Fe ₂ O ₃		1750	85.5	48	92.0	0.19	1630
L-3467A	28.7 ZnO	2.0 Bentonite	1750	90.0	35	88.0	0.20	2500
	54.9 UCI Fe ₂ O ₃							
L-3467B	28.7 ZnO	2.0 Bentonite	1750	75.0	30	90.0	0.32	3180
	54.9 UCI Fe ₂ O ₃							
T-2465M	34.7 ZnO	2.0 Bentonite	1550	89.6	22.5	95.4	0.20	1958
	64.0 UCI Fe ₂ O ₃							

* As provided by the manufacturer United Catalysts, Inc.

Table 2 - Gas Compositions (Volume %) for TGA tests

	Reducing Gas	Sulfiding Gas	Regeneration Gas
H ₂	15.0	15.0	-
CO	8.0	8.0	-
CO ₂	11.0	11.0	-
H ₂ S	-	3.0	-
H ₂ O	30.0	30.0	-
N ₂	36.0	33.0	96.0
O ₂	-	-	4.0

Table 3 - Comparison of Sorbent TGA Reactivity

Sorbent	Maximum Sulfur Capacity (lbs/100 lbs)	Fractional Conversion after 2-hour Sulfidation
L-3404 (1550 °F)	39.1	0.71
L-3406 (1550 °F)	39.1	0.57
L-3407 (1550 °F)	36.4	0.60
L-3407 (1750 °F)	36.4	0.77
L-3409 (1550 °F)	35.0	0.45
L-3467B (1750 °F)	36.2	0.49
T-2465M (1550 °F)	39.1	0.61

Sorbent	Fresh		Sulfided		Oxidatively Regenerated	
	Pore Volume (cc/g)	Pore Volume (cc/g)	% Sulfidation (-)	Pore Volume (cc/g)	Pore Volume (cc/g)	Pore Volume (cc/g)
L-3404 (1550 °F)	0.25	0.13	81.4	0.24	0.24	0.24
L-3407 (1750 °F)	0.25	0.14	97.4	0.20	0.20	0.20
T-2465M (1550 °F)	0.20	0.11	100	NA	NA	NA

Sample	Pore Volume (cc/g)	Mean Pore Diameter (Å)	Crush Strength (lb/pellet)	Attrition Resistance Ambient Temp. (%)
Sulfided:				
Gas Inlet	0.2173	2283	16.00	70.83
Midsection	0.2176	2004	24.93	78.25
Gas outlet	0.2130	2416	22.93	85.30
Regenerated:				
Gas Inlet	0.2107	2221	18.63	65.02
Midsection	0.2036	1795	22.17	70.04
Gas Outlet	0.2318	2440	24.87	73.43
Fresh	0.25	2126	20.0	96.0

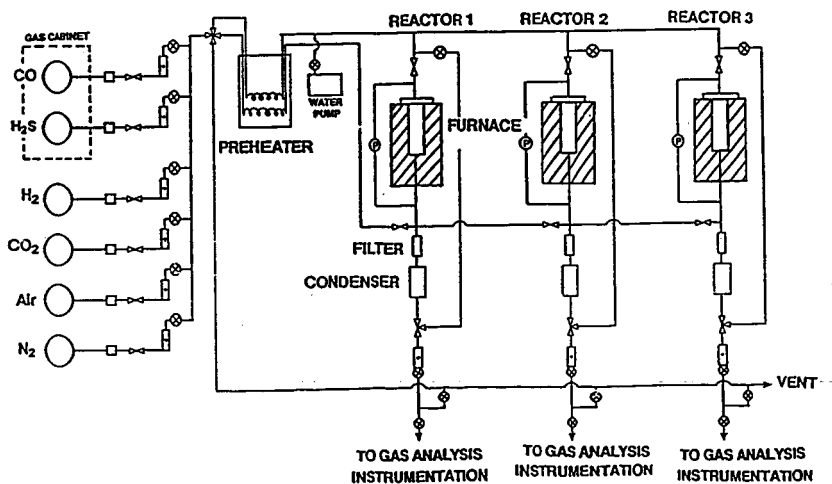


Figure 1. - Schematic Diagram of the Bench-Scale Reactor Unit

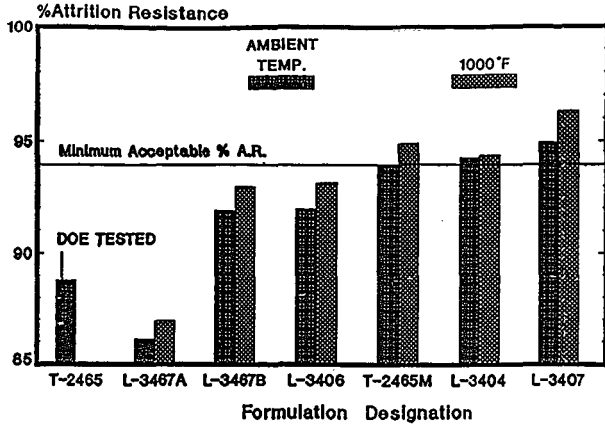


Figure 2. - Attrition Resistance Tests at 1000 °F and Ambient Temperature

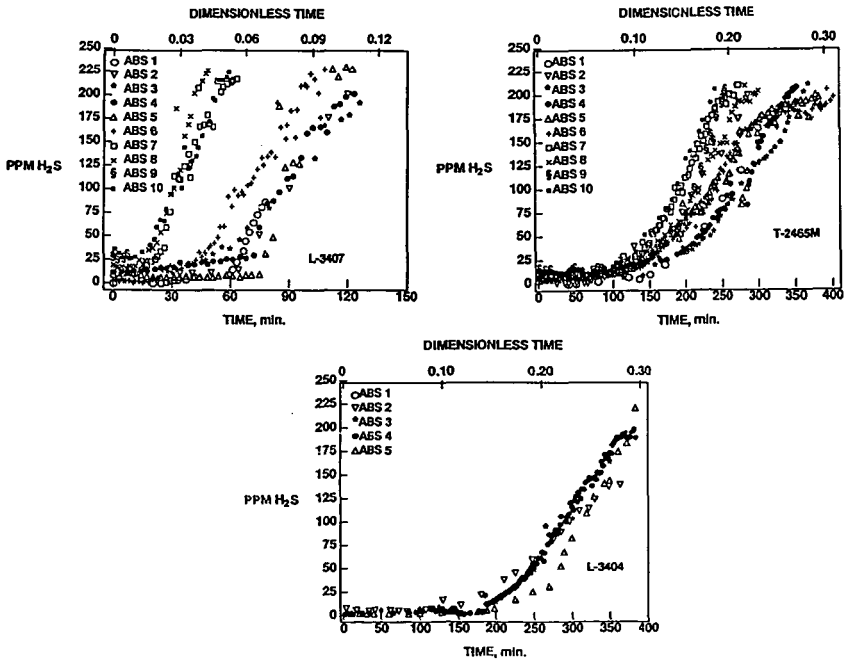


Figure 3. - Breakthrough curves for L-3407, T-2465M, and L-3404

REACTIVE ABSORPTION OF H₂S BY A SOLUTION OF SO₂ IN POLYGLYCOL ETHER

R. Marshall Hix and Scott Lynn
Dept. of Chemical Engineering
University of California
Berkeley, CA 94720

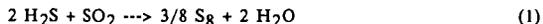
Keywords: Absorption with Reaction, Mass Transfer with Reaction, Plate Efficiency

INTRODUCTION

When coal is gasified, most of the total sulfur content is converted to hydrogen sulfide (H₂S) or, to a lesser extent, carbonyl sulfide (COS). The H₂S concentration in the coal gas depends on the amount of sulfur initially present in the coal and on the nature of the coal-gasification process used. Gas-phase concentrations are typically several thousand ppm H₂S. Because of environmental restrictions and process requirements, H₂S must be removed from coal-derived gas streams.

The required degree of H₂S removal depends on use of the gas. In some cases, selective absorption of H₂S is desirable. In other cases, co-absorption of CO₂ and light hydrocarbons allows these components to be recovered as separate products. To meet this wide range of processing requirements, the U. C. Berkeley Sulfur Recovery Process (UCBSRP) is being developed as a less-costly alternative to conventional sulfur-recovery technology [1]. The reactive absorption of H₂S by a polyglycol ether solution of SO₂ is but one step in this process.

The UCBSRP (Figure 1) consists of six basic steps. First, H₂S is absorbed in the primary absorber by a polyglycol ether (Diethylene glycol methyl ether or DGM). Second, by mixing the H₂S-rich solvent with a slight excess of SO₂ dissolved in the same solvent, all the H₂S can be reacted away to form sulfur by the following irreversible, liquid-phase reaction:



Only a small portion of the absorbed H₂S reacts in the primary absorber; most reacts in the reactor/crystallizers. Third, the dissolved sulfur formed by the reaction is crystallized and separated from the solvent in the reactor/crystallizers. Fourth, the water of reaction and any residual dissolved gases must be stripped from the solvent in the solvent stripper. Fifth, a portion of the recovered, marketable sulfur product is burned with exactly stoichiometric air in the furnace. The heat of combustion of sulfur is recovered in a waste-heat boiler and provides an energy credit for the process. Finally, the SO₂ produced by combustion is absorbed by the cool, lean solvent from the solvent stripper to provide the SO₂-rich solvent stream used in step two.

The key to this process is the irreversible, liquid-phase Claus reaction, equation 1. This reaction, even when carried out at temperatures below 100°C, proceeds rapidly to completion in the presence of an appropriate homogeneous liquid-phase catalyst (3-pyridyl carbinol). By this reaction the large H₂S stripping costs associated with most conventional technologies are avoided, and the cooled H₂S-free solvent from the crystallizer can be recycled back to the primary absorber without further processing. Because the solvent that is fed to the primary absorber is free of H₂S, the treated gas can easily meet a 1-ppm-or-less outlet specification.

Design of both the primary absorber and the SO₂ absorber requires knowing the tray efficiencies. Sieve-tray efficiencies for physical absorption of H₂S and SO₂ were determined at atmospheric pressure. The main solvent fed to the primary absorber contains a small amount of SO₂ that reacts with the H₂S being absorbed on the upper trays. Chemical reaction in the liquid phase can enhance the rate of mass transfer of a gas that is being absorbed. The effect that the simultaneous chemical reaction has on H₂S absorption rates, and thereby tray efficiencies, was studied both by modelling and by experimentation. Tray-efficiency correlations from the literature were used to correlate the experimental data and to predict the high-pressure tray efficiencies that are necessary for designing the high-pressure primary absorber.

TRAY-EFFICIENCY MODELS

One of the most readily available and widely used procedures for estimating tray efficiencies is the procedure developed in the late 1950's by the American Institute of Chemical Engineers (AIChE). This procedure uses mass-transfer correlations first to predict the point efficiency and then to convert the point efficiency to a Murphree tray efficiency. Chan and Fair [2] followed the basic AIChE design strategy but used more current mass-transfer correlations to improve the accuracy of sieve-tray efficiency predictions. The basic procedure, without presenting the correlations, begins with defining the point efficiency, E_{OV} , as

$$E_{OV} = (y_{in} - y) / (y_{in} - y^*) \quad (2)$$

where
$$y^* = m x_{1OC} \quad (3)$$

The inlet and outlet gas compositions to and from the element of solvent are y_{in} and y respectively; y^* is the gas composition that would be in equilibrium with x_{1OC} , the uniform composition of the solvent at the location of interest on the tray. The slope of the equilibrium line is m . A more useful equation for estimating the point efficiency has been derived by analyzing the mass-transfer process by using the addition-of-resistances theory along with the assumption that the gas moves upward, in plug flow, through a well-mixed liquid. The results of the derivation are

$$E_{OV} = 1 - \exp(-N_{OV}) \quad (4)$$

where N_{OV} is the number of mass-transfer units based on the overall gas-phase mass-transfer driving force. The overall number of transfer units is related to number of transfer units based on the mass-transfer driving forces of the individual phases by

$$N_{OV} = [1 / N_v + \lambda / N_L]^{-1} \quad (5)$$

where
$$N_v = k_v a_i t_v \quad (6)$$

$$N_L = k_L a_i t_L \quad (7)$$

$$\lambda = (m V) / L \quad (8)$$

If the individual gas- and liquid-phase mass-transfer coefficients, $k_v a_i$ and $k_L a_i$, and their respective contact times, t_v and t_L , are known or can be estimated reasonably by correlations, the number of gas- and liquid-phase mass-transfer units, N_v and N_L , can be determined. To calculate N_{OV} by equation 5, one needs to know λ , the ratio of the slope of the equilibrium line, m , to the slope of the operating line, L/V . The point efficiency is then calculated by equation 4. It still remains to convert the point efficiency to a Murphree tray efficiency.

Murphree vapor tray efficiency, E_{mv} , as defined by equations 9 and 10 below, is a measure of how closely the change in gas composition across a tray approaches the composition change that would occur if the gas were to leave the tray in equilibrium with the liquid exiting the tray. The gas streams above and below the tray are assumed to be perfectly mixed.

$$E_{mv} = (y_{in} - y_{out}) / (y_{in} - y^*) \quad (9)$$

where
$$y^* = m x_{out} \quad (10)$$

The equilibrium backpressure of the absorbed gas, y^* , for the Murphree vapor tray efficiency is based on the concentration of dissolved gas in the solvent at the tray outlet, x_{out} , whereas the point efficiency is based on local solvent concentration, x_{1OC} , which may be changing as the solvent flows across the tray. By using an eddy-diffusion model for crosscurrent flow to describe liquid mixing on the tray, and by assuming that the inlet gas is perfectly mixed, the two efficiencies can be related to each other through λ and the dimensionless Peclet number, Pe .

$$Pe = Z_L^2 / (D_e t_L) \quad (11)$$

The length of the liquid flow path, Z_L , is the distance between the inlet and outlet weirs on the

tray. The eddy diffusivity, D_e , can be calculated from correlations.

Two limiting regimes are encountered. For complete mixing of the solvent on the tray, corresponding to Pe equal to zero, E_{mv} is equal to E_{ov} . When the solvent flows across the tray in plug flow, corresponding to Pe equal to infinity, the maximum improvement of E_{mv} over E_{ov} is obtained. The Peclet number for the tray and operating conditions used in the present study is approximately equal to 0.01. This low value of Pe indicates that the solvent on the tray is well-mixed and that the measured Murphree efficiencies are equivalent to point efficiencies.

TRAY EFFICIENCY FOR ABSORPTION WITH CHEMICAL REACTION

If absorption with chemical reaction is occurring, the liquid-phase mass-transfer coefficient may increase relative to the coefficient for strictly physical absorption due to the reaction depleting the concentration of the absorbed gas near the gas-liquid interface. To obtain this enhancement, a significant portion of the reaction must occur in the liquid diffusion film near the gas-liquid interface rather than in the bulk solvent. When this is the case, $k_L a_i$ for physical absorption should be multiplied by an enhancement factor, $\phi \geq 1$, to obtain the liquid-phase mass-transfer coefficient for reactive absorption, $k_L^* a_i$, which is then used in equation 7 to obtain N_L .

$$k_L^* a_i = \phi k_L a_i \quad (12)$$

To find ϕ , an appropriate mass-transfer model, such as the film model or the Higbie penetration model must be chosen. The reaction regime (slow, fast, or instantaneous), the order of the reaction, and the reaction equilibrium (reversible or irreversible) must be determined. Then a value for the enhancement factor may be obtained from one of the well-known solutions to the differential equations that describe absorption with chemical reaction under these models [3].

If the tray is well-mixed ($Pe = 0$) the calculation of E_{mv} is straightforward. However, a more rigorous treatment [4] is required when the enhancement factor is a function of one or more of the reactant concentrations and these concentrations vary along the liquid-flow path on the tray. In this case the point efficiency will vary with concentration across the tray and will complicate the calculation of E_{mv} .

In determining efficiencies, the correct value of y^* to use in equations 2 or 9 depends on the reaction rate. For *very fast* reactions, in which most of the absorbed gas reacts in the film and never makes it to the bulk solvent, y^* is equal to zero. For *slow* reactions very little reaction occurs in the diffusion film. Most of the absorbed gas passes into the bulk liquid where it slowly reacts, and y^* should properly reflect the actual concentration of absorbed gas in the bulk liquid. This presents a problem if one desires to determine E_{mv} since it would require an *in situ* method of measuring the concentration of dissolved gas right at the tray outlet to calculate y^* . However, in the case of *slow* reactions, because very little reaction is occurring in the liquid film near the interface, no mass-transfer enhancement is expected, and the tray efficiency for absorption with slow reaction should be equal to the tray efficiency for physical absorption. The system under investigation falls within the *slow* reaction regime.

REACTION IN THE BULK LIQUID ON THE TRAY

In a well-mixed flow absorber operating at steady-state, as for example a sieve-tray absorber, the concentrations of dissolved gas (A) and reactant (B) are uniform throughout the bulk liquid on the tray and remain constant over time. The absorber can then be modeled as a continuously-stirred-tank reactor (CSTR). The design equation for a sieve tray acting as a CSTR/absorber requires the flow of dissolved component A in the liquid being fed to the tray plus the rate of absorption of A from the gas to be equal to the flow of dissolved, unreacted A that leaves the tray plus the rate at which A is consumed by reaction while the liquid is on the tray. For the irreversible, second-order reaction between A and B



with a reaction rate of

$$\text{Rate} = k_2 C_{A0} C_{B0} \quad (14)$$

the CSTR/tray design equations is

$$\bar{R}a_i = \phi k_L a_i (C_{Ai} - C_{Ao}) = (C_{Ao} - C_{Ain})/\tau + k_2 C_{Ao} C_{Bo} \quad (15)$$

The concentration of dissolved A at the interface and in the bulk solution are C_{Ai} and C_{Ao} respectively. The residence time (Q_L/H_L) of the liquid in the tray is τ , where Q_L is the volumetric flow of liquid to and from the tray and H_L is the hold-up (volume) of liquid on the tray. The second-order reaction-rate constant is k_2 , and $\bar{R}a_i$ is the rate of absorption per unit volume.

A *slow* reaction is one for which the reaction term is not negligible although the enhancement factor is still equal to one. For the enhancement factor to be one while substantial reaction is occurring in the bulk solution, the condition that the rate of reaction in the film is much less than the rate of absorption must be satisfied [3]. This condition requires that

$$M = D_{LA} k_2 C_{Bo} / k_L^2 \ll 1 \quad (16)$$

When condition 16 is met, the tray efficiency will remain unchanged from the efficiency for physical absorption even though the rate of reaction in the bulk liquid on the tray is appreciable. The rate of absorption, however, will be greatly improved because the reaction reduces the concentration of component A in the bulk solution (C_{Ao}), thus improving the driving force for mass transfer. When operating within this regime, the reaction rate constant, k_2 , can be calculated from equation 15 if the rate of absorption and the concentrations of A and B are known.

Hydrogen sulfide absorption by solutions of SO_2 is a case of absorption with irreversible, second-order chemical reaction containing a volatile dissolved reactant. Both penetration-model and film-model analyses indicate that condition 16 is met and that the reaction is too slow to cause an enhancement of the liquid-phase mass-transfer coefficient [5]. The reaction, then, occurs predominately in the bulk liquid, and the tray efficiency for reactive absorption should be equal to the efficiency for physical absorption.

PHYSICAL ABSORPTION OF H_2S AND SO_2

Murphree vapor tray efficiencies for physical absorption of H_2S and SO_2 were determined with an apparatus which consisted of a single 0.10-meter (4-inch) sieve tray with 4% free area placed in a circulating gas stream. Solvent was fed to the tray continuously, on a once-through basis. With this apparatus H_2S and SO_2 gas feed rates, gas- and liquid-phase compositions and temperatures, and total gas and liquid flows were measured to determine absorption rates and tray efficiencies. For physical absorption the solvent feed was free of dissolved gas.

Tray efficiencies were determined for physical absorption of SO_2 over an inlet gas concentration range of 400 to 4500 ppm. The liquid and gas flows were constant at 3.55 mole/min (6.97 cm^3/s) and 8.57 mole/min (0.427 m^3/m^2-s) respectively. The total pressure was 122 kPa. The average efficiency for this system was 0.59 ± 0.11 .

Tray efficiencies for physical absorption of H_2S by DGM were determined at 30°C and 40°C for the same total pressure and solvent and vapor flows as above. The inlet gas concentration range was 1200 to 2700 ppm. The H_2S tray efficiencies at 40°C averaged 0.16 ± 0.09 and those at 30°C averaged 0.18 ± 0.08 . These efficiencies are quite a bit lower than the SO_2 efficiencies because of the much lower solubility of H_2S in DGM. Sulfur dioxide is more than ten times as soluble in DGM as is H_2S . The slope of the equilibrium line, m , increases with decreasing gas solubility. For gas absorption under liquid-phase control (which is the case for this system) $\lambda/N_L \gg 1/N_V$. When this is the case, $N_{OV} \approx N_L/\lambda$. Therefore, if m increases due to lower gas solubility, λ must increase in proportion and N_{OV} must decrease, which results in a lower value calculated for E_{OV} . The efficiency for H_2S at 30°C is slightly higher than the efficiency for H_2S at 40°C because of the increased H_2S solubility in DGM at the lower temperature, although the increase in tray efficiency is less than the uncertainty of the efficiency measurements.

Table I compares the measured tray efficiencies for H_2S and SO_2 at various operating conditions to the predictions of the Chan and Fair model [2]. The average absolute error of the tray-efficiency predictions is 9%. This very good agreement with the measured efficiencies provides encouragement for using the model to provide high-pressure tray efficiencies.

HYDROGEN SULFIDE ABSORPTION WITH CHEMICAL REACTION

A. Calculations

Hydrogen sulfide absorption rates were also measured for the case when H₂S is absorbed and undergoes chemical reaction with SO₂ dissolved in the solvent. All the reactive-absorption experiments were with excess SO₂ (from about 2 to 7 times the stoichiometric equivalent). A homogeneous catalyst, 3-pyridyl carbinol (3-PC), was dissolved in the solvent, DGM, to increase the reaction rate. The catalyzed, irreversible, liquid-phase reaction between H₂S and SO₂ was found to be first-order in both reactants by Neumann [6] and Crean [7]. Both Neumann and Crean found that the following rate expression fit their kinetic data.

$$\text{Rate} = k_2 [H_2S] [SO_2] \quad (17)$$

In the present study the rate expression of equation 17 was used in conjunction with the CSTR/tray design equation (eqn. 15) and the reactive-absorption rate data to calculate second-order rate constants at various catalyst concentrations, temperatures, and H₂S feed rates. If the solvent feed to the tray contains no dissolved H₂S, as was the case for all the reactive-absorption experiments, the rate of H₂S absorption ($\bar{K}a_1 H_L$) must equal the rate at which dissolved H₂S leaves the tray in the exiting solvent plus the rate at which H₂S is consumed by reaction on the tray. Equation 15 becomes

$$\bar{K}a_1 H_L (\text{moles } H_2S/\text{sec}) = Q_L [H_2S]_{out} + k_2 H_L [H_2S]_{out} [SO_2]_{out} \quad (18)$$

Use of this equation requires knowledge of the concentrations of dissolved reactants on the tray. Because concentrations could not be measured *in situ*, the concentration of H₂S on the tray was calculated from the tray efficiency for H₂S. If the inlet concentration of SO₂ is known, the concentration of SO₂ leaving the tray can be determined by mass balance. Since the rate of H₂S absorption, tray hold-up, and solvent flow to the tray are measured quantities, equation 18 can be solved for the reaction-rate constant, k_2 .

B. Reactive-Absorption Results

1. Verification of Reaction-Rate Constant

Reactive-absorption rate data were collected at various temperatures, catalyst concentrations, and H₂S feed rates. The concentration of dissolved SO₂ in the solvent feed to the tray was approximately 0.001 m.f. for all the reactive-absorption experiments, and the liquid and gas flows were constant at 3.55 mole/min (6.97 cm³/s) and 8.57 mole/min (0.427 m³/m²-s) respectively. At each catalyst concentration and temperature combination, two absorption runs were done for an H₂S feed rate of approximately 13.0 standard cubic centimeters per minute and two runs were performed with the H₂S feed rate set to achieve an tray-inlet gas concentration of approximately 1900 ppm. For each run the second-order rate constant was calculated by the procedure described above. The first set of reactive-absorption experiments, at a catalyst concentration of 0.015 M 3-PC and a tray temperature of 40°C, returned an average second-order rate constant of 11.2 liter/(mole-s). This value compares fairly well to the rate constant of 32 liter/(mole-s) that was measured at the same catalyst concentration by Neumann [6], who used an adiabatic batch reactor. Extrapolating Crean's data to 0.015 M 3-PC gives a second-order rate constant of 20 liter/(mole-s). Crean's measurements were taken using a stop-flow apparatus connected to a UV-spectrophotometer. This fair agreement among data collected by very different techniques suggests that the method of calculating reaction-rate constants from the reactive-absorption data is valid.

2. Effect of 3-PC Concentration on Reaction-Rate Constant

Figure 2 shows the effect of catalyst concentration on the rate constant at 40°C. The second-order rate constants range from about 10 liter/(mole-s) at 0.015 M 3-PC to about 80 liter/(mole-s) at 0.030M 3-PC. The large error bars result from the uncertainty in the assumed tray efficiency.

The relationship between rate constant and catalyst concentration is fairly linear as was found by Crean and Neumann; however, the negative intercept does not agree with the intercept

through the origin which Crean's data gave. Crean also found a linear dependence of k_2 on catalyst concentration (eqn. 22), whereas this study found a higher order dependency.

$$k_2 = k_3 [3\text{-PC}]_0 \quad (22)$$

where the third-order rate constant, k_3 , does not vary with catalyst concentration. One possible mechanism that would fit this rate expression, although not confirmed, is that H_2S and 3-PC react rapidly and are in equilibrium with the complex they form. The H_2S -catalyst complex then reacts with SO_2 in the rate-limiting step to form a second complex which reacts very rapidly with a physically dissolved H_2S molecule to form sulfur and water. Crean's data are, at least, consistent with this mechanism. Even though a proven reaction mechanism has not been found, the rate expression of equation 17 fits the data fairly well and is simple enough to use easily in numerical calculations.

3. Effect of Reaction on H_2S Absorption

Figure 3 shows the relationship between H_2S absorption rate and reaction-rate constant at an assumed tray efficiency of 0.16. These data were taken at a tray-inlet gas-phase concentration of H_2S of 1900 ppm. Even though the reaction is too slow to cause any enhancement in the liquid-phase mass-transfer coefficient, the reaction does provide significant improvement in the absorption rate of H_2S . It accomplishes this by lowering the bulk liquid-phase concentration of H_2S , which results in a greater overall mass-transfer driving force between the gas and the bulk liquid. This same effect could be achieved in physical absorption by increasing the liquid flow rate to the level that is necessary to achieve the same low concentration of H_2S in the bulk liquid. For example, to achieve the same rate of absorption without reaction that was measured for reactive absorption with a rate constant near 10 liter/(mole-s), the liquid flow would have to be increased by a factor of 2.4. The curve in the figure is from a simulation of a single sieve tray modeled as a CSTR and given the same feed conditions, liquid hold-up, and tray efficiency as the sieve tray in the apparatus. The complex between H_2S and 3-PC was also considered in the model. The two dashed curves represent the uncertainty in the assumed tray efficiency and provide upper and lower bounds for k_2 at a given absorption rate.

SUMMARY

The tray-efficiency model of Chan and Fair adequately predicts, to within about 10%, the measured physical-absorption tray efficiencies for H_2S and SO_2 at low pressure (122 kPa). These correlations will be used to predict tray efficiencies at the high pressures that will be used in designing the primary absorber of the UCBSRP.

A second-order rate expression (first-order in both reactants) and a CSTR-model for the sieve tray were used to calculate second-order rate constants from the reactive-absorption data for H_2S absorption on a sieve tray. The method gave rate constants that were in fair agreement with values that were determined in other studies [6, 7]. The rate constant increases steeply with catalyst concentration, and a rate constant of 100 liter/(mole-s) should be easily achievable at a low catalyst concentration (near 0.03 M). The reaction is too slow to cause enhancement of the liquid-phase mass-transfer coefficient; nevertheless, a substantial improvement in H_2S absorption rate occurs because the reaction lowers the bulk concentration of dissolved H_2S . This is the same effect as seen in physical absorption when the liquid flow rate is increased. Although the rate data that were collected in this study do not fit the proposed rate expression as well as the data of Neumann and Crean, the expression should be adequate for modeling and design of the primary absorber.

REFERENCES

- [1] Lynn, S., D. Neumann, S. Sciamanna, and F. Vorhis, *Environ. Prog.*, 1987., 6, No. 4, p. 257.
- [2] Chan, H. and J. R. Fair, *Ind. Eng. Chem. Proc. Des. Dev.*, 1984, 23, p. 814.
- [3] Dankwerts, P. V., "Gas-Liquid Reactions", McGraw-Hill, Inc., New York, NY, 1970.
- [4] Pohorecki, R. and W. Moniuk, *Inzynieria Chemiczna I Procesowa*, 1983, 4, No. 1, p. 85.

Figure 2: Effect of Catalyst Concentration on Reaction-Rate Constant

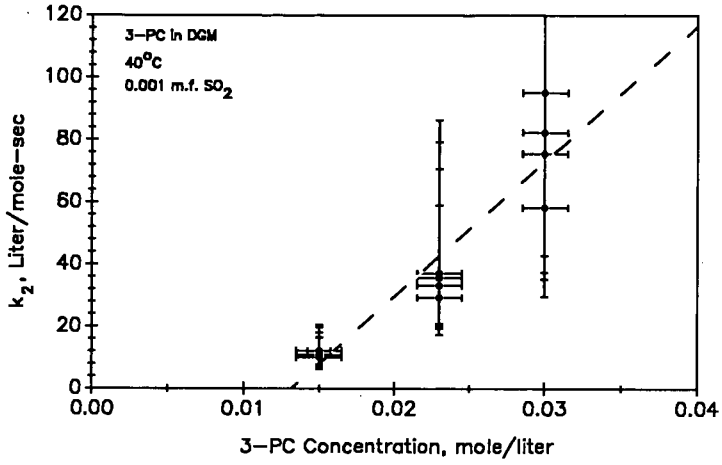
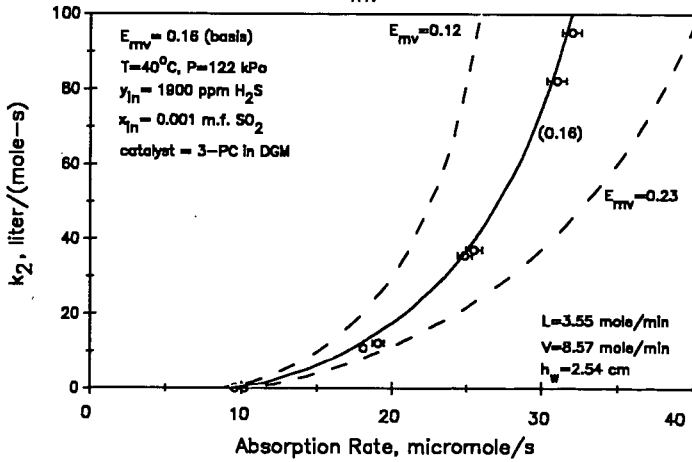


Figure 3: Effect of H₂S Absorption Rate and Assumed E_{mv} on Reaction Rate Constant



HYDROGEN SULFIDE OXIDATION BY NAPHTHOQUINONE COMPLEXES THE HIPERION PROCESS

Robert A. Douglas
Ultrasystems Engineers and Constructors, Incorporated
Irvine, California 92714

Keywords: Hiperion, Hydrogen Sulfide Removal, Naphthoquinone

ABSTRACT: Removal of hydrogen sulfide from gas streams has historically been achieved using a variety of oxidizing agents, including various quinone/metal combinations and iron chelates. Because of its high redox potential, naphthoquinone can be the basis of a highly efficient catalyst system which lends itself to commercial application in an uncomplicated equipment configuration. Both the Hiperion process and its predecessor, the Takahax process (used widely in Japan), make use of naphthoquinone complexes to effectively oxidize hydrogen sulfide to elemental sulfur. The basic chemistry of the process involves oxidation of hydrogen sulfide by a catalyst containing a naphthoquinone/metal complex and re-oxidation of the catalyst by air. This chemistry takes place either in a single absorber/oxidizer column when air is present in the gas or in separate absorber and oxidizer columns for sour gas. Commercial Hiperion units are currently treating refinery gas streams and digester biogas at three locations in the United States. In addition, the process has been demonstrated in pilot plant operation on coal-derived synthesis gas as well as various sour air streams.

Historical Development

During the late 1800's, producers of town gas in England became concerned with the detrimental effects which hydrogen sulfide had on equipment in which their gas was burned. An early attempt at removing the hydrogen sulfide involved passing the gas through beds containing hydrated ferric oxide supported on a media such as wood chips (known as iron sponge). The ferric oxide reacted with the H_2S to form ferric sulfide. These beds could in turn be purged with air to oxidize the ferric sulfide to elemental sulfur and ferric oxide, which could be used to react with additional H_2S . Although this method was relatively effective in removing hydrogen sulfide, it required large plot areas and was very labor intensive. When the bed became completely spent, it was necessary to manually remove and dispose of the iron sponge. This process was made especially difficult by the pyrophoric nature of the spent material.

The next step in the evolution of H_2S removal processes involved a variety of liquid contacting processes. Some of these involved chemistry similar to that employed in the iron sponges, i.e., suspension of iron oxide in an alkaline solution such that reactions similar to those in the iron sponge could occur. Others involved scrubbing with solutions containing various oxygen carriers such as thioarsenates, polythionates, iron-cyanide compounds, and various organic compounds. Many of these found some commercial application but others were either too specialized in application or not commercially viable.

The current generation of hydrogen sulfide removal processes began when it was discovered in the 1920's that certain organic compounds used in the dye industry were effective in oxidizing hydrogen sulfide to elemental sulfur. Several processes using various materials derived from the dye industry were developed in the following decades. These processes, known as liquid redox processes, employed successive cycles of oxidation of hydrogen sulfide by a catalyst containing an oxidizing agent followed by re-oxidation of the catalyst with air.

Work conducted in the 1950's by the Clayton Aniline Company, Ltd. in conjunction with the Northwestern Gas Board of England resulted in the discovery that various quinone compounds were effective oxidants for H₂S. These compounds, shown in Figure 1, which included derivatives of benzoquinone, duroquinone, naphthoquinone, and anthraquinone, had the ability to react with hydrogen sulfide to form the respective hydroquinone along with elemental sulfur. The hydroquinone could in turn be oxidized with air back to the quinone form. This work resulted in the development of the original Stretford process which used anthraquinone di-sulfonic acid (ADA) and which was subsequently applied in several commercial applications. However, the kinetics of the ADA/H₂S reaction were sufficiently slow that large circulation rates and liquid inventories were required. The process was subsequently enhanced by the addition of vanadium salts which significantly increased the kinetics of the reaction and permitted a reduction in circulation rates and liquid inventories. In the modified process, hydrogen sulfide was oxidized by vanadium and the ADA served as a catalyst for the re-oxidation of the vanadium.

Concurrent with the research on ADA and the development of the Stretford process in England, work on other quinone compounds was being conducted in Japan under the sponsorship of Tokyo University and the Tokyo Gas Council. The objective of this research was to develop a hydrogen sulfide oxidation process which would avoid the problems of existing processes (such as side reactions which required a liquid purge and the use of heavy metals), be more efficient, and be tailored to the needs of Japanese industry. The results of this research were used to develop the Takahax process, which uses 1,4 naphthoquinone-2-sulfonic acid as the active agent in the catalyst. This compound has a redox potential which is more than double that of anthraquinone di-sulfonic acid, (refer to Table 1) and thus promotes rapid conversion of H₂S to sulfur without the addition of vanadium or other toxic chemicals. The Takahax process is currently in use at over 200 installations in Japan, with applications ranging from coke oven gas to municipal digester gas.

Following the commercialization of the Takahax process, work with naphthoquinone was continued, and improved methods for synthesis of both 1,4 Naphthoquinone and 1,4 Naphthoquinone-2-sulfonic acid were developed. Further research resulted in the development of a naphthoquinone/metal complex or chelate which permits an increased rate of re-oxidation of the catalyst after reaction with H₂S and therefore results in a significant reduction in reaction residence time requirements as compared to Takahax or other liquid redox processes. This improved process, which is known as the Hiperion process, has been commercialized in the United States and is now in commercial operation at three locations. This paper will discuss the chemistry and flow scheme of the Hiperion process and will review operating results covering a wide range of H₂S removal applications in both the commercial and pilot plant operations.

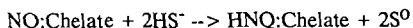
Hiperion Chemistry

The basic reactions for liquid phase oxidation of hydrogen sulfide, with the subsequent reoxidation of the catalyst is similar for all liquid redox processes. The hydrogen sulfide is first dissolved in an alkaline solution where it dissociates to a bisulfide ion and a proton:

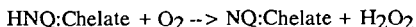


This reaction is, of course, pH dependent. At pH below 7, the undissociated H₂S is the predominant species, and above pH=9 the S²⁻ ion predominates. Since the oxidants used in these processes react with the HS⁻ ion, it is critical that pH be maintained in the range of 8-9.

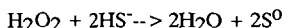
In the Hiperion process, the HS⁻ ion is oxidized by the naphthoquinone chelate to elemental sulfur and the quinone is reduced to the hydroquinone form:



The hydroquinone chelate is subsequently reacted with oxygen in atmospheric air to form the quinone chelate and hydrogen peroxide:



Since hydrogen peroxide is an extremely active oxidation agent, it quickly reacts with any residual HS⁻ to form sulfur and water:



As discussed later in the description of the Hiperion process flow scheme, the oxidized quinone chelate is returned to the absorber column to further react with hydrogen sulfide.

This description of Hiperion chemistry is obviously very rudimentary and does not address the questions of reaction mechanism or the exact nature of the naphthoquinone complex which participates in the redox transfer and results in the reduction of hydrogen sulfide to elemental sulfur. Although a great deal of research has been done into the chemistry of various liquid redox processes, a great deal remains to be learned. The research which has led to the development of the Hiperion process is largely empirical rather than fundamental, and the thrust of this paper is to describe the results of commercial and pilot plant operations using the Hiperion system. Examination of the fundamental chemistry of the process will be left for future papers.

Mass Transfer Packing

Since the reactions involved in the Hiperion process occur virtually instantaneously, the reaction of hydrogen sulfide with the naphthoquinone chelate is limited by mass transfer considerations. Thus effective mass transfer equipment is critical to effective operation of the process. An additional factor in the development of the process was the inherent tendency of solid elemental sulfur to adhere to any available surface. Thus the development of the Hiperion process also involved the development of a packing medium which would provide effective mass transfer and inhibit plugging. The packing consists of finned hollow balls which rotate and become partially fluidized as gas and liquid pass countercurrently through the beds. This mode of operation provides for effective mass transfer as well as inhibiting the settling of sulfur which would result in plugging in the beds. These "windy balls" have been tested in various pilot plant operations and are currently in use in the commercial Hiperion units.

Process Description

The flow scheme of the Hiperion process, which is similar to that of other liquid redox processes and is illustrated in Figure 2, includes two main reaction vessels-- an absorber in which the hydrogen sulfide in the gas is reduced to sulfur by contact with the catalyst and an oxidizer in which the catalyst is regenerated. Equipment is also provided for separation of the solid sulfur from the catalyst.

Sour gas enters the bottom of the absorber column and flows upward through a series of beds of "windy balls" where it is contacted by downflowing catalyst, and the H_2S is oxidized to solid elemental sulfur which is carried off with the liquid catalyst. The sweet gas then passes out of the absorber and to downstream use as dictated by the specific application. The spent catalyst from the absorber flows into a settling vessel where a portion of the suspended sulfur is settled out and the liquid overflow is pumped to the top of the oxidizer column. In the oxidizer, the catalyst is contacted over beds of windy balls with air which is introduced by a blower at the bottom of the column. The spent catalyst is thereby regenerated to the naphthoquinone chelate form, and residual H_2S dissolved in the catalyst is oxidized to sulfur by hydrogen peroxide which is formed in the oxidation reaction. Vent gas from the oxidizer can be discharged to atmosphere or used as combustion air in a furnace or other device.

Periodically, the sulfur which has settled to the bottom of the settler vessel is withdrawn and pumped through a plate and frame filter press where the sulfur is removed and the filtrate is returned to the process. The filter cake from the process is 95-98% sulfur. It contains no heavy metals or hazardous constituents and is suitable for disposal in a Class II landfill or for further purification and sale.

After filtration, the filter cake is water washed and air blown to minimize catalyst losses. The wash water is returned to the system where it serves as a primary source of makeup water to replace that lost by evaporation. Catalyst lost with the filter cake is replaced by addition of a small amount of catalyst concentrate after each filtration cycle. The only other chemical makeup requirements consist of a small amount of alkaline solution for pH control.

As with other liquid redox processes, the Hiperion process operates at ambient temperature and is capable of operating at the full range of normal industrial operating pressures.

Commercial Application

The two naphthoquinone based liquid redox processes, Takahax and Hiperion, have been applied commercially to a wide variety of hydrogen sulfide removal applications, both in Japan and in the United States. As shown in Table 2, Takahax plants are currently being used in Japan for hydrogen sulfide removal from coke oven gas, coal derived gas, town gas, and digester gas. These plants treat gas streams ranging from 2 MMSCFD to over 200 MMSCFD and containing from 700 ppm to 10% hydrogen sulfide. In the United States, the Hiperion process has been commercially applied in oil refinery and municipal digester gas services. In addition, the Hiperion process has been demonstrated on a pilot scale in treating coal derived gas, geothermal gas, offgas from rayon manufacture, and air contaminated with H_2S (see Table 3).

Hydrogen sulfide removal has become an increasingly important consideration to petroleum refiners as environmental restrictions are tightened and as economic and supply considerations dictate a shift to higher sulfur feedstocks. In order to provide the required hydrogen sulfide removal capability, two refiners in California have installed Hiperion units to treat sour gas streams resulting from processing high sulfur crudes.

The first commercial application of the Hiperion process in the United States was in an asphalt refinery where it is part of an indirect method for removing hydrogen sulfide from heavy gas oil (see Figure 3). Heavy gas oil from vacuum distillation is stripped of hydrogen sulfide in a trayed column by a recirculating stream of nitrogen. The H_2S laden nitrogen stream is then fed to the Hiperion absorber column where the H_2S is converted to sulfur. The treated nitrogen stream is then recirculated back to the vacuum gas oil stripper for further sulfur removal. The unit was designed for a nitrogen flow rate of 200 scfm at 20 psig with an H_2S concentration of 4,000 ppm. However, after being put into service, the H_2S concentration

of the nitrogen increased to between 10,000 and 20,000 ppm. With design modifications to accommodate the increased sulfur loading, the unit has been operating for over three years and has removed over 40 tons of sulfur annually.

A Hiperion unit has recently been installed in a second refinery application where the treated stream is a low volume, relatively high H₂S hydrocarbon vent gas stream originating from the overhead system of a vacuum distillation column (see Figure 4). Because of the low flow rate of the sour gas (less than 50 scfm) and the high design H₂S concentration (greater than 10%), this unit was designed with a recycle stream of treated gas which mixes with the incoming sour gas. This approach reduces the concentration of H₂S entering the absorber column and thereby improves removal efficiency and reduces the tendency of sulfur to deposit in the absorber. The treated gas from this unit, which contains less than 100 ppm of H₂S, is used as fuel gas in a refinery furnace.

Hydrogen sulfide removal is also a critical issue in municipal wastewater treatment plants where environmental regulations dictate removal of H₂S from anaerobic digester gas prior to flaring or use in gas engines. As part of a major modernization program, a municipal treatment plant in the southwestern U.S. has recently installed a digester gas treatment and recovery system which includes a Hiperion unit and which will permit compliance with environmental restrictions as well as providing improved energy recovery. A schematic diagram of this application is shown in Figure 5.

In the treatment plant, digester gas, which is composed of approximately equal amounts of carbon dioxide and methane, is generated at a rate of between 100 and 450 scfm and contains between 1,000 and 2,500 ppm of H₂S. Because of the variability of the flow rate, the gas is stored in a constant pressure vessel upstream of the Hiperion unit and a portion of the treated gas from the Hiperion absorber is recycled back to the same constant pressure vessel. A low pressure gas blower is used to provide the small amount of pressure required to overcome pressure loss in the gas system. Gas equal in volume to the net gas input is withdrawn from the treated gas stream and compressed for use in gas engines within the plant. This unit reduces hydrogen sulfide in the gas to less than 100 ppm (generally less than 20 ppm) and produces between one and two tons of sulfur filter cake per month. The filter cake from this plant is disposed in the same landfill which receives sludge from the treatment plant.

Pilot Plant Experience

In addition to those industries described previously where the Hiperion process has been applied commercially, many other industries have similar hydrogen sulfide removal requirements which can be met by the process. Pilot plant work demonstrations of the process have been successfully conducted in a number of these industries.

Steam from geothermal sources provides a major resource for power generation, but in order to utilize this resource, effective means must be provided to remove the hydrogen sulfide associated with geothermal steam. After power has been extracted from the steam, the H₂S is concentrated in the remaining non-condensable vent gas. Application of the Hiperion system to this service has been demonstrated in field pilot plant tests. Vent gas containing 10% H₂S was reduced to less than 100 ppm.

Another area where the Hiperion process can meet sulfur removal needs is in contaminated air streams in municipal treatment plants and other industrial applications. Removal of H₂S from a variety of contaminated air streams has been demonstrated by a single column pilot plant. Since the air required for oxidation of the catalyst is contained in the air being treated, a separate oxidation column is not required. Both oxidation of hydrogen sulfide and oxidation

of the catalyst take place in a single vessel. Pilot plant operations on three separate sour air streams containing from 100 to 5,000 ppm of H_2S has successfully been demonstrated using the single column pilot plant.

Manufacture of rayon is another industry where removal of hydrogen sulfide from an air stream is required in order to meet environmental requirements. Hydrogen sulfide and carbon disulfide are both released from the acid bath in which the rayon is produced. In response to this need, a single column Hiperion pilot plant was constructed and operated to demonstrate H_2S removal in this service. Sour air in this application was consistently reduced from an inlet concentration of 1,400 ppm to an outlet concentration of less than 10 ppm.

The Hiperion pilot plant operation which relates most directly to coal gasification was conducted at the Great Plains coal gasification facility in Buleah, North Dakota. The acid gas from the Rectisol system, which is primarily CO_2 , must be treated for H_2S removal prior to discharge to the atmosphere. Inasmuch as the original treatment system installed at the plant was plagued with operating problems, the plant initiated a pilot plant program to seek a means of improving the operation of the existing H_2S removal system or converting it to another system. During a two month test program, the Hiperion process successfully demonstrated its ability to remove H_2S from streams which were otherwise pure CO_2 . H_2S in the gas was reduced from inlet levels of 1% to outlet levels of less than 100 ppm (Figure 6). In addition, the pilot plant operation successfully demonstrated the effectiveness of the windy ball packing in eliminating plugging of the absorber bed as a major operating problem.

As described above, the various commercial installations and pilot plant operations of the naphthoquinone based Hiperion process (and its predecessor, the Takahax process) have demonstrated the effectiveness of this technology as a tool for removing hydrogen sulfide from gas streams originating from a variety of industrial and municipal sources. The simplicity and effectiveness of the process make it an excellent candidate in any application requiring removal of hydrogen sulfide from a gas stream.

REFERENCES

1. Kohl, Arthur L., Riesenfeld, Fred C., Gas Purification (Gulf Publishing Company, Houston, Texas, 1979)
2. Trofe, T.W., Dalrymple, D.A., Scheffel, F.A., "Stretford Process - Status and R & D Needs", Topical Report Prepared for Gas Research Institute, February, 1987
3. Douglas, Robert A., "Applications of the Hiperion Sulfur Removal Process", Presentation at the 1987 Stretford Conference, October 5, 1987, Austin, Texas
4. Douglas, Robert A., "Hiperion Process Update - Commercial and Pilot Plant Experience", Presentation at the 1989 Liquid Redox Conference, May 7-9, 1989, Austin, Texas
5. "Proceedings of the 1987 Stretford Conference", Gas Research Institute, October 5, 1989, Austin, Texas
6. "Proceedings of the 1989 GRI Liquid Redox Sulfur Recovery Conference", Gas Research Institute, May 7-9, 1989, Austin, Texas

TABLE 1
TYPICAL QUINONE REDOX POTENTIALS
(E⁰ at 25°C)

o Benzoquinone	0.787
p Benzoquinone	0.699
3,4 Phenanthroquinone-1-sulfonic acid	0.677
1,2 Naphthoquinone-4-sulfonic acid	0.625
1,4 Naphthoquinone-2-sulfonic acid	0.535
9,10 Anthroquinone-2-sulfonic acid (ADA)	0.187

TABLE 2
TAKAHAX APPLICATIONS

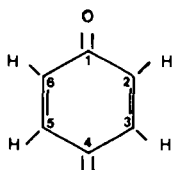
<u>Service</u>	<u>Capacity Range</u> <u>MCFD</u>	<u>H₂S Content</u>
Town Gas	1.5 - 11.5	700 - 10,500 ppm
Coke Oven Gas	1.9 - 239	2,100 - 3,500 ppm
Digester Gas	1.0 - 14.4	1.7% - 2.8%
Chemical Waste Gas	0.1 - 9.6	0.5% - 10%
Flue Gas	62.2	1,400 ppm
Manufactured Gas	7.7	7,000 ppm

TABLE 3
HIPERION PILOT PLANT APPLICATIONS

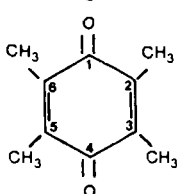
<u>Industry</u>	<u>Service</u>	<u>H₂S Concentration</u>
Rayon Manufacture	Sour Gas	1,400 ppm
Geo Thermal	Vent Gas	10%
Municipal Treatment Plant	Sour Air	300 ppm
Sulfur Manufacturer	Sour Air	700 ppm
Coal Gasification	Acid Gas	1%

FIGURE 1
 QUINONES USED IN
 HISTORICAL LIQUID REDOX STUDIES

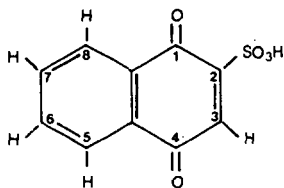
Benzoquinone



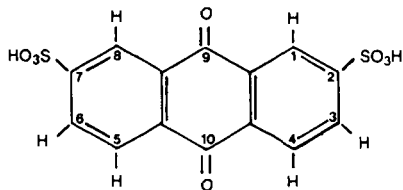
Duroquinone



1,4-Naphthaquinone-2-sulfonic acid



2,7-Anthraquinone-di-sulfonic acid



Source: Reference 2

FIGURE 2
HIPERION PROCESS

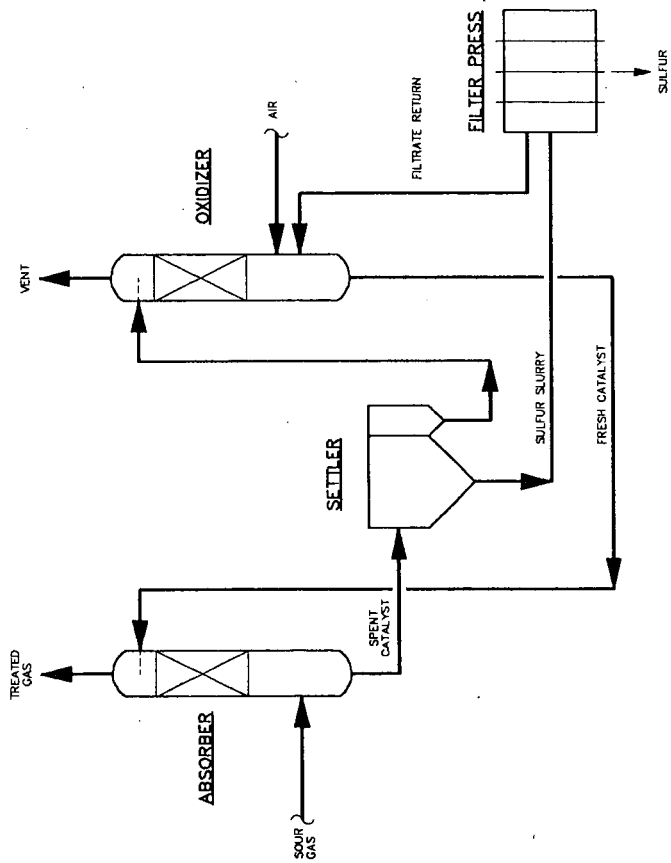


FIGURE 3
HIPERION PROCESS
OIL REFINERY APPLICATION
GAS OIL TREATMENT

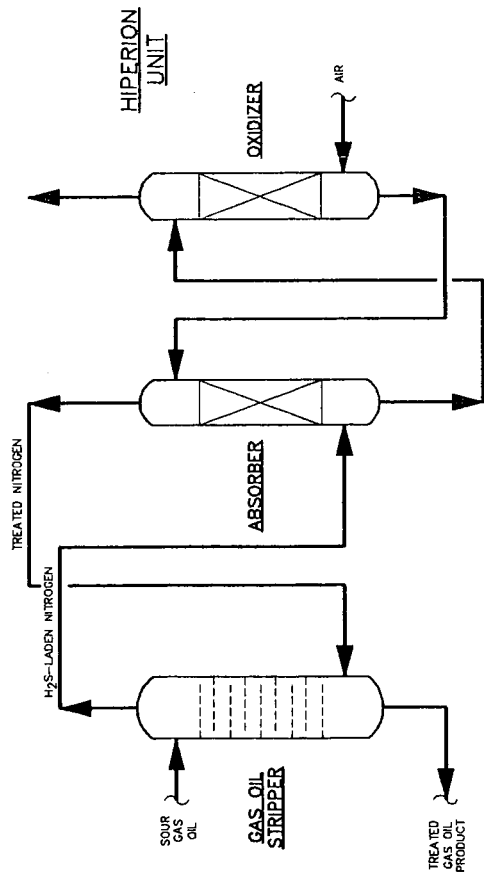


FIGURE 4
HIPERION PROCESS
OIL REFINERY APPLICATION
VENT GAS TREATMENT

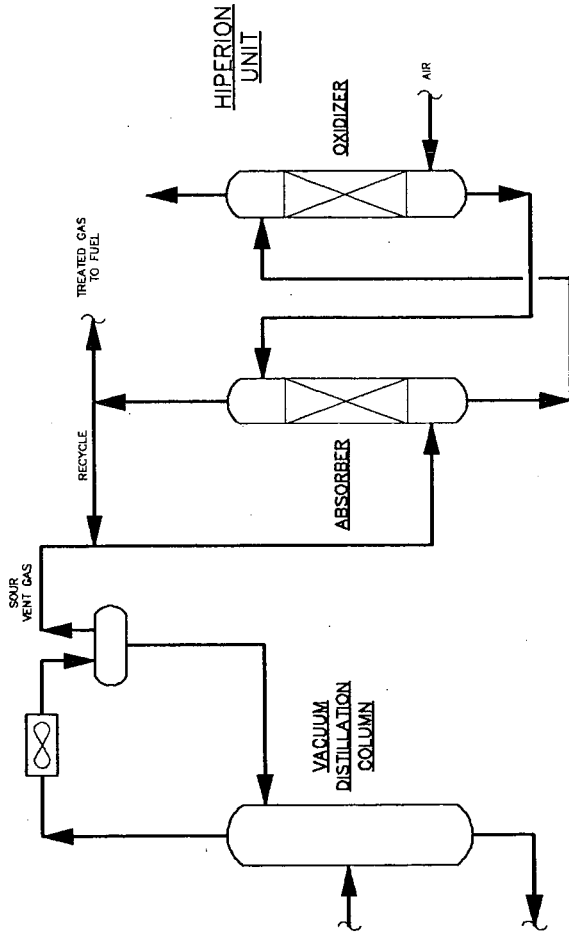


FIGURE 5
HIPERION PROCESS
DIGESTER GAS APPLICATION

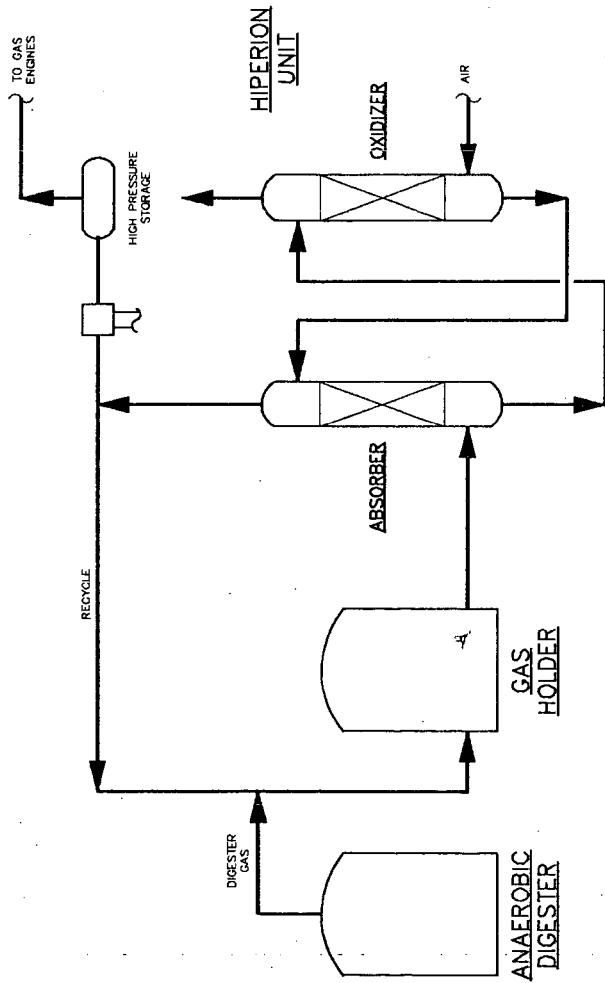
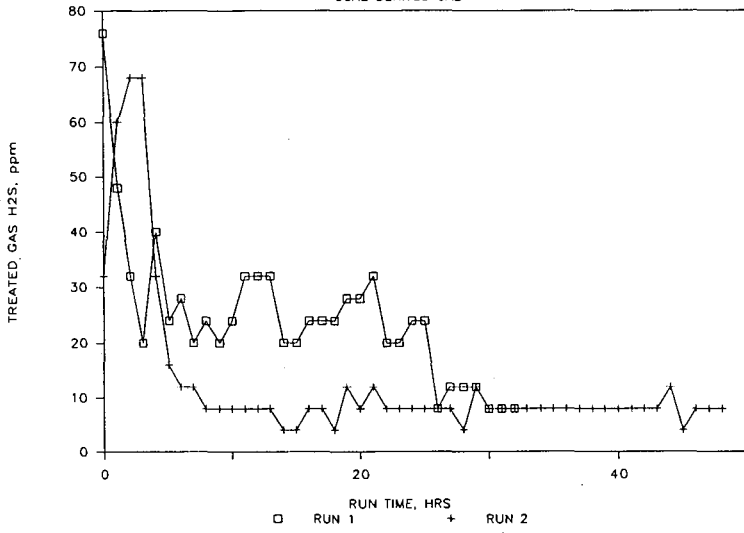


FIGURE 6
HIPERION PILOT PLANT
COAL DERIVED GAS



**INFLUENCE OF COAL TYPE AND DEVOLATILIZATION CONDITIONS
ON SULFUR EVOLUTION DURING COAL PYROLYSIS**

M. Rashid Khan, M. S. Najjar, T. Chakravarty* and P. Solomon**
Texaco, Inc., P. O. Box 509
Beacon, NY 12508

*Bechtel Corporation, Houston, TX 77252

**Advanced Fuel Research, E. Hartford, CT 06118

ABSTRACT

Coal derived products via gasification constitute an attractive alternative source of clean fuels and power compared to pulverized coal combustion. It is well-known that devolatilization of coal is the most important event in the initial stages of all coal conversion processes including gasification. Low- and high-sulfur coals were devolatilized in a number of reactors at various peak temperatures. In addition, a brief review of the available literature data in this area has been performed. The results obtained in this study provide further insights regarding the dependence of the nature of sulfur products evolved during devolatilization on feedstock type.

INTRODUCTION, BACKGROUND AND OBJECTIVES

A fundamental understanding of the physical and chemical transformation of the sulfur present in coal during devolatilization is essential for effective utilization of large reserves of high sulfur coal present in the United States. Coal devolatilization is a key step in various conversion processes including gasification. The organic and inorganic constituents of coal undergo significant changes during devolatilization. The extent of these changes depends on the peak devolatilization temperature, heating rate, gas atmosphere, and most importantly, coal type.

The thermal decomposition of inorganic and organic sulfur in coal forms primarily H_2S , SO_2 , CS_2 , S_2 , and CH_3SH , depending on the devolatilization conditions used. Snow (1932) investigated the conversion of coal sulfur to volatile sulfur at various temperatures and in streams of various gases. In these experiments, Illinois No. 6 coal was heated under flowing gases (H_2 , N_2 , CO_2 , CH_4 , C_2H_4 , and steam) at both slow and (relatively) rapid heating rates. Snow noted that under inert atmospheres, the first traces of H_2S appeared at about $200^\circ C$ and that the H_2S that evolved prior to $270^\circ C$ account for 0.1 percent of total coal sulfur. Snow demonstrated that the maximum desulfurization achievable under the conditions tested (slow heating rate, $10^\circ C/min$; "long" residence time at the peak temperature) is about 50 percent, and this value is essentially reached by $600^\circ C$. Snow also demonstrated that 10 percent of the total coal sulfur is eliminated at $360^\circ C$.

In the Texaco Coal Gasification Process (TCGP), devolatilization of coal occurs in the presence of oxygen. Consequently, it is of interest to better understand the influence of oxygen atmosphere on sulfur evolution. Groves, et al. (1987), studied the decomposition of mineral pyrite in air, 2 percent O₂/N₂, and pure N₂ atmospheres. In these experiments, commercially available samples of mineral pyrite were finely ground and pelletized. The pellets were then placed in a vertical tube furnace with flowing gas atmospheres, and heated for 15 min at temperatures from 300°C to 1,100°C. The decomposition products were analyzed by X-ray diffraction. The results show that pyrite was stable up to 450°C and completely decomposed to form pyrrhotite at 700°C. The pyrrhotite thus formed was stable up to 1,000°C. Above 1,000°C, the pyrrhotite decomposed to form magnetite. The authors also investigated the decomposition of mineral pyrite in a 2 percent O₂/N₂ atmosphere. The authors claim that this atmosphere resembles that of a boiler furnace. In the oxidizing atmosphere pyrite began to decompose at 350°C to form pyrrhotite and haematite. More pyrrhotite and less haematite was formed under these conditions than in an air atmosphere. The final traces of pyrite were detected at 900°C. A maximum amount of haematite was detected at 900°C; above this temperature, haematite steadily decreased while magnetite steadily increased. At 1,100°C, magnetite was the major species present with only trace amounts of pyrrhotite and haematite detected. They also demonstrate that pyrite decomposed to yield pyrrhotite, magnetite and haematite. As the partial pressure of oxygen is decreased, pyrrhotite becomes stable over a larger temperature range, and magnetite is preferentially formed over haematite.

Devolatilization of coal in the TCGP is also influenced by the H₂ atmosphere present in the gasifier. Yergey, et al. (1974), performed nonisothermal kinetic studies on the hydrodesulfurization of coal and mineral pyrite. In these experiments, hydrogen was passed over a finely ground bed of coal placed in a quartz reaction tube. The tube was then placed in a furnace, and the temperature increased at heating rates that varied from 1°C/min to 100°C/min up to temperatures in the range of 27 to 1,027°C. The gas product residence time in the sample bed was determined to be on the order of 7.5×10^{-2} sec. The gases evolved were analyzed by a mass spectrometer. The authors concluded the following: (a) the low-temperature H₂S peak at 412°C associated with two super-imposed organic sulfur removal processes designated as organic I and organic II; (b) H₂S evolution peaks observed at 517°C and 617°C associated with the decomposition of pyrite and iron sulfide; (c) H₂S evolution peaks beginning at 527°C and centered at 657°C associated with hydrodesulfurization of more stable organic sulfur species designated as organic III.

Calkins (1987) flash pyrolyzed various coals to determine the conversion and distribution of products for comparison with data obtained using model compounds. Based on an exhaustive study the following conclusions were drawn: aliphatic and benzylic

sulfides, mercaptans and disulfides are evolved at relatively low temperatures (700°C to 850°C); aromatic sulfides and mercaptans require much higher temperature (900°C) to give high yield of H₂S; thiophene and its derivative show low yield to H₂S even at a temperature as high as 900°C.

Khan (1989a) developed models to predict the distribution of sulfur in the products based on pyrolysis data for 32 different coal samples devolatilized in a fixed-bed reactor. Khan observed that the total sulfur content in the pyrolysis products at 500°C could be correlated to the total sulfur (weight percent of original coal) content. Khan also investigated the influence of the peak devolatilization temperature on sulfur evolution during the pyrolysis of a Pittsburgh No. 8 coal. The relationships are as follows:

$$\text{Total sulfur in gas} = 0.31 \times S_{\text{coal}} \\ [R^2 = 0.93, F = 425, P = 0.0001]$$

$$\text{Total sulfur in tar} = 0.06 \times S_{\text{coal}} \\ [R^2 = 0.85, F = 175, P = 0.0001]$$

$$\text{Total sulfur in char} = 0.61 \times S_{\text{coal}} \\ [R^2 = 0.98, F = 1,475, P = 0.0001]$$

where, R^2 = coefficient of determination
F = mean square of the model divided by the mean square of the error
P = significance value; $P < 0.05$ = significant

One of the above correlations was applied to predict the distribution of sulfur in the condensable fraction of the products generated by a fixed-bed gasification process. For the Pittsburgh No. 8 coal, the predicted percent was 6 percent, which compared well with the estimated sulfur content (5 percent) based on the DOE/METC data from the 42-inch fixed-bed gasifier. This finding confirms that the fixed-bed pyrolyzer utilized by Khan provided a reasonable simulation of the top portion of a fixed-bed gasification process.

Khan (1989a) also performed a multivariate analysis to understand the role of sulfur type (e.g., pyritic versus organic) on their distribution. Multivariate analysis demonstrated that the organic sulfur content of coal plays a stronger role in determining the sulfur content of tar or gases. The pyritic sulfur content of the coal on the other hand plays a key role in determining the sulfur content of the char, at the low-temperature devolatilization conditions. With the increase in the peak devolatilization temperature, however, the gaseous sulfur yield increases at the expense of char sulfur. A summary of the correlations developed by Khan is presented in Table 1.

The objectives of this study are to achieve a better understanding of the chemistry of sulfur evolution by (a)

extending the data base over that previously used (Khan 1989a) for coal devolatilization, and (b) utilization of advanced statistical techniques for data analyses.

EXPERIMENTAL

The details of experimental procedures used in this study are available in the numerous reports published in the literature. The information on devolatilization of coal in a fixed-bed reactor has been described by Khan (1989a, 1989b). A selected number of coals investigated by Khan were also characterized by Curie-point pyrolysis/mass spectrometric (MS) technique at the University of Utah. Curie-point pyrolysis/mass spectrometric technique has been described by Chakravarty et al (1989a, 1989b). During the early 1980s Texaco Inc. commissioned Advanced Fuel Research (AFR) to investigate the devolatilization behavior of a number of coals of interest to Texaco using the AFR's heated-grid technique. In this report devolatilization data on these coals, particularly information on heteroatoms evolved during devolatilization are provided; additional analyses on these data will be reported separately. Information on the heated-grid technique has been widely reported in the literature (e.g., Solomon and Hamblen, 1985).

RESULTS AND DISCUSSION

Pyrolysis of coal in a fixed-bed reactor and comparison with Curie-point pyrolysis/mass spectrometric results

Table 2 summarizes the intensity data of selected masses (chosen to contain sulfur containing molecules) in the spectra of pyrolyzed coals (in-situ in the Curie-point pyrolyzer) evaporated tars and the different forms of sulfur analyzed in fifteen neat coal samples. The coals selected are part of a larger set of data used for statistical analyses performed by Khan (1989a).

In order to sort out the fifteen coals in terms of their underlying sulfur forms (organic, pyritic, and sulfate), factor analysis was performed (figure not shown). For the data set considered, samples 6, 8, and 19 contain significant amounts of organic sulfur. Samples 2, 16, 17, and 24 are relatively high in pyritic sulfur (all of them are Eastern coals) and PSOC 1323 (IL #6, hvBb) stands alone as the one with relatively high sulfate sulfur. The rest of the seven coals are not high in any form of sulfur. In order to achieve a better understanding of how different forms of sulfur influence the composition of sulfur containing molecules in the products, canonical correlations were performed between the MS data sets on the coal and tar samples listed in Table 2. Details of this procedure are provided elsewhere (Chakravarty, Khan and Mauzelaar, 1989b). Canonical correlation assesses the relationship between two or more sets of factors (independent characteristic directions in a data set) on the basis of accounting for a maximum overlap between the two sets of underlying variables. Two significant canonical variates

(correlation coefficient >0.9) were found describing respectively 64% and 58% of the variance in the coal and the tar sets. Figures 1 and 2 describe the sample scores in the space of canonical variate 1 (CV1) and variate 2 (CV2). As we can see the two score plots are alike in terms of their topography (relative location of samples in the space). This means that with respect to the underlying variables (Table 2), the coal samples and the corresponding tars are similar. In other words, the distribution of the twelve sulfur variables will be similar in a tar from a given coal.

The following observation was also aided by numerically extracted spectra. Specifically, we observed that more thiophenes, thionaphthenes and dibenzothiophenes are present in hvAb coals (group of samples at the bottom left marked by circle; Figure 1) and are transferred to the corresponding tars. Our data confirm that coals with high organic sulfur contribute to high aromatic sulfur. This finding, however, is based on a limited data set. Based on the same arguments, the gases (noncondensables at the temperature of MS detector, close to room temperature) from the hvAb coals are expected to contain more aromatic sulfur. Unlike the hvAb coals, the lower rank coals have characteristically lesser m/z 184 (dibenzothiophene) than m/z 134 (thionaphthenes).

The tars from the lower rank coals (hvCb) [Figure 2] show predominantly more hydrogen sulfide, mercaptans and elemental sulfur, except for the IL#6 (hvBb) coal which yields less hydrogen sulfide. For all these coals we note relatively greater amounts of alkyl sulfides. IL #6 coal differs from other lower rank coals in that it also has a high proportion of sulfate sulfur.

Devolatilization of coal using a heated-grid reactor

Tables 3 and 4 provide a summary of results regarding the pyrolysis products generated using a heated-grid reactor. Characterization data such as these are of interest as these coals have been gasified in large scale at the Texaco Coal Gasification Processes (at the Montebello Research Lab and at Cool Water). One obvious conclusion that can be made regarding these results is that the yield of gaseous sulfur products from the Sufco coal is significantly lower than that observed for the Illinois No. 6 coal. Additional analyses of these results will be presented in a future report when further information on sulfur chemistry is generated.

SUMMARY AND CONCLUSIONS

The following conclusions can be drawn based on this study: (a) Advanced statistical techniques appear to be useful to classify coals according to their sulfur type (shown by factor analysis). (b) CV1 and CV2 (results of canonical correlations) space of the pyrolyzed coal and evaporated tar samples indicate that the sulfur distribution relationships between the coals and the

corresponding evaporated tars prepared from the same coals in a fixed-bed reactor follow similar patterns. (c) The upper block Indiana Coal (No. 18, sub-bituminous A), although a lower rank coal, is different in terms of its sulfur constituents than the other (Nos. 8, 19, 23) lower rank coals. (d) The IL#6 (No. 23; hvAb) coal with high pyritic and sulfate sulfur also has high hydrogen sulfide content in the pyrolyzed coal and relatively low hydrogen sulfide in the evaporated tar spectrum. (e) Relatively more thiophenes, thionaphthenes and dibenzothiophenes are present in the hvAb coal and are transferred to the corresponding tars. (f) Results indicate that all lower rank coals have less dibenzothiophenes (m/z 184) than thionaphthene (m/z 134), unlike hvAb coals, and more elemental sulfur. (g) The tars from high volatile coals (hvAb) coals appear to contain lower amounts of aromatic sulfur whereas the tars from the low volatile (hvCb) coal appear to have small amounts of alkyl sulfides. Additional analyses on the influence of devolatilization conditions on sulfur evolution will be presented in a future report.

REFERENCES

- Calkins, W. Energy & Fuels 1987, 1, 59.
Cernic-Simic, S. Fuel 1962, 41 (2), 141.
Chakravarty, T., M. R. Khan and H. Meuzelaar (1989a), accepted for publication, Industrial and Engineering Research.
Chakravarty, T., M. R. Khan, and H. Meuzelaar (1989b), Canadian Journal of Chem Engr, (accepted for publication).
Khan, M. R., Fuel 1989a, 68, 11, 1439-1449.
Khan, M. R., Fuel 1989b, 68, 12, 1522-1531.
Khan, M. R., Third Chemical Congress of North America and 195th ACS International Meeting, Toronto, June 5-10, 1988, Preprint of Fuel Chemistry Division of ACS, pp. 253-264.
Solomon, P. R. and Hamblen, D.G. in Chemistry of Coal Conversion, Editor, R. H. Schlosberg, Plenum Publishing, NY, Chapter 5, pp 121-251, 1985.
Snow, R. D. Ind. Eng. Chem. 1932, 24 (8), 903
Yergey, A. L. et al, Ind Eng. Chem. Proc Des. Develop. 1974, 13 (3), 233.

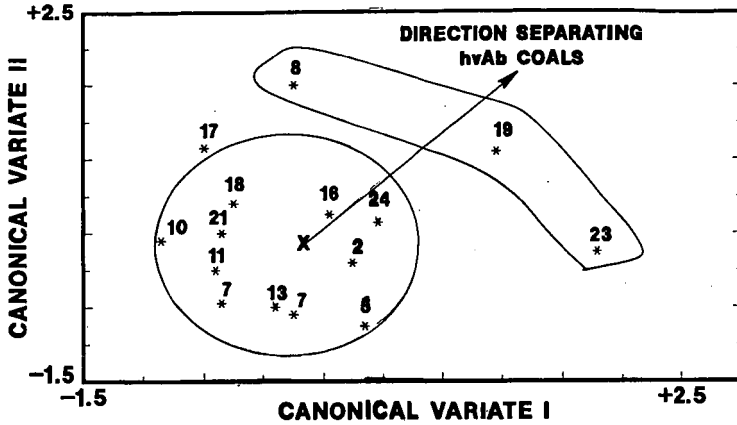


Figure 1 Score plot in CV1/CV2 space obtained from Canonical Correlation Analysis of MS data and on sulfur masses between coals and tars. Note the clustering of groups of pyrolyzed coal samples according to coal rank. The close proximity of PSOC 181 (sub bit A) coal with other hvAb coals could be attributed to relatively higher organic sulfur content of this coal.

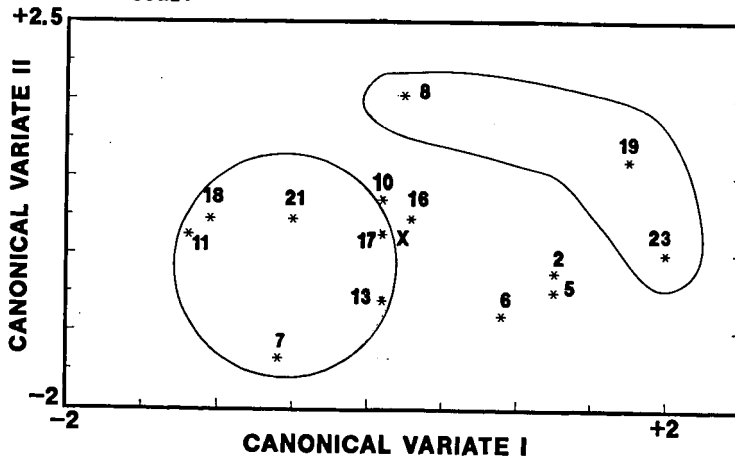


Figure 2 Score plot in CV1/CV2 space obtained from Canonical Correlation Analysis of MS data and on sulfur masses between coals and tars. Note the clustering of groups of tar samples similar to coals based on sulfur containing masses. The close proximity of the tar sample obtained from PSOC 181 (sub bit A) coal with other hvAb coals could be again attributed to relatively high organic sulfur (with no sulfate or pyritic sulfur) of this coal.

Table 3
SUMMARY OF PYROLYSIS YIELDS IN HGR FOR ILLINOIS #6 (Wt% OF DRY COAL)

ILL. #6	Slow Pyrolysis						
	30	31	17	18	19	23	26
Run #	1000	1000	600	800	1500	700	1500
Geometry	Grid	Grid	Grid	Grid	Grid	Grid	Grid
Peak Temperature (°C)	1000	1000	600	800	1500	700	1500
Hold Time (sec)	0	0	15	20	4	25	4
Heating Rate (°C/sec)	1.5	1.50	1.50	400	1333.3	233.3	500
Pressure	1.ATH	1.ATH	VAC	VAC	VAC	2.ATH	2.ATH
Sample Amount (mg)	170.3	141.7	61.1	76.6	62.0	63.8	62.1
Flow Rate (l/min)	0	0	0	0	0	0	0
Mesh Size	(40-60)	(100-200)	(60-100)	(60-100)	(60-100)	(40-60)	(40-60)
PYROLYSIS DISTRIBUTION							
Char	73.0	66.8	77.3	69.2	41.5	77.0	71.2
Tar	10.3	10.5	14.4	17.5	10.8	18.0	8.9
Dry Gas	12.2	10.3	4.8	8.1	17.3	9.5	14.3
Water	2.6	1.0	1.6	2.5	2.5	1.9	1.6
Missing	1.9	11.4	1.9	2.7	7.9	-6.4	4.0
Tar + Missing	12.2	21.8	16.3	20.2	38.7	11.6	12.9
GAS COMPOSITION							
CH ₄	2.55	2.35	1.16	1.90	1.15	1.90	2.68
H ₂	3.50	3.40	.30	1.37	8.16	1.81	4.70
CO			.03	.74	2.27		18.62
Acetylene	3.50	1.61	.49	.01	.22	2.28	2.71
Ethylene		.16	.14	.22	.69	0.22	0.82
Ethane	0.34	0.53	.47	.58	.47	0.40	0.74
Propylene		.30	.20	.22	.26	0.18	0.06
Benzene		0	0	0	0	0	0
Paraffins	1.32	1.52	1.71	1.50	1.17	2.40	1.96
Olefins	0	0	.09	.55	1.15	0	0.67
HCN	0.22	0.25	.08	.51	1.20	0.07	0.32
Amonia	0	1.01	0	0	0	0	0
CUS	0	0	0	0	0	0.01	0
CS ₂	0.64	0.61	0	.02	.03	0.08	0.04
S ₂	0	0.01	.05	.03	.01	0.04	0.04
H ₂ O	2.6	1.0	1.61	2.5	2.5	1.9	1.64
GAS TOTAL	14.89	12.79	6.42	10.64	19.82	11.41	15.95
							27.19

Table 4

SUMMARY OF PYROLYSIS YIELDS IN HGR FOR SUFCO (WT% OF DRY COAL)

<u>SuFCO</u>	<u>Slow Pyrolysis</u>				
Run #	29	32	24	22	21
Geometry	Grid	Grid	Grid	Grid	Grid
Peak Temperature (°C)	1000	1000	700	1000	1500
Hold Time (sec)	0	0	25	10	4
Heating Rate (°C/sec)	.5	.5	33.3	500	1333.3
Pressure	1 ATM	1 ATM	2 ATM	2 ATM	2 ATM
Sample Amount (mg)	148.5	189.3	67.4	53.1	64.5
Flow Rate (l/min)	.7	.7	0	0	0
Mesh Size	(40-60)	(100-200)	(40-60)	(40-60)	(40-60)
<u>PYROLYSIS DISTRIBUTION</u>					
Char	65.5	64.8	65.1	59.5	50.4
Tar	2.3	2.7	10.4	8.3	8.5
Dry Gas	16.2	13.5	15.6	30.1	31.0
Water	1.8	1.0	2.0	2.0	1.0
Missing	14.2	17.3	6.9	0.1	9.1
Tar + Missing	16.5	20.0	17.3	8.4	17.6
<u>GAS COMPOSITION</u>					
CH ₄	2.56	2.40	2.29	3.37	2.50
CO	4.44	4.14	3.13	8.72	17.62
H ₂					
CO ₂	5.2	4.10	3.90	7.25	3.44
Acetylene	0	0	0	0.07	1.35
Ethylene	0.16	0.20	0.41	1.54	0.83
Ethane	0.54	0.30	0.54	0.58	0
Propylene	0.30	0	0.47	1.10	0.28
Benzene	0	0	0	0	0
Paraffins	2.27	2.18	3.77	3.30	0
Olefins	0	0	0.79	3.56	1.19
HCN	0.29	0.19	0.20	0.35	3.65
Ammonia	0.02	0.01	0.01	0.02	0
COS	0	0	0	0	0
CS ₂	0.48	0.48	.08	0.23	0.10
SO ₂	0	0	0	0	0
H ₂ O	1.8	1.0	2.0	2.0	1.0
GAS TOTAL	18.6	15.0	17.59	32.09	31.99

DESULFURIZATION OF HOT COAL-GAS IN A HIGH-PRESSURE FLUID-BED REACTOR

S. K. Gangwal and S. M. Harkins, Research Triangle Institute,
Research Triangle Park, NC 27709 and S. C. Jain, U.S.
Department of Energy, Morgantown Energy Technology Center,
Morgantown, WV 26507

Keywords: Coal Gasification, Desulfurization, High-Temperature

ABSTRACT

Zinc ferrite, a regenerable mixed-metal oxide, is a leading sorbent for removal of H₂S from hot coal-derived gas streams for integrated gasification combined cycle (IGCC) applications. The cyclic nature of the desulfurization process and the highly exothermic regeneration with air impose severe restrictions on the zinc ferrite process in a fixed-bed reactor. Due to several potential advantages of fluid-bed operation, a high-temperature high-pressure bench-scale reactor was constructed and commissioned for testing in the fluid-bed mode. Zinc ferrite (192 μ m mean particle diameter) was tested at a superficial velocity to minimum fluidization velocity ratio of 3.0. Multicycle testing at 15 atm and 600°C with 5000 ppmv H₂S in the inlet simulated fluid-bed coal gasifier (KRW) gas showed that zinc ferrite consistently reduced the H₂S to under 20 ppmv, in a single-stage fluidized bed at a superficial residence time of ~3 seconds. Prior to reaching a bed outlet H₂S concentration of 100 ppmv, a sulfur pickup of 12 g per 100 g sorbent was achieved.

INTRODUCTION

Integrated gasification combined-cycle (IGCC) and coal gasifier/molten carbonate fuel cell (MCFC) power systems employing hot-gas cleanup are two of the most promising advanced technologies for producing electric power from coal. High-temperature desulfurization at conditions that nearly match the pressure and temperature of raw coal gasifier gas has the potential to eliminate the requirements for expensive heat recovery equipment and efficiency losses associated with coal gas scrubbing (U.S. Department of Energy, 1986). High-temperature desulfurization research has focused on the development of mixed-metal oxide sorbents for fixed-bed reactor applications (Gangwal et al., 1989a, 1989b; Grindley and Steinfeld, 1985; Grindley and Goldsmith, 1987). The primary emphasis of this work has been on the development of a zinc ferrite sorbent (a mixed-metal oxide containing zinc oxide and ferric oxide in equimolar proportions) which is a leading candidate for demonstration under the Department of Energy's Clean Coal Program.

Fluid-bed reactors offer several potential advantages over fixed-bed reactors for high-temperature desulfurization of coal-gas. They provide excellent gas-solid contact via vigorous agitation of small particles and thereby also minimize diffusional resistances, give faster overall kinetics, and allow pneumatic transport. Fluidized beds prevent solids segregation at high temperature, offer the capability of continuously adding or removing sorbent, and allow control of highly exothermic sorbent regeneration reactions. It is the need for sorbent regeneration that actually imposes restrictions on fixed-bed technology because a true steady-state is hardly reached in the regenerator off-gas concentration. Fluidized-beds can also withstand a far greater particulate loading in the coal gasifier gas than can fixed-beds.

The objective of the study, motivated by the numerous advantages of fluid-beds, is to develop durable zinc ferrite sorbent formulations suitable for fluid-bed application and test them at conditions simulating coal gasifier gases at high-temperature

high-pressure (HTHP) conditions representative of advanced power plants. High-pressure applications of fluid-bed reactors for desulfurization based on lime and iron-oxide based sorbents have been carried out by Curran (1974) and Isshiki et al. (1987), respectively. The main inferences of significance based on these papers are (1) high attrition resistance of the sorbent will be required and (2) high hydrogen sulfide removal efficiency and stable operation will be possible at HTHP conditions. Our initial results of this on-going study to develop durable zinc ferrite sorbents are presented in this paper.

SORBENT PREPARATION

Zinc ferrite ($ZnFe_2O_4$) is formed by heating to temperatures $>816^\circ C$ ($1500^\circ F$), an approximately equimolar mixture of zinc oxide (ZnO) and ferric oxide (Fe_2O_3) in the presence of a suitable binder such as bentonite. A solid-state reaction takes place giving $ZnFe_2O_4$. A significant data base exists for fixed-bed formulations of this sorbent. The fixed-bed sorbents have been manufactured by AMAX (Jha et al. 1988) and United Catalyst, Inc. (UCI) as 3/16-inch cylindrical extrudates and spherical pellets. More recently, UCI has manufactured a number of zinc ferrite formulations for General Electric (GE) Co. (Ayala et al., 1989) by rounding out the cylindrical extrudates. The rounding process yields 1/8-inch to 3/8-inch ellipsoidal pellets which are believed to possess better attrition resistance in a moving bed because of elimination of sharp edges of the cylindrical extrudates. None of the sorbents manufactured to date is applicable to fluid-beds for which particle sizes on the order of 40 to 500 μm are needed.

Three methods were chosen to prepare fluid-bed zinc ferrite (1) crushing and screening of durable fixed-bed and moving-bed sorbents to desired particle size distribution, (2) spray drying, and (3) impregnating commercial fluidizable support materials such as alumina. The first method is obvious and gives high flexibility in the choice of the desired particle size distribution. However, it may not be the most viable commercial option because of the additional cost associated with crushing, screening, and recycling fines. The particulates formed may be angular with sharp edges which may be subject to high initial rates of attrition. Keeping this in mind, a modification of the first method consisted of fluidizing the crushed zinc ferrite to remove the sharp edges and round the sorbent. Commercially, fluidizable particles such as fluid-cracking catalysts (FCC) consisting of microspheroids are generally prepared by the second method, spray drying. This method, however, does not afford flexibility in particle size which are typically in the 20 to 150 μm range with a mean of about 80 μm . The third method chosen for investigation involved pore volume impregnation of commercially available fluidizable aluminas with a solution of zinc and iron nitrates in the required chemistry followed by drying and calcination at the desired temperature.

SORBENT CHARACTERIZATION

Sorbents were characterized using a variety of techniques prior to testing at the bench-scale. The most important sorbent characteristics included sulfur capacity (defined as grams of sulfur adsorbed per 100 grams of sorbent), regenerability and attrition resistance. Other sorbent properties of importance included mercury pore volume distribution, BET surface area, particle size distribution, weight % of ZnO , Fe_2O_3 , and binder, binder type, and x-ray diffraction (XRD) phase. Sorbent sulfur capacity and regenerability were measured by a thermogravimetric analyzer (TGA) using procedures similar to those developed for fixed-bed sorbents (Gangwal et al., 1989b; Gangwal and Harkins, 1989). The attrition resistance (A_p) of the sorbent was measured using an attrition tester similar to the one described by Anderson and Pratt (1985). Further details of the attrition tester and test procedure are available (Gangwal and Harkins, 1989). Briefly the attrition test consisted of flowing 5 slpm of N_2 for 1 hour through 50 cc of the sorbent in a 1.0-inch diameter quartz tube. The sorbent was supported on a plate with a single 0.4 mm diameter hole in the center. The N_2 emerged at very high velocity through the sorbent near the hole,

thus producing a vigorous shearing effect so that measurable differences in attrition could be produced between different sorbents in a relatively short time. For a sorbent of any particle size distribution, A_r was defined as $A_r = 100(1-B/A)$, where B was the increase in the fines (sizes below the smallest significant particle size) following the attrition test and A was the original amount of sorbent excluding the original fines. The attrition test was designed as a relative (rather than absolute) measure of the tendency of the sorbent to produce fines during fluidization.

BENCH-SCALE UNIT/TEST PROCEDURE

Theoretical modeling, construction of a high-pressure cold fluid-bed system (cold-flow model), and construction of the HTHP bench-scale unit was carried out. The theoretical modeling and the cold flow model were intended to aid in determining the desirable test conditions for the HTHP system. The theoretical modeling followed the approach of Cockrill et al. (1988) and used the bubbling-bed model. The objective of the modeling was to determine the amount of sorbent to be loaded in the reactor, given a set of pressure, temperature, sorbent capacity, gas composition, and sorbent physical properties, so that breakthrough to a level of 10% of the inlet H_2S concentration (0.5 volume %) could be achieved in a reasonable time while operating in the bubbling-bed regime and avoiding slugging.

The modeling was carried out using empirical literature correlations. Unfortunately, nearly all such correlations have been developed using atmospheric pressure test rigs. Thus as a further aid in evaluating fluidization behavior of the sorbents, avoiding slugging, and determining desirable test conditions, a see-through high-pressure apparatus (cold-flow model) was constructed. A commercial porous 1/4-inch thick α -alumina ceramic material with 16 μm pores was used as a distributor in this apparatus. The pipe was made from clear polycarbonate rated to >50 atm. Both 2-inch and 3-inch diameter models were constructed. Since the effect of temperature on fluidization was expected to be minimal, the cold-flow model provided tests of sorbent fluidization behavior which would be representative of the HTHP reactor.

An existing fixed-bed sorbent test facility (Gangwal et al., 1989b) was modified for fluid-bed operation. A schematic diagram of the facility is shown in Figure 1 and a more detailed diagram of the reactor is shown in Figure 2. The system was rated at 35 atm at 788°C (1450°F) and consisted of both 3-inch and 2-inch diameter sorbent cages. The same distributor material as the cold flow model was used. Separate lines and internal cyclones were provided for sulfidation and regeneration. The system provided high flexibility in the choice of gas composition and test conditions (flow rate, pressure, temperature, sorbent amount). The GC system (not shown) could analyze both inlet and outlet gases. Multiple detectors and valve switching arrangement provided for analysis of all permanent gases and sulfur gases. The H_2S , COS, and SO_2 could be analyzed at concentrations down to 0.1 ppmv every 2 to 6 minutes. All parts exposed to hot gases were Alon processed to prevent corrosion. Pressure drop across the bed was measured using a differential pressure gauge. A typical bench-scale test consisted of loading the desired amount of sorbent and bringing the unit up to the desired temperature and pressure. The amount of sorbent loaded in the reactor and the superficial velocity used was guided by preliminary modeling and preliminary tests on the cold flow model. Sulfidation gas of a composition typical of coal gasifier gas from a KRW (originally Westinghouse and now Kellogg) fluid-bed gasifier was then passed through the sorbent at superficial velocity (U_0) to minimum fluidization velocity (U_{mf}) ratio of about 3.0. Sulfidation was terminated when the outlet gas H_2S concentration reached around 500 ppmv (which was about 10% of the inlet H_2S concentration). Regeneration of the sorbent was then carried out with a gas containing 2% O_2 and 98% N_2 at maximum temperatures up to 760°C (1400°F) and similar U_0/U_{mf} ratio as sulfidation. Previous fixed-bed experience with zinc ferrite showed that 760°C was required to prevent sulfate formation. End of regeneration was indicated when SO_2 in the off-gas fell below about 200 ppmv. The sulfidation-regeneration cycle was then repeated as many times as desired. The sorbent was characterized before and after each test for its particle size distribution and attrition resistance (A_r).

RESULTS AND DISCUSSION

Sorbent preparation activities initially concentrated on spray-drying followed by rotary calcination at temperatures up to 1750°F. UCI conducted bench-scale and pilot-scale trials to produce a spray dried zinc ferrite comparable in attrition resistance to FCC material. Bench-scale trials used up to 20% binder consisting of bentonite, Al₂O₃ gel, SiO₂ gel, and TiO₂. Two formulations (L-3392 with 15% binder and L-3393 with 20% binder) were prepared. The mean particle sizes of the L-3392 and L-3393 sorbents were 102 μm and 88 μm respectively. The attrition resistances of these sorbents were compared to a standard FCC material. Both L-3392 and L-3393 were subjected to greater attrition ($A_R \approx 70$ for L-3392 and L-3393 VS 97 for FCC) than FCC and thus were considered unacceptable for fluid-bed application. TGA tests of these sorbents showed very desirable capacity and reactivity, however. In order to increase attrition resistance, UCI increased the binder level to 25% and 50% in pilot-scale trials. In both cases agglomeration occurred and bricks rather than free-flowing particles were formed. The bricks were crushed and tested for attrition resistance. Although these materials showed high attrition resistance, they no longer possessed sulfur capacity as shown by the TGA. At this point UCI decided to terminate their effort to produce fluidizable zinc ferrite by spray drying.

With the failure of spray-drying as a potential technique, activities were initiated for sorbent preparation by impregnation. Commercial fluidizable γ -alumina and α -alumina powders were chosen for initial preparations. α -alumina was successfully loaded with up to 20 weight zinc ferrite. The procedure consisted of impregnating zinc and iron nitrates in a liquid volume equal to the pore volume of the alumina. This was followed by drying (120°C) and calcination at temperatures from 600°C to 840°C. The samples were tested for capacity by TGA. Sorbents calcined at temperatures up to 750°C quickly sulfided to their maximum capacity and were regenerable over 1.5 cycles, with no loss in capacity during the second cycle. The sample calcined at 840°C did not attain maximum capacity. Tests were not successful with the γ -alumina which showed poor reactivity presumably due to a strong chemical interaction of the reactive alumina with the active ZnO and Fe₂O₃. The attrition resistance of the impregnated α -alumina zinc ferrite was somewhat less than a zinc ferrite prepared simply by crushing and screening a zinc ferrite prepared as ellipsoids for moving bed applications as discussed below.

Other potential methods, including modification of the impregnation method, are presently being investigated for producing a durable zinc ferrite sorbent. To initiate bench-scale testing, it was decided to select one of the available moving bed sorbents and prepare the desired particle size sorbent by crushing and screening. UCI had recently prepared a 20,000 lb batch of zinc ferrite designated T-2465M for GE. The properties of this sorbent are shown in Table 1. The low pore volume (0.2 cc/g) and high density (2.57 g/cc) of this sorbent compared to other sorbents (Ayala et al., 1989) made it a good candidate for testing in the fluid-bed mode. The sorbent was obtained from GE and crushed and screened to give a particle size distribution from -48 to +150 mesh (105 to 297 μm).

The results of two 10-cycle tests conducted with the T-2465M sorbent are reported herein. Both tests were conducted without a cyclone. Test 1 was conducted using the 2-inch diameter sorbent cage with 179 grams of the sorbent, whereas Test 2 was conducted with the same cage but with twice as much sorbent. The nominal conditions of the tests are shown in Table 2. U_{mf} was calculated using standard correlations presented by Kunii and Levenspiel (1969). The U_0/U_{mf} ratio of ≈ 3.0 was guided by experiments at 15 atm in the cold flow model which showed a vigorously bubbling bed at U_0/U_{mf} of 2.6 and slightly slugging bed at U_0/U_{mf} of 3.0. The first cycle H₂S breakthrough curves for the two tests are presented in Figure 3. As can be seen, doubling the contact time improves the cleanup efficiency significantly. Estimated superficial contact time for Test 1 was ≈ 1.6 seconds whereas that for Test 2 was ≈ 2.9 seconds. The superficial contact time is calculated by dividing the estimated

expanded bed height (approximately 1.3 times the static bed height) by the superficial velocity. The static bed height is estimated from the particle density of 2.57 g/cc with the assumption of 40% voids in the bed. The results suggest that ~2.9 second superficial contact time is sufficient to obtain high cleanup efficiency in a single-stage fluid-bed.

The reason for using 179 g of sorbent for the first test was because this amount was indicated by modeling, following the approach of Cockrill et al. (1988) and using Kunii and Levenspiel's bubbling bed model. It was calculated that a breakthrough time (defined as the time to reach an outlet H₂S concentration equal to 10% of the inlet) of about 2 hours will be required. The actual breakthrough time from Figure 3, however, was only 0.5 hours. The model calculations had assumed an infinitely fast intrinsic rate constant. TGA tests, however, suggest that the intrinsic rate of reaction, in addition to gas and emulsion phase mass transfer rates, could represent a resistance to reaction. Also, product layer diffusion resistance through the -48 to +150 mesh particles could be important as shown by the TGA and could account for the flattening of the breakthrough curve for Test 1 past 50 minutes. The model is presently being refined based on the TGA results.

The sulfur capacity at a breakthrough level of 500 ppmv H₂S for each of the 10 cycles of Test 2 is shown in Figure 4. The sorbent is seen to retain a significant portion of its capacity over 10 cycles. The sorbent was subjected to particle size distribution measurement and attrition testing before and after each test. These results, shown in Table 3, indicate that fines continue to be created over the 10 cycles for both tests. Attrition resistance of the sorbent following testing appears to decrease with increased bed height. The reason for this may be increased particle-particle interaction in a deeper bed. The attrition resistance of the freshly crushed and screened T-2465M sorbent is similar to commercial fluidizable aluminas, as indicated earlier. The reduction in attrition resistance over 10 cycles is believed to be due to thermal cycling and chemical transformations during sulfidation and regeneration.

CONCLUSIONS

A zinc ferrite sorbent reduced the H₂S in coal gasifier gas to less than 20 ppmv in a single stage fluidized-bed at HTHP conditions. Crushing and screening of a durable ellipsoidal 1/8-inch to 3/8-inch zinc ferrite sorbent (T-2465M) produced a reasonable 192 μ m fluid-bed media whose initial attrition resistance was comparable or better than commercial fluidizable aluminas. The sorbent needs to be tested over a large number of cycles (~100) to further assess its durability under fluidizing conditions.

ACKNOWLEDGEMENTS

Financial support for this work from the U.S. Department of Energy, Office of Fossil Energy, Morgantown Energy Technology Center under Contract No. DE-AC21-88MC25006 is gratefully acknowledged. The sorbent T-2465M, manufactured by UCI, was supplied free of cost by GE. Helpful discussions were held with Dr. D.P. Harrison of Louisiana State University.

REFERENCES

- Anderson, J.R., and K.C. Pratt, 1985, Introduction to Characterization and Testing of Catalysts, Academic Press, Orlando, Florida, pp. 196-190.
- Ayala, R.E., E.M. Gal, and S.K. Gangwal, 1989, "Enhanced Durability of Desulfurization Sorbents for Moving-Bed Applications," Proc. Ninth Ann. Gasif. Gas Stream Cleanup Cont. Rev. Mtg., U.S. Department of Energy, Morgantown Energy Technology Center, Morgantown, WV, June 27-29.

- Cockrill, D.E., F.R. Groves, and D.P. Harrison, 1988, "Modeling of a High-Temperature Fluidized-Bed Desulfurization Reactor," Paper No. 9b, National AIChE Meeting, New Orleans, March 6-10.
- Curran, G.P., 1974, "The CONOCO Process for Hot Desulfurization of Fuel Gas: A Status Report," Proc. Fourth, Int. Conf. Fluid-Bed Comb., Energy Research and Development Administration.
- Gangwal, S.K., and S.M. Harkins, 1989, "Enhanced Durability of Desulfurization Sorbents for Fluid-Bed Applications," Proc. Ninth Ann. Gasif. Gas Stream Cleanup Cont. Rev. Mtg., U.S. Department of Energy, Morgantown Energy Technology Center, Morgantown, WV, June 27-29.
- Gangwal, S.K., S.M. Harkins, M.C. Woods, S.C. Jain, and S.J. Bossart, 1989a, "Bench Scale Testing of High-Temperature Desulfurization Sorbents," Environmental Progress, 8(4), 265-269.
- Gangwal, S.K., J.M. Stogner, S.M. Harkins, and S.J. Bossart, 1989b, "Testing of Novel Sorbents for H₂S Removal from Coal Gas," Environmental Progress, 8(1), 26-34.
- Grindley, T., and H. Goldsmith, 1987, "Development of Zinc Ferrite Desulfurization Sorbents for Large-Scale Testing," AIChE Annual Meeting, Session 114d, New York, November 15-20.
- Grindley, T. and G. Steinfeld, 1985, "Desulfurization of Hot Coal Gas by Zinc Ferrite," Acid and Sour Gas Treat Proc., Gulf Publ. Co., Houston, Texas, pp. 419-465.
- Isshiki, A., T. Sugitani, S. Kobayashi, and J. Fukui, 1987, "Hot Gas Cleanup Technology for Integrated Gasification Combined-Cycle Power Generation," Sekitan Riyo Gijutsu Kenkyu Happyokai Koenshu, 9, 233-269.
- Jha, M.D., M.H. Berggren, and D.P. Harrison, 1988, "Enhanced Durability and Reactivity for Zinc Ferrite Desulfurization Sorbent," Proc. Eighth Ann. Gasif. Gas Stream Cleanup Cont. Mtg., DOE/METC-88/6092, Vol. 1 (DE88010253), pp. 83-92.
- Kunii, D. and O. Levenspiel, 1969, Fluidization Engineering, John Wiley and Sons, Inc., New York, pp. 72-73.
- U.S. Department of Energy, Morgantown Energy Technology Center, 1986, Hot Gas Cleanup for Power Generating Systems, DOE/METC-86/6038 (DE-86006607), pp. 1 -5.

Table 1. Properties of Sorbent T-2465M

ZnO : 34.0%	Pellet density : 2.57 g/cm ³
Fe ₂ O ₃ : 64.0%	Surface area : 4.6 m ² /g
Bentonite : 2.0%	Pore volume : 0.2 cm ³ /g
Size : 1/8 to 3/8 inch	Mean pore diameter : 1958 Å
Shape : ellipsoidal	Crush strength : 22.5 lb/pellet
Calcination Temperature : 843°C (1550°F)	Attrition resistance : 95.4%
Bulk Density : 1.44 g/cm ³	Theoretical sulfur capacity : 39 g/100 g

Table 2. Nominal Bench-Scale Test Conditions (Reactor I.D. = 2.0-inch)

	Sulfidation		Regeneration
	Inlet	Outlet	Inlet
Pressure (atm)	15		15
Temperature (°C)			
Maximum	630		760
Inlet	600		675
Average	615		Not applicable
Gas composition (vol. %)			
	Inlet	Outlet	Inlet
H ₂	9	13	--
CO ₂	5	9	--
H ₂ O	19	15	--
H ₂ S	0.45	0.001	--
N ₂	Balance	Balance	98.0
CO	16	12	--
O ₂	--	--	2.0
Flow (slpm)	35.0		32.0
U _{mf} (cm/s)	2.0		1.8
U _o * (cm/s)	6.2		6.1
U _o /U _{mf}	3.1		3.4

*Based on average temperature for sulfidation; inlet temperature for regeneration.

Table 3. Particle Size Distribution (Weight %) and Attrition Resistance (A_R) of Fresh and Used T-2465M Sorbent

Size (μm)	Fresh T-2465M	Test 1 after		Test 2 after	
		4 cycles	10 cycles	6 cycles	10 cycles
>297	0.00	0.02	0.34	0.79	0.08
250 to 297	13.46	8.27	4.59	13.14	11.36
177 to 250	44.87	43.36	43.19	37.42	37.81
149 to 177	10.43	12.03	11.63	11.46	10.71
125 to 149	24.07	17.48	18.50	18.47	19.58
105 to 125	7.16	13.06	14.53	13.85	13.41
<105	0.00	5.77	7.22	4.87	7.04
Average size (μm)	192	181	171	184	180
A _R	94.1	--	85.4	--	78.4

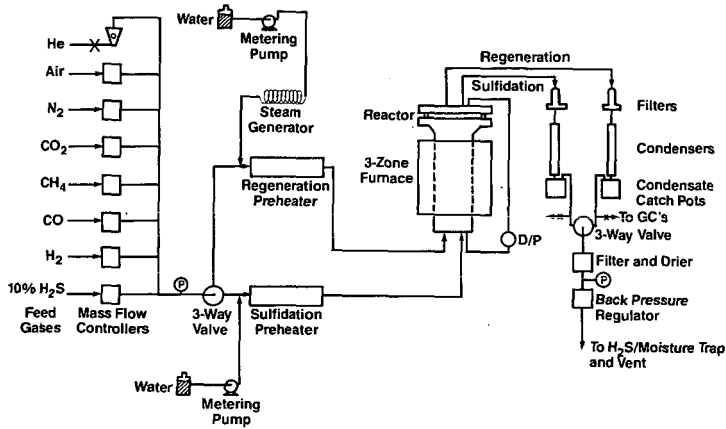


Figure 1. Bench-scale fluid-bed sorbent test facility.

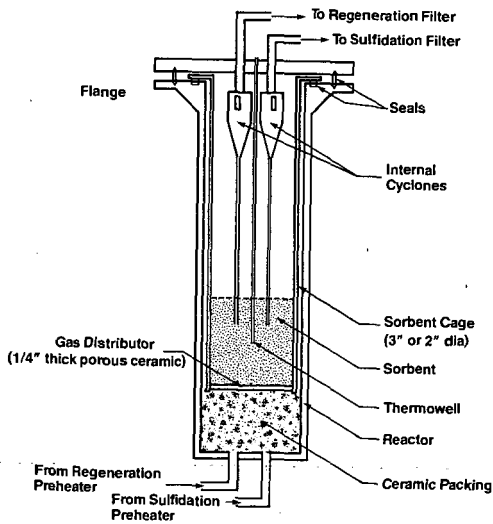


Figure 2. Fluid-bed reactor.

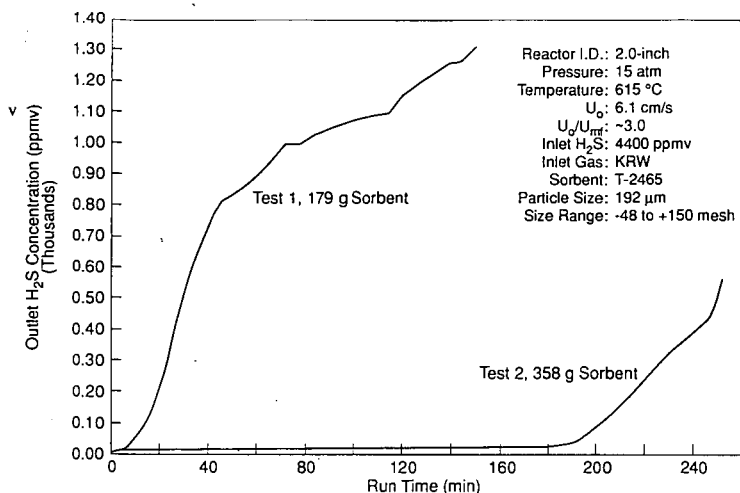


Figure 3. Effect of sorbent amount on H_2S breakthrough profile.

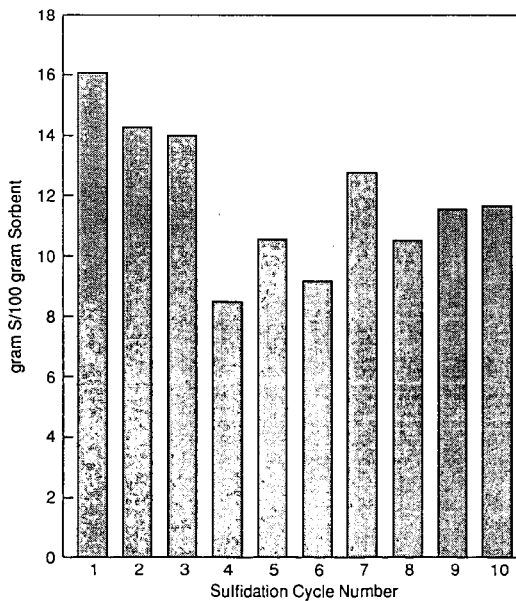


Figure 4. Sulfur capacity at 500 ppmv H_2S in outlet gas for Test 2 over 10 cycles (inlet H_2S = 4400 ppmv).

HIGH TEMPERATURE H₂S REMOVAL
FROM PROCESS GASES IN A STEAM REGENERATIVE PROCESS
USING MnO OR FeO ON γ -ALUMINA ACCEPTORS

J.P. Wakker, A.W. Gerritsen
Delft University of Technology,
Laboratory of Chemical Process Technology,
Julianalaan 136, 2628 BL Delft, The Netherlands.

Keywords: H₂S removal, high temperature, steam regenerative

Abstract

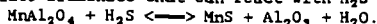
During gasification of coal the sulfur compounds are converted mainly into H₂S and COS. A process to remove these compounds at temperatures of 400-800 °C has been developed. The acceptors used are based on MnO or FeO on a γ -alumina carrier. Regeneration takes place at the same temperature with a gas containing steam, while more than 15 % of H₂S can be obtained in the dried reactor off gas. The main advantage of steam regeneration is that no oxidation or noticeable heat effect is involved. A packed bed microreactor was used to study sulfidation- and regeneration behaviour extensively in cyclic experiments. It showed that H₂S can be removed to a level of 0-50 ppmv depending upon gas composition. After several hundreds of cycles only little deactivation was observed. The effects of various compounds in the feed were studied.

Introduction

Thermodynamics of the reaction $MnO + H_2S \rightleftharpoons MnS + H_2O$ in the temperature range 400-800 °C indicate that the equilibrium is shifted completely towards the metal sulfide. This means that MnO can remove H₂S at these temperatures quite deep but also that steam will not regenerate a sulfur loaded acceptor. Consequently it may sound strange that a MnO on γ -Al₂O₃ acceptor is proposed here! However, fact is that such an acceptor can remove H₂S effectively at 400-800 °C and is regenerated easily with steam at the same temperature [1, 2].

Other H₂S acceptors often use air for regeneration, resulting in sulfur oxides as well as an oxidized acceptor, both needing a reducing agent like H₂ to obtain acceptable products. The heat produced may result in temperature control problems and sintering of the acceptor material. In contrast the MnO on γ -Al₂O₃ acceptor is regenerated without a noticeable heat effect, resulting in a stable acceptor. As regeneration does not change the oxidation state of the acceptor, no reduction is needed either. The H₂S formed can be used directly to generate sulfur, e.g. in a Claus plant. This ability to regenerate MnO on γ -Al₂O₃ acceptors with steam is not incidental, on the contrary: -after a relative short stabilization time- the acceptors can be exposed to more than 400 sulfidation-regeneration cycles without a change in activity.

At Delft University of Technology (DUT) several investigations were performed to determine which compound(s) are responsible for the fact that steam regeneration is possible [3]. It is supposed that regenerable acceptors are formed from a monolayer of MnO which reacted with the γ -alumina carrier and produced a surface alumininate. In other words: free MnO on Al₂O₃ is expected to be non-regenerable, while MnO with a crystalline structure close enough to that of the γ -Al₂O₃ carrier will form a surface-alumininate that can react with H₂S according to:



The equilibrium constant of this reaction can be estimated and compared with that of pure manganese oxide. In figures 1a and 1b are shown, respectively, the thermodynamic equilibrium constant for FeO and MnO, in contact with a H₂S-H₂O gas mixture and the reaction enthalpies for the sulfidation. For the pure metal oxides the sulfidation equilibrium is shifted completely towards the metal sulfide at temperatures from 400 to 800 °C. As can be seen from figure 1a the thermodynamic constants of the corresponding aluminates MnAl₂O₄ and FeAl₂O₄ indicate that their equilibrium with a H₂S-H₂O gas mixture is not pronounced to one side. In these

figures both Fe and Mn oxides are shown because it was found that not only MnO on γ -Al₂O₃ can be used in a steam regenerative process to remove H₂S. Quite similar behaviour is found with FeO on γ -Al₂O₃, the same holds even for Zn, Ni and Co. However, only FeO on γ -alumina comes close to MnO on γ -alumina, the others are far less attractive.

Several investigations support that an aluminate is the active substance. Atomic absorption measurements in combination with sulfidation-regeneration experiments of acceptors with different metal oxide levels show that, up to a certain coverage, all metal sulfide formed can be regenerated with steam. That coverage corresponds to a number of metal oxide moles equal to the number of alumina moles exposed at its surface.

Although the assumption that manganese aluminate is the active compound could not be confirmed by röntgen diffraction, this technique did not prove the opposite either. No lines characteristic for this compound could be found, probably due to its high dispersion on a carrier of poor crystallinity. Irregenerable acceptors however show lines that correspond with those of pure MnO. Diffuse reflectance spectroscopy at reaction conditions shows that regenerable acceptors have bands characteristic for MnAl₂O₄ (as indicated by their grey colour) while irregenerable acceptors have a MnO spectrum (and a brown colour). Another technique used is Mössbauer spectroscopy, although it could only be applied to iron oxides as manganese has no Mössbauer activity. From this study it can be concluded that on steam-regenerative acceptors the Fe²⁺ ions are highly dispersed on the support and built-in into the alumina. This agrees with the formation of FeAl₂O₄.

Experimental

Acceptor preparation

Using the wet impregnation technique the carrier is contacted with a solution of a metal salt at ambient temperature. After approximately 16 h the impregnated material is filtrated and dried, generally overnight, at about 110 °C. In some cases, e.g. in case a metal acetate or -oxalate was used, the drying was combined with calcination at 300 °C. Finally the material, with the metal still in a high oxidation state (e.g. MnO₂), is reduced with H₂ at 600 °C. Depending on the metal content desired the complete process is repeated a number of times.

Table 1 shows that the number of preparation cycles and the molarity of the salt solution not only determine the amount of manganese obtained on the carrier, but also whether or not such an acceptor can be regenerated completely. Although not indicated in the table, with each salt it is possible to obtain an acceptor which can not be regenerated completely. This is done by raising the manganese content above 8-10 %w. Notably this agrees with a 1:1 mole ratio of metal to surface alumina.

Instrumental

The apparatus used to obtain the sulfidation-regeneration data is described schematically in figure 2. The heart of the apparatus is a tubular quartz reactor with an internal diameter of 9 mm. Normally 3 g acceptor, with a mean particle diameter of 0.4 mm, result in a bed length of approximately 70 mm. The reactor is kept at a constant temperature, which can be chosen between 400 and 800 °C. The reactor is used in a cyclic way: about 1.5 hour it is used to remove H₂S from the gas stream fed (the sulfidation- or acceptance phase), then for about half an hour the sulfur is removed from the acceptor (the regeneration phase). The cycle is completed with a flush phase of another half hour.

In the acceptance phase the feed to the reactor is obtained by mixing gases from cylinders. Generally the H₂S content is 1 %v and the hydrogen content 10 %v, the balance being N₂. The total flow rate is 100 ml/min at ambient conditions. Several other gases, notably CO and CO₂, can be added as well. If the influence of small amounts of H₂O is studied, the feed is passed through a bed of FeSO₄.7aq. This results in a H₂O content of 0-5 %v, depending upon the temperature of the FeSO₄,

bed. If the H_2O concentration has to be higher than 5 %v, liquid water is injected into the reactor. This will evaporate before reaching the acceptor bed.

Quite different amounts of water are needed during regeneration. In this phase the H_2S supply is closed and a small stream of water injected, resulting in a flow with approximately 50-80 %v of steam.

The H_2S content in the outlet is monitored by passing the gas through a stirred vessel with a $CdSO_4$ solution, kept at a constant pH of 4 by introducing NaOH as well. Under above conditions the flow of NaOH supplied equals the flow of H_2S leaving the reactor. The concentration of H_2S can be obtained as the first derivative of this flow towards time. Other compounds (CO , CO_2 , H_2S and H_2O) in the reactor effluent can be detected with a gas chromatograph. In this way e.g. the shift-reaction can be followed.

A typical breakthrough curve, which describes the outlet H_2S concentration during the acceptance phase, is shown in figure 3. At the start of an experiment all H_2S supplied is captured by the acceptor. After approximately 20 minutes a sudden increase of the H_2S concentration indicates breakthrough. Within a few minutes this concentration raises to about 30-40% of the inlet value. Of course in practice breakthrough will never be waited for. Some time before this moment is expected, another reactor with fresh or regenerated acceptor will be used. During our investigations the outlet concentration is monitored for about 1 h more because the complete curve gives valuable information about the concentration profile within the acceptor bed in the time-span BEFORE actual breakthrough.

After enough data are gathered the H_2S supply is switched off and steam introduced. Now H_2S is being produced. Again the H_2S content is monitored as a function of time to obtain kinetic data. This proceeds until all sulfur captured during acceptance has been released.

Results and discussion

An interesting variable is the amount of sulfur captured at breakthrough (qb) as a function of the time on stream. As can be observed in figure 4 a fresh acceptor will take up some 2 % of its weight as sulfur at 600 °C. This decreases gradually to approximately 1 % in the first week and remains constant at that level afterwards, at least until some 80 days, or approximately 400 cycles, later. This deactivation can, to a certain extent, be explained by the decrease in surface area which was determined in parallel to this experiment. The corresponding BET surfaces are shown in the figure. It should be noted here that the temperature was kept at 600 °C all the time. At this temperature the deactivation will also take place if the acceptor is NOT subjected to acceptance-regeneration cycles but left in a reducing atmosphere only. If a fresh acceptor is used and the temperature maintained at 400 °C, no or little deactivation takes place. At 800 °C the acceptor will take up 2.7 %w S, but this capacity decreases in about five weeks to approximately 1 %w S, probably due to sintering of the carrier material.

The influence of temperature on a "stabilized acceptor" is shown in figure 5. Lowering the temperature from 600 °C to 400 °C results in a decrease of sulfur capture at breakthrough by approximately one half. When the acceptors are stabilized at 800 °C instead of 600 °C lowering the temperature from 800 °C to 600 °C results in a decrease of the breakthrough capacity from 2.7 %w sulfur to approximately 0.5 %w sulfur. The same behaviour is observed for iron containing acceptors. This decrease is attributed to both kinetics and thermodynamics.

The influence of the H_2S concentration itself on the breakthrough capacity is given in figure 6. At low H_2S concentrations the capacity is somewhat higher than at high concentrations. This can be explained by summation of two processes. The first process is a fast equilibrium between H_2S and surface aluminate; the corresponding acceptor capacity is not influenced by the H_2S concentration. The second process is slow and corresponds to sulfur that moves to sites that are not easily reached. This means that when low H_2S concentrations are used (while the volumetric flow rate is kept constant) the second, relatively slow process can proceed longer before breakthrough is measured, resulting in a higher capacity.

In all experiments hydrogen is added to the feed to prevent decomposition of H₂S into hydrogen and sulfur. As long as the feed gas only contains N₂, H₂ and H₂S the H₂ concentration does not influence the reaction rate in the range of 7 to 90 %.

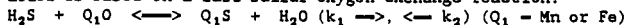
The results discussed so far are obtained with a feed of 1 % H₂S, 10 % H₂, the balance being N₂. In general, however, the feed will contain CO, CO₂ and H₂O as well. As could be expected from the possibility to use steam as the regenerative agent, H₂O has a negative effect on the amount of sulfur captured at breakthrough. This is demonstrated in figure 7a. In this figure the relative breakthrough capacity is shown as a function of the water content of the feed. The relative breakthrough capacity is the observed breakthrough capacity divided by the breakthrough capacity of the same acceptor using a standard feed gas without water. In this way the capacities of different acceptors can be compared easily. The retention level decreases drastically by 15 % of H₂O. However, CO in the feed has a positive effect on the sulfur retention capacity as is demonstrated in figure 7b, which shows that 50 % CO will increase that capacity by a factor of approximately 1.4 for the manganese acceptor and a factor 1.7 for the iron containing acceptor. From this figure the influence of the hydrogen concentration can be seen clearly too. The positive effect of 50 % CO is a factor 1.9 if the feed gas contains only 10 % hydrogen instead of 40 % hydrogen. A combination of both effects, the negative water influence and the positive CO influence, can be observed in figures 8a and b.

The effect of CO can be explained by the shift reaction: $CO + H_2O \rightleftharpoons CO_2 + H_2$. Both the water fed to the reactor and the water produced in the reaction of H₂S with the acceptor react with CO to form a CO₂/H₂ mixture. Another effect of introducing CO is the formation of COS by the analogous equilibrium: $CO + H_2S \rightleftharpoons COS + H_2$. Fortunately it showed that COS only appears in the effluent after H₂S breakthrough, indicating that COS is effectively removed by the acceptor as well. The COS formation is quite fast, the COS in the gas leaving the reactor is almost in equilibrium with the other gas constituents.

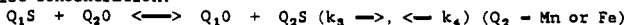
Other compounds which may be found in practical feedstocks are hydrocarbons as CH₄, C₂H₆ and lower alkenes. Experiments showed that these compounds have no influence on acceptor behaviour if their content is lower than 10 %. Even higher levels are allowed, although some influence may start to be visible, especially in case of alkenes.

Recently the regeneration of the acceptors has been studied in more detail [4]. Figure 9 shows the amount of steam needed to regenerate acceptors which were previously completely loaded with sulfur. By dividing this amount by the amount needed stoichiometrically, the relative steam use RSU is obtained. It can be seen that two-third of the sulfur captured can be regenerated easily, the rest needs a higher amount of steam. Similar figures are available for different steam concentrations, all indicating that a high steam concentration and a low steam space velocity is best. The resulting off gas may contain up to 25 % of H₂S on wet basis or 40 % or more on dry basis. Such a gas can be used quite well in a Claus unit.

Another part of the study is focussed on a mathematic model to describe the results. The model is based on a fast sulfur-oxygen exchange reaction:



A slow sulfur-oxygen exchange reaction is added to explain the slow rise of the outlet concentration:



Next "Langmuir" adsorptions are needed to account for the amount of H₂S that can be desorbed from a loaded acceptor without using any steam; it is assumed that the same sites also adsorb H₂O:



Mathematically this set of equilibria is difficult to solve, mainly because the H_2S and H_2O concentrations are independent. In practice 4 stiff partial differential equations have to be solved simultaneously.

Results obtained with this model are given in figures 10a and b. With the model a good fit is obtained. The fact that the calculated H_2O outlet curve is not in agreement with the experimentally found curve is not taken too serious because the H_2O analysis was much less reliable.

The parameters used to obtain these curves are summarized in table 2. Of course much work is still to be done in this field, e.g. we are to determine some of the parameters of the last table by independent other techniques like thermogravimetrics, and the effect of CO has to be incorporated in the model.

Also in the field of practical experiments progress is made. In the near future the acceptors will be tested in a larger unit to desulfurize a sub-stream of gas leaving the experimental 200 kW (thermal) gasifier build at the Energy Research Centre of the Netherlands in Petten. The unit consists of 3 reactors (1.5 liter volume each) which are used intermittently. While one is in the acceptance phase the acceptor in one of the others is regenerated. This work is described extensively in next paper presented at this congress.

Conclusions

The acceptors developed at DUT can remove H_2S from a fuel gas and can be regenerated with a gas containing steam. This behaviour can be explained by the formation of a surface $MeAl_2O_4$ (Me = Mn or Fe) spinel.

The amount of sulfur captured at breakthrough varies between 0.25 and 3.0 Zw , depending upon temperature and gas composition. The regeneration off-gas contains up to 40 Zv H_2S , enough to be fed to a Claus plant. The acceptors have a long lifetime: they can be used during at least 400 sulfidation-regeneration cycles.

SYMBOLS USED:

BET	B.E.T. surface area of acceptor	[m^2/g]
C_i	outlet concentration of component i	[Zv]
C_i^f	inlet concentration of component i	[Zv]
d_p	particle diameter of acceptor	[mm]
ΔH	reaction enthalpy sulfidation reaction	[kJ/mol]
K	equilibrium constant sulfidation reaction	[-]
K_{H_2O}	equilibrium constant H_2O adsorption Langmuir sites	[m^3/mol]
K_{H_2S}	equilibrium constant H_2S adsorption on Langmuir sites	[m^3/mol]
k_1, k_2	rate constants fast exchange reaction	[$m^3/(mol.s)$]
k_3, k_4	rate constants slow exchange reaction ($k_3 = k_4$)	[$m^3/(mol.s)$]
L	length acceptor bed	[mm]
q_b	breakthrough capacity, sulfur captured at breakthrough	[Zw]
$q_{b,rel}$	relative breakthrough capacity = observed breakthrough capacity divided by the breakthrough capacity of the same acceptor using standard feed gas	[-]
Q_{theor}	theoretical maximal capacity of acceptor	[mol/m^3]
Q_1	stoichiometric capacity of fast exchange sites	[mol/m^3]
Q_2	stoichiometric capacity of slow exchange sites	[mol/m^3]
Q_3	stoichiometric capacity of Langmuir sites	[mol/m^3]
T	temperature	[$^{\circ}C$ or K]
θ	H_2S throughput parameter = amount of sulfur fed during acceptance divided by an arbitrary amount of sulfur	[-]
#	number of impregnation cycles	[-]

Literature:

- [1] J. Barin, O. Knacke, O. Kubachewski, "Thermochemical Properties of Inorganic Substances", Springer Verlag, Berlin, 1973, Supplement, 1976.

- [2] D.R. Stull, H. Prophet, "JANAF Thermochemical Tables", 2nd ed., National Bureau of Standards, Washington D.C., 1971.
- [3] T.H. Soerawidjaja, "Steam regenerative removal of H₂S at high temperatures using metal oxide on alumina acceptors", Thesis, Delft University Press, 1985.
- [4] R. van der Heijden, A.W. Gerritsen, I²-Procestechnologie, 10, 11-18 (1987).

TABLES TABLES TABLES TABLES TABLES TABLES TABLES TABLES

Table 1. Influence of salt, molarity and number of impregnations on ability to be regenerated by steam.

Salt	# mol	Mn	Regeneration
		%w	%
Nitrate	1 x 2.0	7.9	69
	4 x 0.7	10.1	95
	4 x 0.5	8.0	100
Sulfate	3 x 0.5	7.2	100
Acetate	1 x 2.0	7.7	100

Table 2. Parameters of the model at 400 and 600 °C

Param	Dimension	400 °C	600 °C
k_1/k_2	-	4.7	3.6
k_1	m ³ /(mol.s)	0.4	0.4
Q_1	mol/m ³	160	209
$k_3=k_4$	m ³ /(mol.s)	1E-3	7E-7
Q_2	mol/m ³	140	210
K_{H_2S}	m ³ /mol	1.38	1.36
K_{H_2O}	m ³ /mol	14.7	12.4
Q_3	mol/m ³	140	168

FIGURES FIGURES FIGURES FIGURES FIGURES FIGURES FIGURES FIGURES

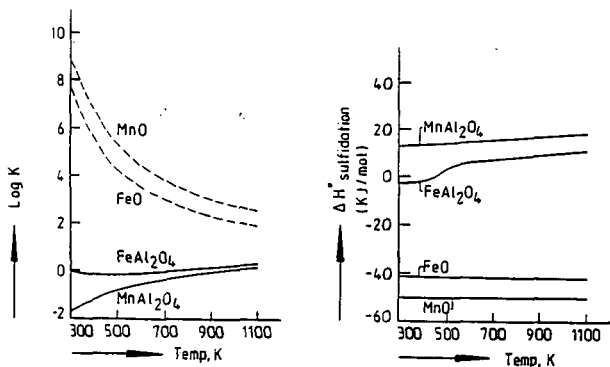


Figure 1: Thermodynamic data of sulfidation.
a: Equilibrium constant.

b: Heat of reaction.

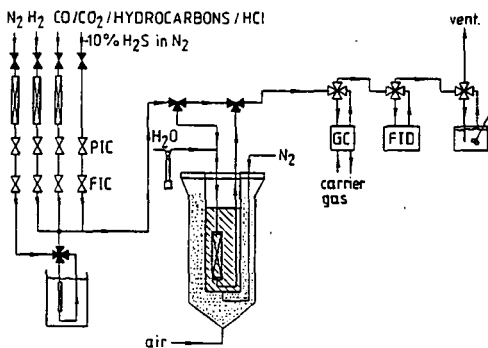


Figure 2: Apparatus used for sulfidation-regeneration experiments.

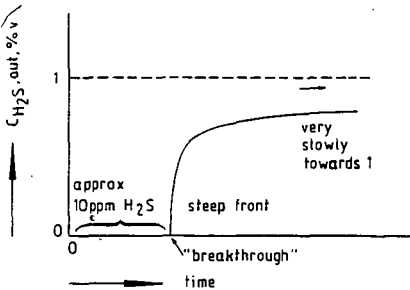


Figure 3: Typical H₂S breakthrough- or elution curve.
Response of C_{H₂S,out} on stepwise increase of C_{H₂S,in} at time = 0.

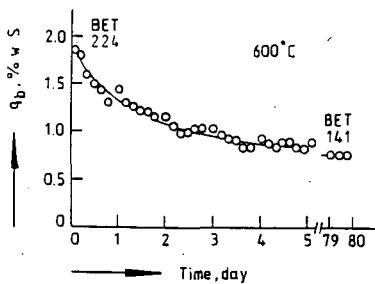


Figure 4: Stabilisation of acceptor at 600 °C. Sulfur captured at breakthrough as a function of time.

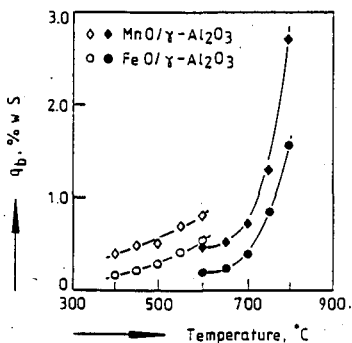


Figure 5: Influence of temperature on breakthrough capacity. Acceptors: 9.1 kw Mn on γ-alumina (open diamonds) 8.2 kw Mn on γ-alumina (solid diamonds) 6.5 kw Fe on γ-alumina (open circle) 4.6 kw Fe on γ-alumina (solid circle)

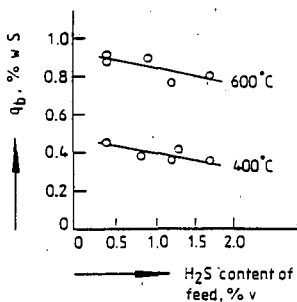


Figure 6: Influence of H₂S content of feed on breakthrough capacity. Acceptors: 9.1 kw Mn on γ-alumina. Temperature: 400 and 600 °C.

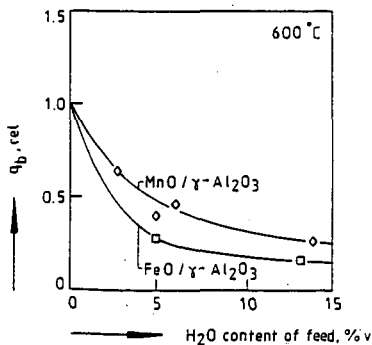
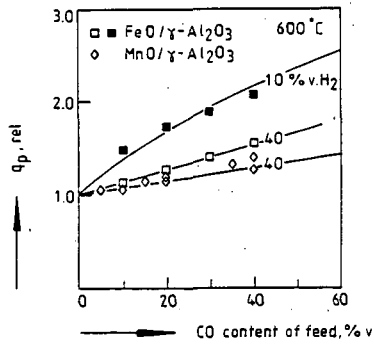


Figure 7: Influence of H₂O content, CO and H₂ content of feed on breakthrough capacity. Temperature: 600 °C. Acceptors: 9.1 kw Mn on γ-alumina 4.6 kw Fe on γ-alumina.



b: Influence of CO and H₂ content

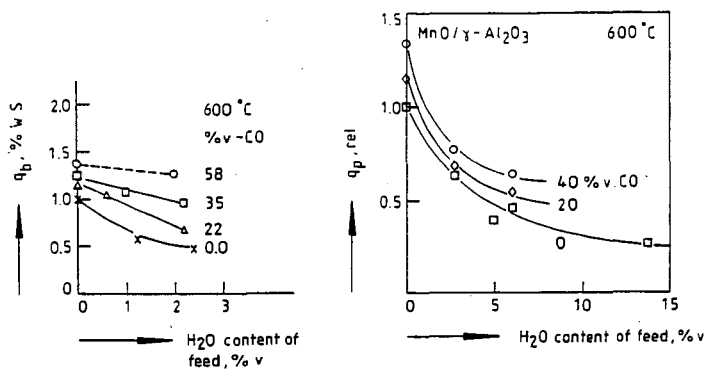


Figure 8: Combined influences of H₂O and CO in feed on breakthrough capacity. Acceptor: 8.1 %w Mn on γ -alumina. Temperature: 600 °C.
a: 10 %v H₂ b: 40 %v H₂

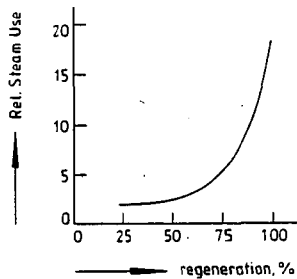


Figure 9: Relative Steam Use (RSU) as a function of percentage of acceptor that is regenerated. RSU is the amount of steam supplied during generation, divided by the amount needed stoichiometrically for complete regeneration. Acceptor: 8.1 %w Mn on γ -alumina. Temperature: 600 °C.

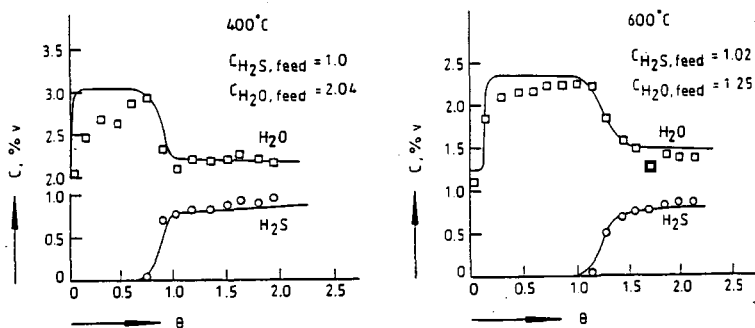


Figure 10: Comparison of experimental and simulated breakthrough curves. a: Temperature 400 °C. b: Temperature 600 °C.

COAL GASIFICATION: HIGH TEMPERATURE
H₂S REMOVAL IN A STEAM REGENERATIVE PROCESS
UNDER REALISTIC CONDITIONS.

J.P. Wakker, A.W. Gerritsen,
Delft University of Technology,
Laboratory of Chemical Process Technology,
Julianalaan 136, 2628 BL Delft, The Netherlands.

Keywords: H₂S removal, high temperature, steam regenerative

Abstract

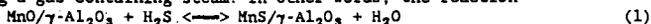
During gasification of coal H₂S, COS and some other impurities are formed. To remove H₂S and COS a steam regenerative process using MnO or FeO on γ -alumina acceptors has been developed. The acceptors can be used in the temperature range of 700-1100 K. Regeneration takes place at the same temperature with a gas containing steam. Using a 200 kW thermal coal gasification plant available at ECN in Petten the acceptors have been tested under realistic conditions at pilot plant scale. In this way the effects of other impurities and upscaling on acceptance and regeneration behaviour could be studied. No deactivation of the acceptors was found during four weeks of continuous sulfidation-regeneration cycles. Used/spent acceptors are analysed for capacity and contaminants.

Introduction

As the world oil and natural gas sources are limited quite some research effort is aimed at the utilisation of coal to replace oil and natural gas. The positive results of the demonstration plant in Cool Water, California, are now available. Also in the Netherlands the application of coal gasification for electricity production meets renewed interest which leads to a lot of new short and long term research proposals. The long term proposals mainly concern high temperature gas cleaning because this can lead to improvement of efficiency and lower investments in CGCC plants [1].

When coal is gasified it reacts with steam and air or oxygen at temperatures in the range of 800-2000 K. The raw gas produced by a gasifier generally contains a number of impurities, of which sulfur compounds are the major ones. Requirements of either downstream processes or environmental regulations usually dictate that these impurities must be removed from the gasifier effluent. The principle sulfur compound formed during gasification of coal is H₂S beside smaller amounts of COS, CS₂ and mercaptans. The total amount of H₂S produced can vary between 0.2-1.4 %v. After removing the sulfur compounds the gas can be used as a fuel, a synthesis gas or a reducing gas.

Both the gasification and the combustion of the purified gas are carried out at high temperatures. If purification is carried out at low temperature (e.g. in case ethanol amines are used) the raw gas must be cooled before entering the purification unit and reheated prior to combustion. However, if purification is also carried out at a high temperature the cooling and reheating can be eliminated or at least be simplified. The overall thermal efficiency of the whole plant will increase. Unfortunately, almost all commercially available processes for the removal of H₂S operate at low temperatures or can not be regenerated easily. Van der Linde [2] found that MnO on γ -Al₂O₃ can remove H₂S from gases at 700-850 K, while the sulfided product can be regenerated to MnO on γ -Al₂O₃ at the same temperature using a gas containing steam. In other words, the reaction



is reversible.

It has been shown by Soerawidjaja [3] that acceptors based on manganese or iron are superior to those based on cobalt, nickel and zinc. The active component in the reaction seems to be a surface spinel, MnAl₂O₄ or FeAl₂O₄. Using available thermodynamic data [4,5], equilibrium constants and enthalpy changes can be estimated. The thermodynamic equilibrium constants of the sulfidation of MnAl₂O₄ and FeAl₂O₄ in the temperature range of 700-1100 K become close to unity, while

those of MnO and FeO are large (greater than 100), see figure 1. This means that the sulfidation of $MnAl_2O_4$ and $FeAl_2O_4$ is reversible, whereas that of MnO and FeO is irreversible. From figure 2 it can be seen that the enthalpy changes accompanying sulfidation of these metal oxides, is small in case of $MnAl_2O_4$ and $FeAl_2O_4$.

Experimental.

Acceptor preparation.

Up till now the research has taken place in a laboratory set-up using approximately 3 g of grinded and sieved alumina extrudates with particle diameters between 0.25 and 0.42 mm while a synthetic gas mixture of N_2 , H_2 and H_2S was used. The experiments described here not only concern the use of a realistic gas but also involve upscaling: 1 kg acceptor per reactor. Also the particle diameter of the acceptor increased. The γ -alumina extrudates used (Ketjen/Akzo 001-1.5E) have an average length of 4.8 mm and an average diameter of 1.7 mm. Because of the increased particle diameter and the larger amount of carrier material the impregnation method had to be adjusted to maintain the metal content and sulfur removal capacity.

For acceptor preparation the scheme in figure 3 is followed. Normally the impregnation fluid is shaken a few times during impregnation (method 1), resulting in a good acceptor. However, this technique can not be used for larger amounts of acceptor material. The main problem with the large amount of material and coarse extrudates is contacting the impregnation fluid with the carrier material in such a way that each particle is filled with the impregnation fluid. A number of techniques to improve contacting between fluid and carrier are investigated: stirring fluid only (method 2), stirring of both fluid and solids (method 3) and recycling impregnation fluid through a packed bed of carrier material (method 4). Each acceptor batch prepared is analysed for attrition, distribution of the metal oxide in each particle and between particles, metal content and capacity for H_2S removal, the last property both under laboratory conditions and under realistic conditions.

The first two criteria are evaluated qualitatively only. The metal oxide distribution can, because the oxides are dark coloured, be evaluated easily. The metal content is determined by Atomic Adsorption Spectroscopy (AAS). The equipment used for determining breakthrough capacity under laboratory conditions is described elsewhere [6].

Equipment

The breakthrough capacity and deactivation under realistic conditions are measured in an experimental set-up situated at the Energy Research Foundation (ECN) in Petten, The Netherlands. The gasifier (200 kW thermal) is build especially for research purposes and produces a fuel gas that can be used for a number of different experiments; the unused gas is flared.

The pilot plant can be divided into two main parts: the coal gasifier which supplies the realistic fuel gas and the equipment for high temperature H_2S removal in which the acceptors can be tested.

The coal gasifier can be subdivided into: the reactor, the coal feed system, the air system and the hot fuel gas system

The co-current moving bed reactor consists of a steel vessel internally fully isolated with ceramic material. At the bottom an asymmetric ashcone rotates with a low variable speed and forces the ashes and unconverted coal into the ashes waste pipe.

The air needed for gasification is sucked into the reactor through two air inlets, one situated at the top and another in the middle of the reactor. This means that the gasifier is used at underpressure, preventing gas leakage to the environment.

The coal bed can be divided into three zones:

1. the pyrolysis zone at top of the coal bed. In this zone devolatilisation of the coal takes place. Light hydrocarbons and heavy tar products are formed. Particularly the heavy tar products can cause problems when they condensate. They are nearly completely converted in the oxidation zone.
2. the oxidation zone under the pyrolysis zone. In this zone tar and hydrocarbons are oxidized by the air which is led into the reactor just above the coal bed. Moreover, part of the coal is converted into CO_2 and H_2O to produce the heat needed by the reactions in the reduction zone. The temperature raises quickly to a level of 1600-1900 K.
3. the reduction zone at the bottom of the coal bed. In this zone the products of the oxidation zone, CO_2 and H_2O , react with coal to form CO and H_2 . Because these reactions are relatively slow the reduction zone covers the greatest part of the coal bed. The fuel gas exit is situated at the bottom of the reduction zone. In case browncoal is used as feed, as in the study presented here, the fuel gas leaves the reactor at about 1000 K.

The coal feed system consists of a storage bunker, a moving band to the top of the reactor and a lock hopper on top of the reactor.

The air system can be divided into the start-up system and the main system. At a cold start air is sucked through a separate pipe in which an electric heater is mounted. When the temperature of the coal has reached such a level that spontaneous combustion takes place and partial oxidation generates enough heat to support the gasification process the electric heater is switched off and the main supply system is used.

Dust and ashes are removed from the gas stream by two cyclones. From the cyclones the gas is led into a cooler where the temperature is lowered to approximately 315 K to protect the rootsblower which sucks the air through the reactor.

Part of the hot fuel gas (approximately 900 K) is drawn off before entering the cooler and sent to the equipment for H_2S removal.

In the equipment for H_2S removal (figure 4) the following parts can be distinguished: pretreatment of the fuel gas, reactor section, gas analysis, pretreatment of regeneration- and flush gas and process control, data acquisition and registration

The fuel gas leaves the gasifier with a temperature of about 900 K. As the gas cooles down during transport to the desulfurization unit it is reheated electrically to 880 K. The hot gas passes through a silicium carbide filter, in which the dust content decreases from about 1 g/Nm^3 to about 20 mg/Nm^3 , and flows to the reactor section.

The equipment is designed in such a way that H_2S can be removed continuously. Three reactors are required (R1..R3). During operation one reactor is in the acceptance stage, a second in the regeneration stage while the third reactor is flushed. After H_2S breakthrough of the reactor in the acceptance stage all reactors are switched to their next stage.

Each reactor is filled with 1 kg of acceptor material, MnO or FeO on a γ -alumina carrier. The temperature is kept at about 880 K by a heating jacket.

The raw fuel gas is sent downwards through the reactor. Regeneration and flushing take place in the opposite direction. In this way the removal of H_2S from the acceptors is faster and more complete (after acceptance most of the H_2S is accumulated in the top of the acceptorbed). For the regeneration a H_2O , H_2 , N_2 -mixture is used. Flushing is done with an H_2 , N_2 -mixture.

The H_2S concentrations in the raw fuel gas, the cleaned fuel gas and the regeneration off gas are needed to calculate mass balances and breakthrough capacities. Moreover, the CO_2 , CO and H_2O concentrations in the raw fuel gas are measured.

Three different analysis apparatuses are used: a Beckman gas chromatograph, a Radas H_2S -monitor and a Metrohm titration unit. The H_2O concentration in the raw fuel gas is measured from time to time separately. The gas chromatograph measures the composition of the raw fuel gas. The monitor registers the H_2S concentration in the

cleaned fuel gas by means of UV absorption. Two ranges can be chosen: 0-500 and 0-5000 ppm. The titration unit is used to measure the amount of H_2S produced during regeneration. For this purpose a pump continuously sucks a flow through a critical capillary from the regeneration off-gas into a titration vessel. By using different capillaries the flow can be changed (50, 100 or 150 Nml/min). The titration unit is the same as described with the laboratory set-up [5].

The mini plant is automated by a system which consists of a Tulip AT personal computer, equipped with a Keithley 570 interface and runs under the software package Asyst.

The system has the following tasks:

- control of the acceptance-regeneration cycles in the three reactors, using 12 channels. A number of boundary conditions, e.g. time elapse of the stages, measurement of breakthrough and safety, are taken into account.
- data acquisition of three different channels and filing of the data gathered in a clear structure.
- presentation of the data in such a way that mass balances can be calculated and the course of the breakthrough capacity as a function of time (days) can be followed.

The plant can be used 24 hours a day. Each acceptance-regeneration cycle results in three sets of data: the H_2S concentration in the raw- and in the cleaned fuel gas (gas chromatograph and monitor respectively) and, from the regeneration stage, the amount of H_2S in the regeneration off-gas (from the titration unit).

Results and discussion

Table 1 shows the necessity of improving contact between impregnation fluid and carrier material. Shaking of the fluid from time to time (method 1) results in a poor distribution of the metal oxide, a low metal content and a low capacity (batch 1). Stirring the fluid only (method 2) gives attrition. This attrition could be lowered by stirring at a lower speed, but applied to larger quantities the contact is influenced negatively. The results of batch 3 show that stirring of both fluid and solids (method 3) results in too large attrition as well. The results of batch 4 show, in contrast with methods 1, 2 and 3, that method 4 (recycling the impregnation fluid through a packed bed of carrier material) improves contact between carrier and impregnation fluid. Attrition, distribution of the metal, metal content and capacity correspond with previous work [3]. Batches 5 to 9 confirm these observations.

The breakthrough capacities obtained in the laboratory set-up are generally somewhat lower than the optimum capacity (0.70-0.85 with regard to 0.80-1.0 $X_w S$). The use of larger particles is the main reason.

Decreasing impregnation time from about 18 hours to 2 to 3 hours has no influence on breakthrough capacity.

The results of the iron containing batches 10 and 11 are similar to those of previous work [3] if attrition, distribution of the metal, metal content and breakthrough capacity are taken into account.

Batches 10, 6 and 9 were tested continuously during four weeks under realistic conditions in reactors 1, 2 and 3 respectively. Each reactor was submitted to about 50 acceptance-regeneration cycles. The measurements which are most reliable with respect to their mass balance are discussed below. Examples of the acceptance and regeneration curves are shown in figures 5 and 6.

In figures 7, 8 and 9 the breakthrough capacities, the amount of H_2S released during regeneration and the CO and H_2O concentrations are presented as a function of cycle number. Most of the H_2O concentrations in the figures were not measured quantitatively but result from equilibrium calculations, in which it is supposed that thermodynamic equilibrium between CO, CO_2 , H_2 and H_2O is reached at the desulfurization reactor inlet. As the measured points (the dots in the figures) lie somewhat higher than the calculated points, the calculated points only give an indication of the course of the water concentration.

It can be noticed easily that the acceptance- and regeneration capacities follow the CO concentration line. Increasing the CO concentration increases the

breakthrough capacity. This effect was expected because the shift reaction will consume H_2O formed during acceptance and H_2O from the feed gas according to:



From the figures it can also be concluded that the breakthrough capacity remains almost constant. In tables 2 and 3 the average breakthrough capacity and the average composition of the raw fuel gas are given.

If the breakthrough capacities obtained under realistic conditions are compared with those obtained in the laboratory set-up with a gas containing 20 %v CO, 10 %v H_2 , 5 %v H_2O and 1 %v H_2S there is a reasonable agreement. The breakthrough capacity is about 0.40 %w S for a manganese containing acceptor. The influence of the CO_2 and the higher H_2 concentration (both causing a somewhat lower capacity) is not corrected for.

When the desulfurization process described here would be applied to the Shell coal gasification process the breakthrough capacity would be much higher. As the raw fuel gas contains about 65 %v CO, 26 %v H_2 and 2 %v H_2O [7], a breakthrough capacity of approximately 1.5 %w S can be expected.

The H_2S concentration in the cleaned fuel gas depends upon gas composition, e.g. H_2O - and CO concentration. Before breakthrough the concentration in the cleaned fuel gas is lower than 40 ppmv and generally lower than 20 ppmv. Purification to a level below 1 ppmv is measured frequently.

Recently testing of new batches of the acceptors has started. At this moment batches 7, 11 and 8 (reactors 1, 2 and 3 respectively) are used during two weeks. The breakthrough capacities and regeneration behaviour are better than the results of batches 10, 6 and 9, see figure 10. From the figures it can be concluded that the acceptors show the same initial deactivation as observed during experiments in the laboratory. After this initial period the breakthrough capacity remains almost constant. Because the acceptors are still being used, they are not tested under laboratory conditions yet. Results will be available in the first half of 1990.

The H_2S concentration in the dried regeneration off gas is about 15 %v, high enough to be delivered to a Claus plant. This concentration can be increased by optimizing the composition of the regeneration gas. Under laboratory conditions, concentrations up to 40 %v (on a dry base) have been measured [8].

After the experiments at EGN the used/spent acceptors were tested again under laboratory conditions. The breakthrough capacities showed to be lower than expected, probably due to sintering of the carrier material. This sintering can be caused by undesirable high temperatures (up to 1000 K) as were measured in the reactors. In table 4 the results are summarized. The breakthrough capacities of the fresh and used/spent acceptors are obtained under exactly the same conditions. The breakthrough capacity of the manganese based acceptors decreased stronger than that of the iron based acceptor. This difference could be explained by the fact that the iron based acceptor is not used for testing the equipment. Some samples of the used/spent acceptors were analysed with XPS (X-ray Photoelectron Spectroscopy) and ESCA (Electron Spectroscopy for Chemical Analysis) to determine surface composition of the acceptors. Clearly some carbon, sulfur, nitrogen and chloride is present and, of course, aluminium and manganese or iron.

Conclusions

From the experiments it can be concluded that:

- the experimental set-up for testing acceptors under realistic conditions including process control and data acquisition operates without any serious problems.
- during the test period no deactivation of the acceptors is observed.
- during the second test period the acceptors have a higher capacity.
- the fuel-gas is cleaned to a level of 0-20 ppmv.
- the breakthrough capacity of the acceptors is quite low, a feasibility study has to indicate whether this is a main problem.

- the iron based acceptor seems to be less sensitive to deactivation caused by the use of a realistic fuel gas than the manganese based acceptors, but this difference could be explained by testing the equipment with the manganese containing acceptors.
- the H₂S concentration in the regeneration off-gas is high enough to deliver to a Claus plant, and can be optimized further.

Literature

1. J.J.M. Snepvangers, J. Stork, Kolanvergassing anno 1987, NEOM Publication, 874703/2319, August 1987.
2. B.J. van der Linde, An experimental study on the use of manganese oxide on γ -alumina acceptors for the flue gas desulfurization, Thesis, Delft University Press, 1982.
3. T.H. Soerawidjaja, Steam regenerative H₂S removal at high temperatures using metal oxide on alumina acceptors, Thesis, Delft University Press, 1985.
4. J. Barin, O. Knacke, O. Kubachewski, Thermochemical Properties of Inorganic Substances, Springer Verlag, Berlin, 1973, Supplement 1976.
5. D.R. Stull, H. Prophet, JANAF Thermodynamical Tables, 2nd ed., National Bureau of Standards, Washington D.C., 1971.
6. J.P. Wakker, A.W. Gerritsen, High Temperature H₂S Removal from Process Gases in a Steam Regenerative Process Using MnO or FeO on γ -alumina Acceptors, presented at this meeting.
7. L. David Smith (ed.), Deer Park unit points the way, Modern Power Systems, 3(8), August 1988.
8. R. van der Heijden, A.W. Gerritsen, Regeneratieve verwijdering van zwavelwaterstof bij 600°C, I²-Procesttechnologie, 10, 11-18, 1987.

Table 1. Results of acceptor preparation and characterization.

Batch #	Metal	Preparation				Results				
		Alumina (kg)	Volume (l)	Impregnation		Attrition	Metal distribution		Metal content (Zwt)	Capacity (Zwt S)
				Method	Time (h)		Per particle	Between particles		
1	Mn	0.02	0.07	1	18	no	bad	bad	6.10	0.50
2	Mn	0.02	0.07	2	18	yes	good	bad	5.03	0.45
3	Mn	0.02	0.07	3	18	yes	good	bad	5.17	0.55
4	Mn	0.45	1.50	4	18	no	good	good	8.26	0.80
5	Mn	1.08	3.54	4	18	no	good	good	8.44	0.70
6	Mn	1.80	5.94	4	18	no	good	good	7.51	0.80
7	Mn	1.80	6.00	4	24	no	good	good	8.46	0.70
8	Mn	2.00	6.00	4	3	no	good	good	8.09	0.85
9	Mn	1.90	6.30	4	2	no	good	good	8.98	0.70
10	Fe	1.90	6.30	4	18	no	good	good	6.95	0.55
11	Fe	1.50	5.00	4	3	no	good	good	5.17	0.55

Table 2. Average breakthrough capacities of acceptors under realistic conditions.

Acceptor	Breakthrough capacity (Zw S)
FeO (reactor 1)	0.25
MnO (reactor 2)	0.20
MnO (reactor 3)	0.18

Table 3. Average fuel gas composition.

Compound	Zv
CO	16.6
H ₂	17.0
CO ₂	12.6
H ₂ O	3.8 (from eq. calc.)
H ₂ S	0.3-0.4
CH ₄	0.9
dust	20 mg/Nm ³

Table 4. Breakthrough capacities of fresh and used/spent acceptors.

	Batch	Acceptor	Capacity fresh (Zw S)	Capacity used/spent (Zw S)	Deactivation (%)
Reactor 1	10	FeO	0.55	0.35	36
Reactor 2	6	MnO	0.80	0.39	51
Reactor 3	9	MnO	0.70	0.35	50

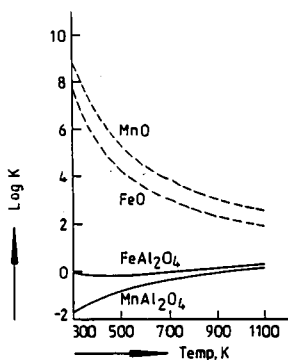


Figure 1. Thermodynamic data of sulfidation, equilibrium constants.

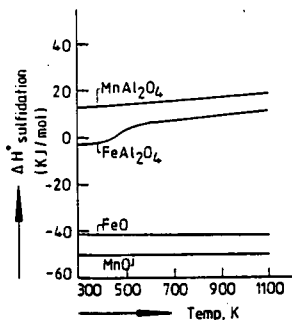


Figure 2. Thermodynamic data of sulfidation, heat of reaction.

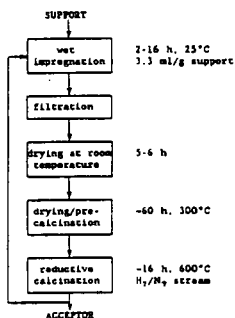


Figure 3. Preparation of acceptors.

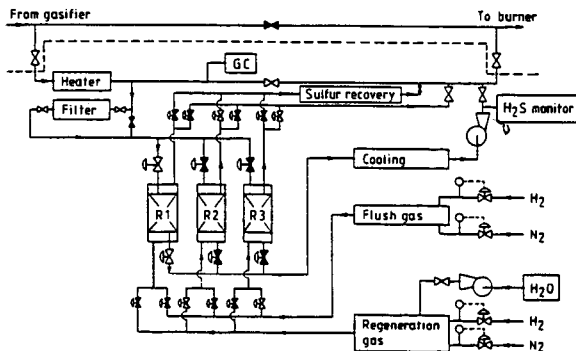


Figure 4. Schematic flow sheet of the pilot plant for H_2S removal.

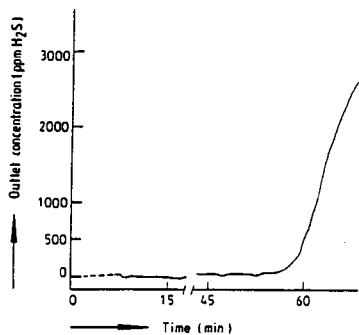


Figure 5. Measured breakthrough curve.

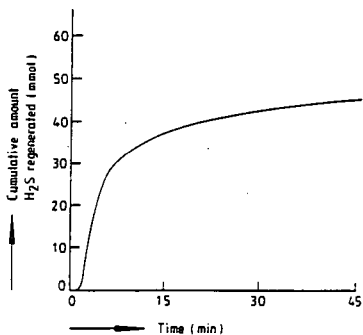


Figure 6. Measured regeneration curve.

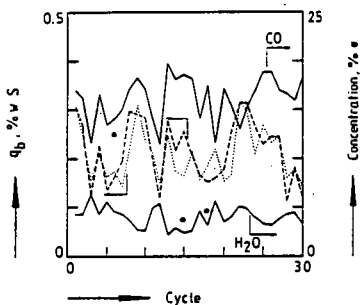


Figure 7. Captured and regenerated amount of sulfur of reactor 1. $\text{FeO}/\gamma\text{-Al}_2\text{O}_3$, batch 10 and the CO and H_2O concentrations.
 - - - - Captured amount sulfur
 - - - - Regenerated amount sulfur
 • Measured H_2O concentration

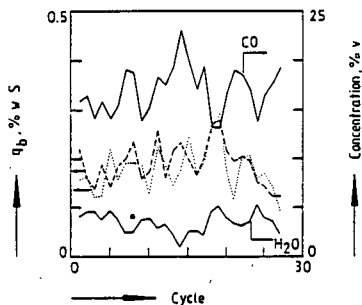


Figure 8. Captured and regenerated amount of sulfur of reactor 2. $\text{MnO}/\gamma\text{-Al}_2\text{O}_3$, batch 6 and the CO and H_2O concentrations.
 - - - - Captured amount sulfur
 - - - - Regenerated amount sulfur
 • Measured H_2O concentration

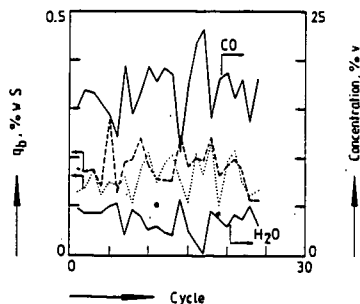


Figure 9. Captured and regenerated amount of sulfur of reactor 3. $\text{MnO}/\gamma\text{-Al}_2\text{O}_3$, batch 9 and the CO and H_2O concentrations.
 - - - - Captured amount sulfur
 - - - - Regenerated amount sulfur
 • Measured H_2O concentration

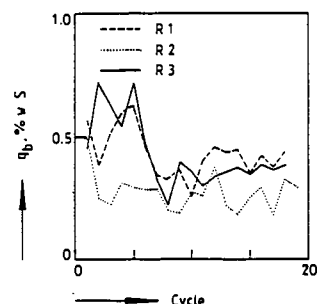


Figure 10. Breakthrough capacities of batches 7 (---), 11 (....) and 8 (—).

INTEGRATION AND TESTING OF HOT DESULFURIZATION
AND THE TEXACO COAL GASIFICATION PROCESS FOR POWER GENERATION

Allen M. Robin, Jimmy C. Wu, Jerry S. Kassman
Texaco Inc., Montebello Research Laboratory
P.O. Box 400, Montebello, California 90640

Keywords: Texaco Gasifier, Coal Gasification, In-Situ and
External Desulfurization.

OBJECTIVE:

The overall objective of this project is to develop and demonstrate an improved, high efficiency, integrated coal gasification combined cycle (IGCC) electric power generation system on a process development unit (PDU) scale. The work includes investigations of in-situ desulfurization and hot gas cleanup as applied to the Texaco Coal Gasification Process. New specialized instrumentation, being developed by DOE/METC for coal gasification, also will be tested during this project.

BACKGROUND STATEMENT:

The Texaco Coal Gasification Process (TCGP) is a second generation, commercially proven coal gasification process that is capable of meeting all present and proposed environmental regulations. There are currently three commercial plants in operation (excluding the Cool Water plant which has been shut down after a five year successful demonstration) with two more under construction.

The TCGP is a continuous, entrained flow, pressurized gasification process for converting coal, coal derived materials, or other suitable solid carbonaceous feedstocks into syngas, which is composed primarily of hydrogen and carbon monoxide. The solid feedstock is ground and fed as a concentrated water slurry into a refractory-lined pressure vessel through a special burner where it is mixed with an oxidant such as pure oxygen, air or oxygen enriched air to produce syngas. Syngas cooling is accomplished either indirectly by a syngas cooler or directly by quenching with water, depending on the end use for the gas. The syngas cooler mode is typically selected for process sequences in which methanol or fuel gas is the desired end product. The direct water quench mode is particularly attractive for those applications where pure hydrogen is required for ammonia or petrochemical synthesis.

Currently, gas contaminant removal is accomplished by conventional methods that require the gas to be cooled to ambient temperature or below. As in the TCGP based Cool Water 120-megawatt IGCC electric power plant, sulfur emissions are reduced to 10% of the New Source Performance Standards (NSPS). Economic studies indicate that, compared to a conventional pulverized coal plant with stack gas cleanup, a TCGP based IGCC system would be 15% more efficient, and have comparable investment costs. An additional increase in process thermal efficiency and a major reduction in capital cost can be realized if the hot gas does not have to be cooled down to ambient

temperature for cleaning before being fed to a combustion turbine. However, the major hot gas contaminants which include sulfur compounds, particulates, volatile metals and nitrogen compounds, still have to be removed.

Desulfurization, specifically, can be accomplished either in-situ, by including a sulfur sorbent with the coal water slurry feed to the gasifier, or external, by contacting the gas with a sorbent downstream of the gasifier vessel. In-situ desulfurization could provide the lowest investment cost and simplicity of design. External desulfurization has a potential for very high sulfur removal and the production of a salable by-product. A significant amount of work has been done by other investigators in the areas of in-situ and external desulfurization using either a fluidized bed or a moving bed coal gasifier. However, little work, except for that reported here, has been done to study hot desulfurization in conjunction with an entrained bed gasifier such as that used in the TCGP.

PROJECT DESCRIPTION:

To help achieve the goal of clean, low cost power generation from coal, Texaco submitted an unsolicited proposal in July, 1986 to develop and demonstrate the integration of high temperature desulfurization with the TCGP. The proposal resulted in a Cooperative Agreement with the DOE/METC which was awarded on September 30, 1987. This project is expected to take five years to complete at a cost of \$17 MM which will be shared between Texaco and the DOE/METC.

The test program is divided into five phases defined as follows:

- o Phase I - Preliminary Desulfurization Research.
- o Phase II - Process Optimization.
- o Phase III - Prepare Integrated System.
- o Phase IV - Integrated System Commissioning.
- o Phase V - Integrated PDU Tests.

The first three years (Phases I and II) are devoted to proof of concept and selection of the optimum processes which will make up the integrated system. The following two years (Phases III - V) will be devoted to the design, construction and operation of the integrated system. The project is currently in its third year. This paper discusses the results achieved during the Phase I and part of the Phase II work.

THEORETICAL STUDIES AND BENCH SCALE TESTS

Theoretical studies and bench scale tests were done to select suitable in-situ and external high temperature desulfurization sorbents for later evaluation on a process development unit (PDU) scale. These studies and tests were done at three different locations: Texaco Research Center, Beacon (TRCB), Texaco's Montebello Research Laboratory (MRL), and the Massachusetts Institute of Technology (MIT).

The work done at TRCB⁽³⁾ and MRL was to identify and characterize in-situ desulfurization sorbents suitable for use with the TCGP. The

results indicated that for in-situ desulfurization, only two throw-away systems; iron oxide and iron oxide/sodium oxide, had potential for success during oxygen and air gasification in the slagging mode. The results also indicated that the most effective use of calcium oxide would be to inject it into hot syngas at a location after the slag has solidified.

The work done at MIT was to identify external desulfurization sorbents suitable for use with the TCGP. Four different mixed metal oxide sorbents (Zn-Fe-O, Zn-Ti-O, Cu-Al-O, Cu-Fe-Al-O) were synthesized and tested. Also, a commercial iron oxide and a zinc ferrite (L-3201/UCI) sorbent were evaluated in cyclic sulfidation-regeneration tests. The MIT results indicated that the ZnO-based sorbents were limited to operating temperatures below 1100 deg. F in the highly reducing TCGP syngas streams. The Zn-Ti-O sorbent showed a higher temperature capability up to 1300 deg. F. The Cu-Fe-Al-O sorbent showed merit for regenerative desulfurization of TCGP syngas at all temperatures up to 1400 deg. F.

PDU TESTING - IN-SITU DESULFURIZATION

The PDU testing was conducted at MRL using an existing pilot plant gasification unit modified to test in-situ and external desulfurization. The gasifier in the PDU is equipped with a syngas cooler in addition to a water quench. The gasifier is normally operated at a pressure of 350 psig and at a temperature between 2000 and 3000 deg. F. The capacity of the PDU is 15-20 tons/day of moisture free coal. A PFD of the modified MRL pilot plant is shown in Figure 1. Sulfur removal was accomplished primarily in-situ by including sorbent(s) with the coal water slurry feed to the gasifier. External high temperature desulfurization was examined in a downstream fixed bed system using a slip stream of syngas generated during PDU operations.

During the Phase I PDU testing, a 1-day shakedown run and three 3-day screening runs were completed. All of the runs were made at a gasifier pressure of 350 psig using high purity oxygen (99.75 vol%) as the oxidant. A medium sulfur Pittsburgh No.8 coal (2.1 wt% S) was used for all runs except the last run; in the last run, a high sulfur Powhatan coal (5.1 wt%) was gasified. Table 1 lists the key properties of the two coals. Two different in-situ sulfur sorbents, Fine OX (high purity iron oxide, Fe₂O₃) and soda ash (high purity sodium carbonate, Na₂CO₃), were selected for testing based on the results of thermodynamic calculations and bench scale tests. Soda ash was tested only as a co-sorbent with Fine OX.

Limestone or dolomite initially selected for use as an in-situ sulfur sorbent, was rejected when the bench scale testing indicated that the calcium would preferentially react with the silicate phase in the coal slag instead of with the H₂S in the syngas.

A summary of the operating conditions and %H₂S reduction in the syngas for each test period/run is shown in Table 2. The data indicate that a nominal 50% reduction of H₂S in the syngas was achieved at a normal gasifier operating temperature, using iron oxide as the in-situ sulfur sorbent. The slag generated during the tests was stable. This level of H₂S reduction in the syngas was achieved

Figure 1 MRL GASIFICATION PDU FOR TESTING HIGH TEMPERATURE DESULFURIZATION

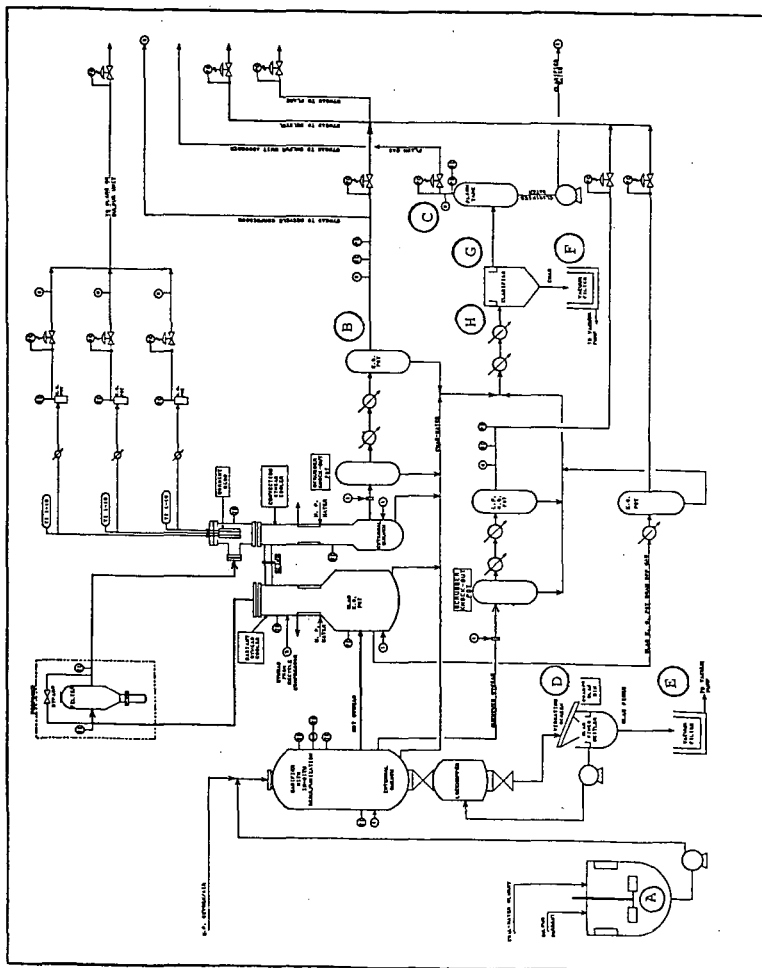


Table 1 Charge Stock Test Results

Coal	Pitts. No.8	Powhatan
Moisture	2.80	4.36
Proximate Analysis (dry basis)		
Volatile Matter, wt%	37.37	41.13
Fixed Carbon	56.08	48.07
Ash	6.55	10.80
Ultimate Analysis (dry basis)		
Carbon	78.41	71.16
Hydrogen	5.13	5.09
Nitrogen	1.45	1.04
Sulfur	2.14	5.07
Ash	6.55	10.80
Oxygen (by diff.)	6.32	6.84
Gross Heating Value, btu/lb	14092	13037
Ash Fusion Temp., deg. F		
Initial	1995	1960
Softening	2195	2005
Hemispherical	2280	2095
Fluid	2350	2355

Table 2 Phase I In-Situ Desulfurization Test Matrix

Run/Test Period	Length * Run/Test Period (Hr)	In-Situ Sulfur Sorbent Dosage (Lb/Lb S in Coal)		Gasifier Temp. (deg.F)	Vol% H2S In Gas	%Reduct. In H2S
		Fine OX	Soda Ash			
1/	26.4/	0	0	To	0.47	-
2/	69.4/					
A	14.4	3.5	0	To	0.26	44.7
B	16.7	3.5	0	To-200	0.23	51.1
C	9.3	3.5	0	To-300	0.17	63.8
D	15.5	3.5	0	To-100	0.26	44.7
E	11.0	4.5	0	To-100	0.26	44.7
3/	59.3					
A	11.6	3.5	1.5	To	**	-
B	13.0	3.5	1.5	To-200	**	-
C	23.0	3.5	2.0	To	0.20	57.4
D	9.0	3.5	2.0	To-100	0.20	57.4
4/	84.0					
A	15.3	0	0	To	1.50	-
B	12.0	1.7	0	To	0.90	40.0
C	12.0	1.7	0	To-150	0.83	44.7
D	12.0	2.6	0	To	0.76	49.3
E	12.0	2.6	0	To-150	0.71	52.7
F	12.0	2.6	0.25	To-125	0.69	54.0
G	6.2	2.6	0.25	To-175	0.71	52.7

* Run Length = Total on-stream time including the time between steady state operating periods.
 ** No stable readings from on-line mass spectrometer were available.

for both the medium sulfur Pittsburgh No.8 coal and the high sulfur Powhatan coal. Higher levels of desulfurization were achieved by lowering the gasifier temperature. However, this resulted in lower carbon conversions which produced too much char to be effectively handled in the PDU.

A higher H₂S reduction of about 60% in the syngas was achieved at a normal gasifier operating temperature using iron oxide plus a high dosage of sodium carbonate added to the Pittsburgh No.8 coal slurry. However, the slag generated was unstable (i.e. sulfide in the slag would oxidize on exposure to ambient air) and there were solids handling and plugging problems experienced during the tests because of the extremely small solid particles produced which were cemented together with condensed sodium compounds. A low dosage of sodium carbonate, tested during the Powhatan coal run, resulted in no improvement in H₂S reduction. Because of these results we decided to abandon further testing of sodium carbonate.

Most of work in the current Phase II program involves air gasification in the PDU. Three runs have been completed, using Pittsburgh No. 8 coal, in the same gasifier used for the Phase I PDU testing. A 4-day baseline run, a 3-day Fine OX in-situ desulfurization run and a 3-day dolomite desulfurization run have been made. The results indicate that a nominal 24% reduction of H₂S in the syngas was achieved at a normal gasifier operating temperature, using Fine OX as the in-situ sulfur sorbent. Higher levels of desulfurization were achieved by lowering the gasifier temperature or increasing the dosage of Fine OX. The highest level of H₂S reduction in the syngas achieved was 38%. Again, this resulted in lower carbon conversions which produced too much char to be effectively handled in the PDU.

Preliminary data indicate that a 65-70% reduction of H₂S in the syngas was achieved during the dolomite desulfurization run. The dolomite was injected as a water slurry into the syngas in the radiant syngas cooler. Most of the slag had been removed or solidified at the point of injection to prevent undesirable reactions between calcium and silica. Typical wet syngas compositions from the oxygen and air gasification runs with in-situ sulfur sorbent(s) can be seen in Table 3.

Table 3 Typical Wet Syngas Composition

Coal	Pitts. No.8	Powhatan	Pitts. No.8
Oxidant	Oxygen	Oxygen	Air
Syngas Composition			
A, mole%	0.06	0.10	0.64
H ₂	29.96	28.39	11.36
CO	38.91	37.17	14.70
CO ₂	9.88	11.89	8.82
N ₂	1.57	2.28	53.78
CH ₄	0.09	0.00	0.04
H ₂ S	0.35	1.18	0.20
COS	0.03	0.05	0.00
H ₂ O	19.15	18.94	10.46
Total	100.00	100.00	100.00

PDU TESTING - EXTERNAL DESULFURIZATION

Four different external sulfur sorbents (zinc ferrite/T-2465, zinc ferrite/E-13A, zinc copper ferrite/L-2952, and zinc titanate/L-3014) were selected for the Phase I PDU testing based on the results of theoretical studies and the recommendations of METC. The external sorbent testing system, as shown in Figure 1, consists of three parallel, fixed sorbent beds mounted in the top of the convection syngas cooler vessel. The four external sorbents were evaluated in single pass sulfidation using a slip stream of 1000-1300 deg. F syngas fed to each of the three beds, with an H₂S concentration between 1,600 and 14,500 ppm.

The H₂S concentration was constant throughout each sorbent bed run; the variation in H₂S levels is a result of the different gasifier operating temperatures, in-situ sulfur sorbents and dosages, and the different coals used. The following conclusions and recommendations were made based on the Phase I performance of the external sorbents:

- o All four sorbents evaluated achieved H₂S removals greater than 99.9% before breakthrough.
- o The ferrite based sorbents evaluated are not suitable for use with the TCGP oxygen blown syngas because of a severe loss in crush strength that occurs after only a single sulfidation, and the catalyzing of the methanation reaction.
- o Zinc titanate retained more of its crush strength and had a higher sorbent utilization in sulfidation only testing.
- o Formulations of zinc titanate with more zinc should be tested to see if the maximum sulfur loading can be increased.

In the Phase II program, three external sulfur sorbents (zinc ferrite/T-2465, zinc titanate/L-3014/0.8 ZnT, and zinc titanate/1.5 ZnT) have been evaluated in single pass sulfidation using a slip stream of syngas during the air gasification baseline run at an inlet H₂S level of 2900 vppm. All three sorbents achieved H₂S removal of greater than 99.9% before breakthrough. Examinations of the spent sorbents after the baseline run indicated that all three were in good condition. The zinc titanates were expected to retain their crush strengths. However, we were pleasantly surprised to find that the zinc ferrite, which disintegrated during the previous oxygen gasification runs, had also retained much of its crush strength during the air gasification runs.

ADVANCED INSTRUMENTATION AND WESTINGHOUSE CERAMIC CROSS FLOW FILTER EVALUATION

Several advanced instruments being developed by METC, which could be used for process control and on-line measurements in entrained bed gasification systems with integral hot desulfurization, were identified for testing in the PDU. On-line testing of the instruments started in Phase II.

A Westinghouse ceramic cross flow filter, which was installed in the PDU, has been tested with over 100 hours of on-stream time. This

project is sponsored by the DOE with Texaco acting as a subcontractor to Westinghouse. The objective is to demonstrate the use of the filter to remove solids from the hot syngas.

FUTURE WORK:

We are currently making PDU equipment modifications to improve the reliability of the limestone/dolomite injection system for the air gasification runs.

External desulfurization testing will continue with emphasis on optimized formulations of zinc titanate. An iron oxide sorbent which we obtained from METC will also be tested.

We are continuing the testing of the advanced instrumentation and the Westinghouse ceramic cross flow filter.

REFERENCES:

- (1) Power Magazine, April 1985, p. 24-25
- (2) Robin, A.M., Becker, W.M., Leininger, T.F., "Integration and Testing of Hot Desulfurization and Entrained Flow Gasification for Power Generation Systems", Paper presented at Seventh Annual Gasification and Gas Cleanup Systems Contractors Review Meeting, June, 1987.
- (3) Robin, A.M., Wu, C.M., Najjar, M.S., "Integration and Testing of Hot Desulfurization and Entrained Flow Gasification for Power Generation Systems", Paper presented at Eighth Annual Gasification and Gas Cleanup Systems Contractors Review Meeting, May, 1988.
- (4) Robin, A.M., Wu, C.M., Kassman, J.S., "Integration and Testing of Hot Desulfurization and Entrained Flow Gasification for Power Generation Systems", Paper presented at Ninth Annual Gasification and Gas Stream Cleanup Systems Contractors Review Meeting, June, 1988.
- (5) Robin, A.M., Wu, C.M., Kassman, J.S., "Integration and Testing of In-Situ Desulfurization and the Texaco Coal Gasification Process for Power Generation", Paper presented at Sixth Annual International Pittsburgh Coal Conference, September, 1988.

H₂S REMOVAL FROM FUEL GAS DURING COAL GASIFICATION

by

Javad Abbasian, Amir Rehmat
Institute of Gas Technology, 3424 S. State Street, Chicago, IL 60616

Dennis Leppin
Gas Research Institute, Chicago, IL

Daniel D. Banerjee
Center For Research on Sulfur in Coal, Carterville, IL

Key Words: H₂S Removal, In-Situ Sulfur Capture, Sulfidation Kinetics

Introduction

The United States has large reserves of high-sulfur, caking Eastern bituminous coal. Because of the restrictive environmental emission requirement, this coal cannot be used directly for generation of power, unless the station is equipped with sulfur dioxide scrubbers, which raises the cost of power. One approach to meet the environmental emission requirement and to maintain or improve the overall power generation efficiency is the development of hot gas cleanup systems to remove sulfur and particulate contaminants from the fuel gas thereby eliminating the efficiency losses associated with the cold gas cleanup methods such as wet scrubbing.

Simplicity, efficiency, and cost containment are all integral parts of the development of the sulfur removal systems. An attractive system for coal gasification is one in which high-sulfur coal is gasified; sulfur in the coal is retained within the gasifier with ash, eliminating the need for gas cleanup; gas is available for use without first cooling it to preserve the sensible energy; and water vapor is retained in the product gas to make a substantial contribution in the combined-cycle power output. These criteria can be met through the use of a calcium-based sorbent such as limestone or dolomite directly in the fluidized-bed gasifier, which acts as both a catalyst for the gasification reactions and captures sulfur as calcium sulfate.

The Institute of Gas Technology (IGT) has already developed the U-GAS Process to produce fuel gas from coal. The U-GAS process uses a single-stage fluidized-bed reactor to efficiently convert any type of coal, either run-of-mine or washed, into low- or medium-Btu fuel gas that can be used in industrial plants or utility power plants.(2) The process has been developed during 10 years of testing in a 30 tons of coal per day capacity pilot plant located in Chicago and is currently being commercialized. In a new configuration of the U-GAS process, the U-GAS One-Step Desulfurization Process, limestone or dolomite is fed into the coal gasifier to capture and remove sulfur compounds from the fuel gas within the gasifier. Under the reducing conditions of the gasifier, limestone reacts with sulfur compounds to significantly reduce the sulfur content of the fuel gas.

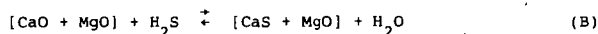
The Gas Research Institute (GRI) was interested in developing a process whereby in-situ desulfurization was used in a coal gasification process to produce power or synthesis gas (for the production of methane) as co-product.(1) Under the sponsorship of GRI and the Department of Energy, a limited number of tests were conducted at pilot plant facilities that verified the feasibility of in-situ sulfur removing techniques(2,3). IGT has recently conducted a series of in-situ desulfurization tests with coal and limestone co-feeding to a high-pressure coal gasifier (see Figure 1). The purpose of these tests was to determine the effects of pressure and temperature on the extent of in-situ sulfur removal within the gasifier. These tests were conducted at gasification pressures ranging from 1 to 3 MPa in the high-pressure Process Development Unit (PDU), which is based on IGT's U-GAS fluidized-bed coal gasification process. The result of these recent high-pressure tests indicates that the approach to equilibrium usually exceeds 84%.(4)

Researchers in the field of chemical kinetics of limestone/dolomite reactions with hydrogen sulfide(5-14) have already verified the potential use of these sorbents for sulfur capture. The reaction of calcined limestone/dolomite is very rapid, and the reaction almost approaches equilibrium. On that basis, it is possible to capture substantial quantities of sulfur and discharge it with the ash. Based on equilibrium considerations, it is feasible to remove up to 90% sulfur using this process.

Work on the desulfurization reactions in the literature has not sufficiently addressed the reaction conditions in the context of coal gasification processes and the kinetics of the sulfidation reaction at the gasification conditions.

This study, which was jointly funded by the Gas Research Institute and the State of Illinois Center for Research on Sulfur in Coal (CRSC), was undertaken to obtain comprehensive experimental data on the sulfidation reactions at gasification conditions to determine the kinetics of this gas/solid reaction.

In the process, the primary sulfidation reactions take place within the fluidized-bed gasifier under reducing conditions. The limestone is calcined at gasification conditions; sulfur capture occurs through the reaction of calcium oxide with hydrogen sulfide:



The specific information obtained in this investigation includes --

1. Determination of the effects of the following variables on the rate of Reaction B.

- Temperature
- Pressure
- H₂S Concentration
- Sorbent Particle Size

2. Determination of the kinetic rate expression for Reaction B as a function of the above variables.

Experimental

The sulfidation reaction tests involving the reaction between CaO and H₂S were conducted in a quartz thermobalance at atmospheric pressure. The effects of sample weight, gas flow rate, particle diameter, H₂S concentration, and temperature on the reaction rate were determined. The thermobalance apparatus and the test operating procedure have been discussed elsewhere(14).

The sorbent chosen for the complete kinetic study in this program was obtained from New Enterprise Stone & Lime Co., Inc., located in Pennsylvania. This material has already been used by the Institute of Gas Technology (IGT) and KRW Energy Systems, Inc. in fluidized-bed gasification tests. Elemental analysis were conducted on this sorbent, the results of which are given in Table 1.

The sorbent (dolomite) was screened and divided into four batches of different particle size range. The range of particle size for the four batches was -80, -45+50, -25+30, and +16 mesh. The complete particle size distribution is given in Table 2.

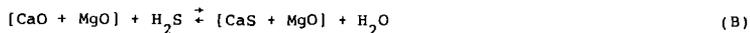
Previous investigation(15) had indicated that the reaction of CaO with H₂S does not depend on the gas composition as long as a constant level of H₂S is maintained. Therefore, in all the tests conducted in this study, the reactant gas consisted of H₂S/H₂/He mixtures. The ratio of hydrogen to hydrogen sulfide was maintained at about 3:1 to prevent dissociation of hydrogen sulfide to elemental sulfur.

To determine the effect of hydrogen sulfide on the reaction rate, and the order of the reaction with respect to H₂S concentration, a series of four tests were conducted with a sample from batch No. 1 (-80 mesh) at 980°C. The concentration of H₂S in this series of runs was 0.8%, 1.6%, 2.5%, and 3.75%. A plot of CaO conversion versus time is presented in Figure 2.

Sulfidation reaction tests were conducted using samples from batch nos. 1, 3, and 4 to determine the effect of intraparticle diffusion on the reaction rate. These tests were conducted at 980°C with a reactant gas containing 3.75% hydrogen sulfide. Figure 3 shows the conversion of calcium oxide versus time as a function of particle size.

Results and Discussions

The conversion of calcium oxide in the sulfidation reaction is calculated using the following formula:



$$\% \text{ Conversion} = \frac{56 X (\text{weight gained})}{16 X (\text{calcined sample weight}) X (\% \text{ CaO in the calcined sample})} \quad (1)$$

where 16 is the difference in the atomic weight of gained sulfur and lost oxygen and 56 is the molecular weight of calcium oxide.

The rate expression for Reaction B is --

$$-r_{\text{CaO}} = \frac{-1}{S_r} \frac{dN_{\text{CaO}}}{dt} = \bar{K}_s [\text{H}_2\text{S}]^n \quad (2)$$

where r_{CaO} is the rate of the reaction, N_{CaO} is the number of moles of calcium oxide, S_r is the surface of unreacted core of the particle, $[\text{H}_2\text{S}]$ is the concentration of hydrogen sulfide, and \bar{K}_s is the overall reaction rate constant.

Assuming the particles are spherical, Equation 2 can be written as --

$$-r_{\text{CaO}} = \frac{-1}{4\pi r_c^2} \frac{dN_{\text{CaO}}}{dt} = \bar{K}_s [\text{H}_2\text{S}]^n \quad (3)$$

The rate constant \bar{K}_s can be expressed as --

$$\bar{K}_s = \frac{1}{\frac{1}{K_d} + \frac{1}{K_s}} \quad (4)$$

K_s is the intrinsic reaction rate constant and K_d is the measure of the conductance due to diffusion. The intrinsic reaction rate constant is usually expressed in Arrhenius form --

$$K_s = K_s^0 \text{Exp}(-E_a/R_g T) \quad (5)$$

where E_a is the activation energy for the reaction, T is the absolute temperature, and R_g is the ideal gas law constant. The diffusion conductance is usually expressed as --

$$K_d = \frac{D_{\text{eff}}}{L} \quad (6)$$

In Equation 6, D_{eff} represents the effective diffusivity and L is the average thickness of the diffusion layer.

Integrating Equation 3, it can be shown that --

$$1 - (1 - x_{\text{CaO}})^{1/3} = \frac{t}{\tau} \quad (7)$$

where

$$\tau = \frac{\rho_{\text{CaO}} R}{K_s [\text{H}_2\text{S}]^n} \quad (8)$$

In the above equations τ is the time required for complete reaction of a particle, x_{CaO} is the conversion of calcium oxide, ρ_{CaO} is the molar density of the sorbent, R is the average radius of the solid particles, and t is the time of reaction. It follows that $1 - (1 - x_{\text{CaO}})^{1/3}$ should be a linear function of time and the slope of such linear plot will be $1/\tau$. A plot of $1 - (1 - x_{\text{CaO}})^{1/3}$ versus time is presented in Figure 4. The order of reaction with respect to hydrogen sulfide concentration was obtained by determining the slope of the line when $\ln(\tau)$ was plotted against $\ln([\text{H}_2\text{S}])$ (Figure 5), indicating that the reaction is first order with respect to hydrogen sulfide concentration (that is, $n=1$).

From the experimental data of this study, the value of intrinsic rate constant was obtained to be 2.99 cm/s, while the effective diffusivity within the solid particle was determined to be 0.692 cm²/s. The diffusivity of hydrogen sulfide in a binary mixture of H₂S/He was calculated using the correlation by Fuller, *et al*(16) to be 7.97 cm²/s. The ratio of the effective diffusivity of H₂S within the solid particle to the open space diffusivity is 0.086. This ratio was reported by Pell(8) to be 0.056.

Tests for the effect of temperature on the sulfidation reaction rate were conducted in the temperature range of 650° to 1040°C. Figure 6 shows the Arrhenius plot of the intrinsic rate constant versus reciprocal of absolute temperature. The slope of this curve indicates that the activation energy for this material in the temperature range of 650° to 1040°C is about 7.7 Kcal/g mole. The overall rate of reaction can be written as --

$$\frac{-1}{4\pi r_c^2} \frac{dN_{\text{CaO}}}{dt} = \frac{-1}{4\pi r_c^2} \frac{dN_{\text{H}_2\text{S}}}{dt} = \left(\frac{1}{\frac{R}{2D_e} + \frac{1}{66.44} \exp\left[\frac{3889}{T}\right]} \right) [\text{H}_2\text{S}] \quad (9)$$

In Equation 9, R is the average diameter of sorbent particles in cm, T is the reaction temperature in °K, and $[\text{H}_2\text{S}]$ is the concentration of hydrogen sulfide in gram mol/cm³.

Integrating Equation 10 leads to --

$$1 - (1 - x_{\text{CaO}})^{1/3} = \left(\frac{1}{\frac{R}{2D_e} + \frac{1}{66.44} \exp\left[\frac{3889}{T}\right]} \right) \frac{[\text{H}_2\text{S}]}{\rho_{\text{CaO}} \cdot R} \cdot t \quad (10)$$

where ρ_{CaO} is the molar density of CaO in gram mol/cm³ and X_{CaO} is extent of conversion of calcium oxide.

The intraparticle diffusivity was calculated by applying the correlation by Fuller, et al(16) to the experimental data from this work. The resulting correlation is —

$$D_e = 2.6 \times 10^{-6} T^{1.75} P^{-1} \quad (11)$$

where D_e is in cm²/s, T is in degrees Kelvin and P is in atmosphere.

The results of experimental tests conducted at elevated pressure (0.2 to 3 MPa) indicated that the overall reaction rate observed in the high pressure thermobalance reactor is controlled by a combination of gas film diffusion and interparticle diffusion. The effective diffusivity and the intrinsic reaction rates could not be determined from the high pressure data.

Conclusion

The rate of reaction between a fully calcined dolomite and hydrogen sulfide have been determined and described by a rate expression that is first order with respect to hydrogen sulfide concentration. The overall reaction rate is controlled by the chemical reaction and intraparticle diffusion. The shrinking core model for spherical particles with unchanging size appears to fit the observed data very well. The activation energy was 7.7 Kcal/g mol and the effective diffusivity through the pore of the solid sorbent at 980°F and 1 atmosphere was 0.692 cm²/s, which is 8.6% of the effective diffusivity of hydrogen sulfide in gas phase.

ACKNOWLEDGEMENT

The financial support for this work was provided by the Gas Research Institute and the State of Illinois Center for Research on Sulfur in Coal.

REFERENCES CITED

1. Leppin, D., "Process Development of In-Situ Catalytic Desulfurization Fluidized-Bed Gasification for Combined Power and SNG Manufacture." Paper presented at the Eighth Annual EPRI Conference on Coal Gasification, Palo Alto, California, October, 1988.
2. Jones, F. L. and Patel, J. G., "Performance of Utah Bituminous Coal in the U-GAS Gasifier." Paper presented at the Fifth EPRI Contractors Conference on Coal Gasification, Palo Alto, California, October 1985.
3. Weldon, J., Haldipur, G. B., Lewandowski, D. A. and Smith, K. J., "Advanced Coal Gasification and Desulfurization With Calcium Based Sorbents," Am. Chem. Soc., Div. Fuel Chem. Prepr. 33, 3, 1986.

4. Bryan, B. G., Goyal, A., Patel, J. G. and Ghatge, M. R., "Results of In-Situ Desulfurization Tests in the U-GAS Coal Gasification Process." Paper presented at the Fifth Annual International Coal Conference, Pittsburgh, Pennsylvania, September 1988.
5. Rehmat, A., Abbasian, M. J., Leppin, D. and Banerjee, D. D., "Reaction of Calcium-Based Sorbents With Sulfur in Coal During Gasification." Paper presented at the International Conference on Coal Science, Eurohal, The Netherlands, 1987.
6. Chang, E. and Thodos, G., "Complex Nature of the Sulfation Reaction of Limestone and Dolomites," AIChE J. **30**, 3, 1984.
7. Keairns, D. L., Archer, D. H., Newby, R. A., O'Niell, F. P. and Vidt, E. J., "High Temperature Sulfur Removal System Development Unit," Am. Chem. Soc. Div. Fuel Chem. Prepr. **21**, 1976.
8. Borgwardt, R. H., Roache, N. F. and Brene, K. R., "Surface Area of Calcium Oxide and Kinetics of Calcium-Sulfide Formation," Envir. Progr. **3**, 2 (1984).
9. Pell, M., "Reaction of Hydrogen Sulfide With Fully Calcined Dolomite." Ph.D. Thesis, City University of New York, 1971.
10. Squires, A. M., Graff, R. A. and Pell, M., "Desulfurization of Fuels With Calcined Dolomites," Chem. Eng. Progr. Symp. Ser. **115**, 67 (1971).
11. Freund, M., "Intrinsic Global Rate Constant for the High Temperature Reaction of CaO and H₂S," Ind. Eng. Chem. Fund. **23** (1984).
12. Ruth, L. A., Squires, A. M. and Graff, R. A., "Desulfurization of Fuels With Half Calcined Dolomite," Environ. Sci. Tech., **b**, 12 (1972).
13. Kamath, V. S. and Petrie, T. W., "Path of Reaction of Hydrogen Sulfide-Carbonyl Sulfide Mixture With Fully Calcined Dolomite," Envir. Sci. Tech., **15**, 3 (1981).
14. Roache, N. F., "Reaction of H₂S and Sulfur With Limestone Particles," Ind. Eng. Chem. Process Des. Dev., **23**, 1984.
15. Abbasian, M. J., Rehmat, A., Leppin, D., Banerjee, D. D., "Desulfurization of Fuel Gas With Calcium-Based Sorbents," Fuel Proc. Tech. (to appear March 1990).
16. Fuller, E. N., Schettler, P. D. and Giddings, J. C., "A New Method for Prediction of Binary Gas-Phase Diffusion Coefficient," Ind. Eng. Chem., **58**(5), 18, 1966.

Table 1. ELEMENTAL ANALYSIS OF THE SORBENT

<u>Analysis</u>	<u>wt. %</u>
Calcium	28.5
Magnesium	4.79
Silicon	3.11
Potassium	0.46
Iron	0.34
Strontium	0.10
Carbon Dioxide	40.84

Table 2. PARTICLE SIZE DISTRIBUTION OF THE SORBENT USED

<u>Size</u>		<u>Batch No. 1</u>	<u>Batch No. 2</u>	<u>Batch No. 3</u>	<u>Batch No. 4</u>
<u>Sieve</u>		<u>(-80 mesh)</u>	<u>(-45+50 mesh)</u>	<u>(-25+30 mesh)</u>	<u>(+16 mesh)</u>
<u>Micron</u>	<u>(mesh)</u>	<u>wt % retained</u>			
1400	14	--	--	--	--
1180	16	--	--	--	100
710	25	--	--	--	--
600	30	--	--	100	--
355	45	--	0.80	--	--
300	50	--	99.2	--	--
180	80	8.83	--	--	--
150	100	57.10	--	--	--
75	200	10.73	--	--	--
45	325	9.78	--	--	--
	Pan	<u>13.56</u>	--	--	--
		100.00	100.00	100.00	100.00
$\bar{d}_p = \sum_i \bar{d}_{pi}$		140 μ	327 μ	655 μ	1290 μ

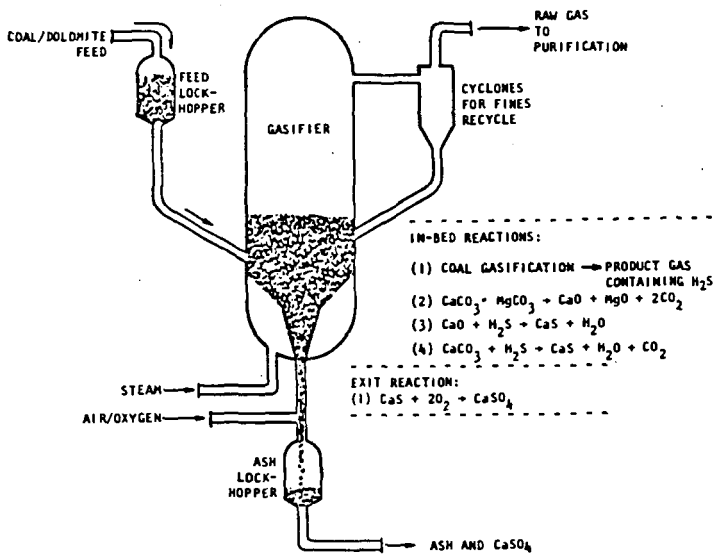


Figure 1. COAL GASIFICATION WITH IN-SITU SULFUR CAPTURE

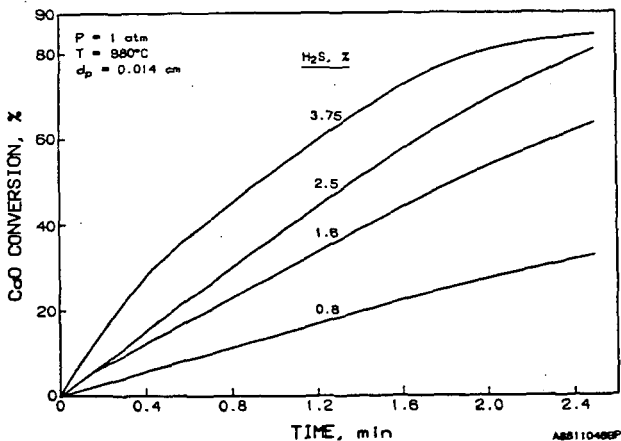


Figure 2. THE EFFECT OF H₂S CONCENTRATION ON THE SULFIDATION REACTION RATE

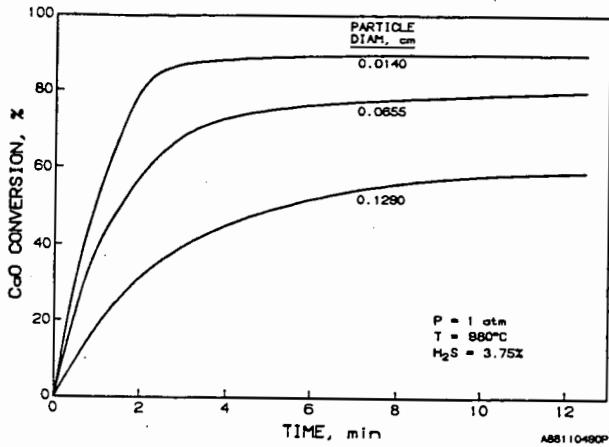


Figure 3. THE EFFECT OF PARTICLE SIZE ON THE SULFIDATION REACTION RATE

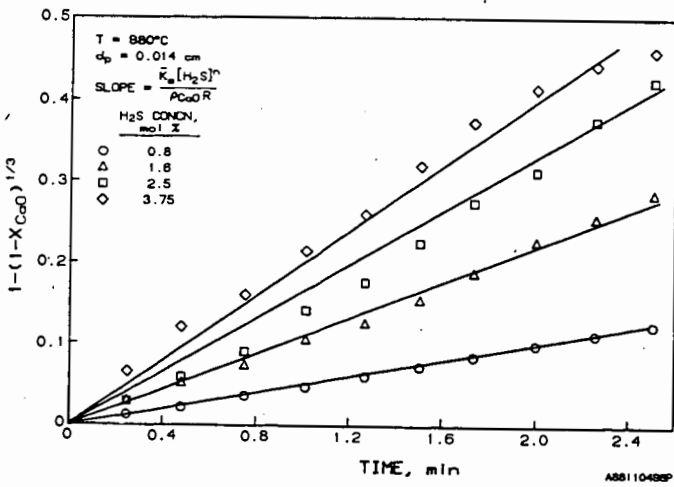


Figure 4. PLOT OF $1-(1-X_{CaO})^{1/3}$ VERSUS TIME

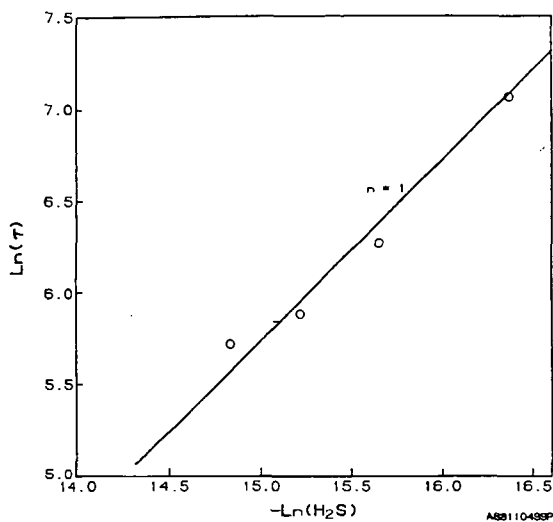


Figure 5. DETERMINATION OF THE ORDER OF THE SULFIDATION REACTION WITH RESPECT TO H_2S CONCENTRATION

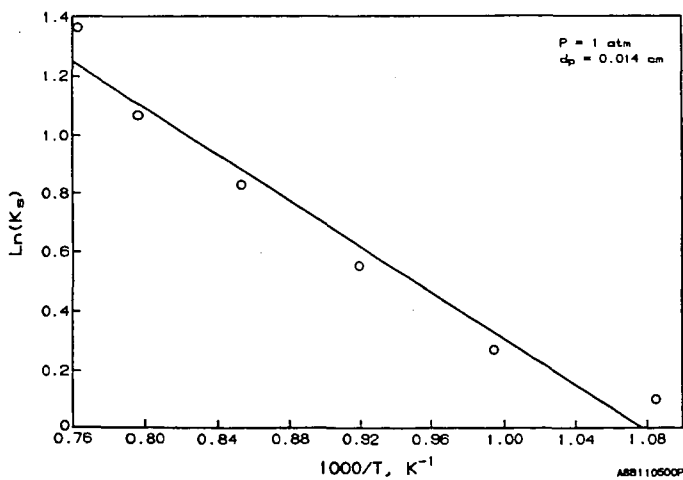


Figure 6. ARRHENIUS PLOT FOR THE SULFIDATION REACTION

DIRECT SULFUR RECOVERY PROCESS FOR ELEMENTAL SULFUR RECOVERY FROM GAS

Thomas P. Dorchak¹ and Santosh K. Gangwal²

¹Morgantown Energy Technology Center

Morgantown, West Virginia 26505

²Research Triangle Institute

Research Triangle Park, North Carolina 27709

ABSTRACT

Research Triangle Institute, under contract to the U.S. Department of Energy, has investigated several processes for recovering elemental sulfur from tail-gas that contains SO₂. The work focuses on a dilute tail-gas that is produced by the oxidative regeneration of mixed metal oxide sorbents. The sorbents have been proposed for hot gas cleanup of raw coal gas, upstream of a gas turbine in an integrated, gasification/combined-cycle system. Initially, SO₂ in the tail gas was absorbed on a specially prepared sodium alumina sorbent, followed by reductive regeneration, to produce a concentrated stream of hydrogen sulfide (H₂S), which is a suitable feed for a Claus plant to recover elemental sulfur. It was found that elemental sulfur could be continuously recovered from the tail-gas, thereby eliminating the Claus processing. In a single stage, over 90% of the SO₂ was converted to elemental sulfur using the new direct sulfur recovery process (DSRP). In a two-staged system, overall recoveries of over 99.5% are expected. The effectiveness of the new catalytic process on gases that contain H₂S has also been demonstrated. Tests were conducted to evaluate the effects of pressure, temperature, stoichiometry, space velocity, and steam content.

INTRODUCTION

In the U.S., elemental sulfur is recovered by steam injection from underground deposits using the thermally inefficient Frasch process. Concern is growing that this source may dwindle in capacity and productivity by the year 2000 (Joseph 1988). Natural gas and petroleum processing is another large source. Dwindling production of natural gas and petroleum in the U.S. will further limit the supply of sulfur. Sulfur is mostly used to produce sulfuric acid, the largest single chemical produced in the U.S. The U.S. consumed over 11 million long tons of sulfur in 1988 (U.S. Bureau of Mines 1988). Elemental sulfur production offers an alternative to flue gas and other gas treatment processes, which produce large volumes of throwaway waste that must be disposed of in an environmentally safe manner.

Increasingly stringent environmental emission standards here and in Europe are another driving force for the high efficiency 99%-recovery of sulfur. The U.S. Environmental Protection Agency standards of October 1, 1985 (40 CFR, Part 60, Subpart LLL), limit natural gas processing plants to sulfur emissions of less than 2 long tons per day. Petroleum refineries are limited to emissions of less than 90 ppm. These limitations require sulfur removal of 99% efficiency, above the conversions achieved in simple, multi-stage Claus plants of 95 to 97%. The European Economic Community will require a minimum of 98.5% recovery rates from Claus plants by 1992. Currently, Federal Republic of Germany regulations require up to 99.5% recovery. Environmental concerns and improved process economics have engendered the commercialization of a number of modified Claus processes enhanced with tail-gas treatment processes (Goar 1986).

The U.S. Department of Energy's (DOE's) Morgantown Energy Technology Center has developed and advanced a hot, coal-gas desulfurization concept that is based on a regenerable zinc ferrite sorbent (Grindley 1988). The potential benefit of hot gas cleanup is most significant when the clean coal gas is used to fuel a gas turbine in

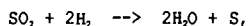
an integrated, gasification/combined-cycle system. In the zinc ferrite process, H₂S reacts with zinc ferrite, which is then regenerated by a dilute air stream. This produces a hot regeneration off-gas containing 1 to 3% SO₂, which must be disposed of in an environmentally acceptable manner. Other desulfurization sorbents can be used in a similar manner that produce an off-gas that contains SO₂. Alternative throwaway processes, such as the hot lime bed developed by the Esso Research Centre (Kowszun 1979), lead to the generation of a large amount of waste, which must be disposed of under an increasingly stringent regulatory burden.

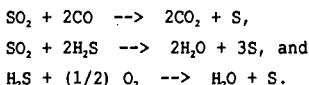
Among the options for the ultimate disposal of off-gas containing SO₂, production of elemental sulfur is attractive. The Ralph M. Parsons Company, under contract to DOE, has evaluated the technical and economic feasibility of candidate processes that can recover sulfur from hot coal gas desulfurization processes (O'Hara et al. 1987). Elemental sulfur, an essential commodity for industrial and military use, is easily stored and transported. Research Triangle Institute, under contract to DOE, has investigated several processes that can recover elemental sulfur from the off-gases that contain SO₂ (Harkins and Gangwal 1988). The initial work focused on absorption of SO₂ on a novel sorbent (Gangwal et al. 1988), followed by reductive regeneration, to produce a concentrated stream of H₂S that would be a suitable feed for recovery of elemental sulfur at a Claus plant. During these investigations, it was found that elemental sulfur could be continuously recovered from the off-gas, thereby eliminating the need for Claus processing. In a single stage, over 90% of the SO₂ was converted to elemental sulfur. In a two-staged system, overall recoveries of over 99.5% are expected. The effectiveness of the new catalytic process on gases containing H₂S has also been demonstrated.

PROCESS PRINCIPLES

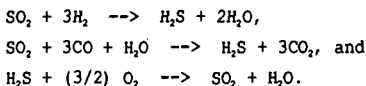
The new direct sulfur recovery process (DSRP) is capable of converting over 90% of the sulfur in gas streams that contain reduced or oxidized gaseous sulfur compounds to elemental sulfur in a direct continuous process. No preconcentrating, oxidation, or reduction is necessary. The residual sulfur in the effluent can be obtained either as essentially all H₂S or as all SO₂ by controlling the inlet gas composition. The DSRP can also reversibly convert oxidized gaseous sulfur compounds such as SO₂ to reduced sulfur compounds such as H₂S and vice versa. Conversion of H₂S and carbonyl sulfide to elemental sulfur has also been demonstrated, confirming the reversible nature of the DSRP. However, the work has focused largely on conversion of SO₂ to elemental sulfur.

The primary gas stream to be treated is mixed with a small flow of a secondary gas stream, and is contacted with a catalyst at temperatures from about 400 to 700 °C and at pressures up to 20 atmospheres. If the primary gas stream to be treated contains mainly oxidized sulfur gases, then the secondary gas stream should be reducing in nature. Near stoichiometric quantities are desirable to promote the conversion to elemental sulfur and to reduce reaction with other components in the gas stream. It is possible to have oxidizing gases such as steam and CO₂ in the secondary gas stream as long as the gas is overall reducing. If the primary gas stream already has close to the desired stoichiometry, then a secondary gas stream is not required. On the other hand, if the primary gas stream contains mainly reduced sulfur gases, then the secondary gas stream should be oxidizing in nature (e.g., containing oxygen or other oxidants). In all cases, if elemental sulfur is the desired product, the mixture of the primary and secondary gas streams should have close to such stoichiometry that the sulfur gases can be completely converted to elemental sulfur. Simple examples of these stoichiometries are



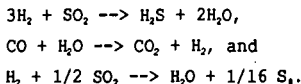


It is also possible to convert oxidized sulfur gases to reducing sulfur gases and vice versa by shifting the stoichiometry of the inlet mixture toward the desired gas and by choosing the proper temperature and pressure. Simple examples of the stoichiometries are



The chemistry of the process invariably involves multiple intermediary reactions at or near the surface of the catalyst. When SO_2 and reducing gases are simultaneously contacted with the catalyst, steady state is quickly reached, and SO_2 is continuously converted to elemental sulfur. When H_2S and oxidizing gases are simultaneously contacted with the catalyst, H_2S is continuously converted to elemental sulfur as steady state is reached. The yield of elemental sulfur increases with increasing temperature between 400 and 700 °C and with increasing pressures from above atmospheric to 20 atmospheres.

These observed results have been verified by thermodynamic equilibrium analysis of the seven compounds: H_2 , CO_2 , CO , H_2S , SO_2 , H_2O , and S_8 (or S_2). Since the number of compounds is seven and the number of atoms is four (H, C, O, S), only 7 - 4 or three reactions between these compounds were needed to completely describe the system from the standpoint of thermodynamic equilibrium. The following reactions were selected (others are possible) to completely define the system from a thermodynamic standpoint:



The state of the catalyst is constant and was not incorporated into the analysis.

Starting with a mixture containing about 2% SO_2 , 4% $\text{CO} + \text{H}_2$, 4% $\text{CO}_2 + \text{H}_2\text{O}$, and the balance N_2 , the predicted yield of elemental sulfur as S_8 is about 60% of the inlet sulfur at 20 atmospheres and 700 °C. Since more than 90% yield was observed experimentally, it is postulated that the elemental sulfur products obtained may be combinations of S_2 , S_8 , S_4 , and S_6 or higher polysulfides. It is known that S_2 , S_4 , and S_6 are not stable at 700 °C at 1 atmosphere. However, data are not available at 20 atmospheres. The thermodynamic analysis, in any event, lends credence to the results obtained in the laboratory.

EXPERIMENTAL APPARATUS

Tests were performed using the fixed-bed reactor system shown in Figure 1. The system consists of a 1-in. O.D., 0.87-in. I.D., Alon-processed 316 stainless steel reactor, a gas feed system, and a filter/condenser for the removal of elemental sulfur and water. Premixed gases flow from pressure regulated gas bottles, controlled by mass flow controllers. A high pressure, positive displacement pump injects water into the gases before an electric heater prior to entering the bottom of

the reactor. After exiting the reactor, the gas is cooled to 160 °C to condense sulfur on the filter. Water is removed in a condenser and then the dry gas flows through a back pressure regulator, which controls the bed pressure. A sample of gas is continuously withdrawn before the back pressure valve. The gas is analyzed for H₂S and SO₂ by gas chromatography and a continuous SO₂ analyzer. The outlet gas flow rate is measured periodically using a soap bubble meter.

EXPERIMENTAL RESULTS

Tests were conducted to evaluate the effects of pressure, temperature, space velocity, and steam content on sulfur recovery in the DSRP. These tests were conducted over a wide range of pressures up to 40 atmospheres and at temperatures from about 390 to 700 °C. Space velocities ranging up to 5500 standard cubic centimeters per cubic centimeter hour, scc/(cc).hr were evaluated. Steam content ranged up to 25% by volume. The work focused on the reduction of SO₂ to elemental sulfur with simulated coal gas; however, a number of runs demonstrated the oxidation of H₂S and the reversibility of the reactions. A large database was generated that deals with the conversion of SO₂ to elemental sulfur over the range of conditions and inlet gas compositions shown in Table 1.

All experimental runs were carried out in a single-stage fixed-bed reactor with either 25 or 50 cm of catalyst. The two sizes allowed investigation of a range of space velocities within the capacity of the gas delivery system. Blank runs without the catalyst showed the reactor walls to be essentially inactive. Experimental results are summarized in Figures 2 through 6.

The initial investigations focused on the effects of pressure, space velocity, and temperature on the conversion rate of SO₂ to elemental sulfur. By far the greatest effect was observed by varying the pressure at a near constant temperature of 650 °C. (See Figure 2.) Beginning slightly above atmospheric pressure, conversion to elemental sulfur was about 20%, which quickly rose to near 60% at 10 atmospheres and then to over 90% near 20 atmospheres. Doubling the pressure to 40 atmospheres increased the conversion to 95%. In comparison, one stage of a Claus reactor may result in a 60 to 70% conversion, resulting in the typical commercial practice of using three stages of Claus reactors with intercooling between each stage to obtain 90% conversion. In addition, the hourly gas space velocity in a Claus ranges near 1000 scc/(cc).hr, while the results shown in Figure 2 were obtained at a space velocity near 1800 scc/(cc).hr. The higher pressure of the DSRP permits higher space velocities and therefore smaller size reactors, or higher through-put with a fixed size of reactor. Even space velocities higher than 1800 scc/(cc).hr can be used in the DSRP as shown in Figure 3.

Data presented in the upper band of Figure 3 were obtained at a constant pressure of 20 atmospheres and at temperatures from 550 to 650 °C. Up to a maximum space velocity of 5500 scc/(cc).hr, conversion was impacted to a small degree, essentially remaining above 90% at the extreme flow rate. Space velocities ranging from 1800 to 5500 scc/(cc).hr resulted in conversion rates varying between 90 and 95% near 550 °C. The variation was less pronounced at temperatures near 650 °C, remaining closer to 95%. In contrast, the impact of space velocity at the lowest pressure of near 1.5 atmospheres was dramatic.

The lower line in Figure 3 illustrates the impact. A variation in space velocity from 400 to 1800 scc/(cc).hr cuts the conversion rate in half, i.e., from about 46% to near 20%. As a result, the slope of the lower line is much steeper than the upper band obtained at 20 atmospheres pressure. We can also compare the results at varying pressures but at a fixed space velocity of 1800 scc/(cc).hr and a temper-

ature of 650 °C (i.e., point A at 1.5 atmospheres to point B at 20 atmospheres). At the lower pressure, the conversion is near 20% while at the higher pressure, the conversion is well over 90%. This shows that pressure plays an important role in the DSRP.

The data in Figure 3 also confirm the much higher throughput possible at higher pressure. At the lowest space velocity while at the lower pressure, conversion does not even approach the 90% achieved at higher pressure, which prevents an exact comparison. At the higher pressure, the conversion is hardly affected at the highest space velocity, which was at the limits of the laboratory gas supply system. Therefore, high conversion rates can be achieved using the DSRP even at extreme flow rates, provided the pressure is sufficiently high.

Somewhat analogous to the effect of pressure is the effect of temperature, but to a much lesser degree as shown in Figure 4. At 440 °C and above, conversion to elemental sulfur remains well above 90% and is essentially unaffected by any increase in temperature. These results obtained at a constant pressure of 40 atmospheres are significant because the insensitivity of both conversion rate and catalyst to temperature rise and thermal degradation is demonstrated. The catalyst has yet to show any sign of deactivation over hundreds of hours of testing, including repetitive testing of a single catalyst material and even with an accidental excursion to 760 °C. The possible effects of thermal degradation may become more evident as the DSRP is scaled-up to pilot-scale and larger size.

The effect of the steam content of the gas on conversion of SO₂ to elemental sulfur was evaluated. The Claus equilibrium is limited by the water content of the gas, which must be removed in the intercooling step between stages. However, this disadvantage is not experienced with the DSRP at high temperature and pressure. Figure 5 shows results at 20 atmospheres of pressure and at temperatures varying from 600 and 700 °C. Steam content in the inlet gas ranged from about 1 to 25% and produced virtually no impact on the conversion rate above 5% steam. The effect below 5% may be questionable since data from some early runs are included that may not have been at optimal conditions. However, the insensitivity to steam indicates that the conversion is not limited by the Claus equilibrium, at least at first. As the overall sulfur content in the gas drops to the ppm level and as H₂S and SO₂ levels become comparable, an equilibrium may be established that is not affected by steam content at high temperature and pressure. In contrast, the equilibrium and conversion rate are definitely dependent on stoichiometry.

Figure 6 presents the concentration of SO₂ and the reduced sulfur compounds COS and H₂S that are found in the outlet as the molar ratio of reducing gases was varied. The molar ratio was varied closely, at about a stoichiometric ratio of two moles of reducing gas, either as H₂ or CO, to one mole of SO₂ in the inlet. As the reducing content in the gas increased, the residual content of SO₂ in the gas decreased and the reduced compounds of sulfur increased. This confirms the equilibrium nature of the DSRP and demonstrates that the components in the outlet can be controlled. Figure 6 also shows that sulfur conversion is optimized as the stoichiometric ratio of 2.0 is approached, demonstrating the importance of controlling molar ratios. The data also suggest that H₂S in a gas stream could be efficiently converted to elemental sulfur.

The direct conversion of hydrogen sulfide to elemental sulfur was confirmed in a short series of experiments. In one preliminary experiment, an 88.2% conversion rate was observed when 2.5% H₂S and 0.6% COS in nitrogen were reacted over a catalyst with a stoichiometric amount of oxygen at a one-to-one molar ratio. In a more carefully controlled experiment, over 95% conversion to elemental sulfur was ob-

tained. These initial experimental results require further confirmation. It can be significant that the DSRP removes reduced sulfur species either as H_2S or COS from a gas stream. This introduces the possibility of treating a variety of industrial gas streams.

CONCLUSIONS

Experimental results indicate that the Direct Sulfur Recovery Process, DSRP, can convert SO_2 , COS and H_2S directly to elemental sulfur at conversion rates near 95% in a single stage, and above 99.5% after two stages.

Pressure has the most significant effects in terms of increased conversion to elemental sulfur and increased throughput with the DSRP. Gas hourly space velocities over 5500 scc/(cc).hr and above can increase the throughput.

Above a threshold temperature and depending on pressure, conversion rates remain above 90% with little impact caused by further increases in temperature.

The DSRP is insensitive to the steam content of the gas, which distinguishes it from other processes that rely on Claus equilibrium reactions.

Gas streams containing concentrations of sulfur compounds as low as 0.85%, possibly even lower, can be treated using the DSRP to efficiently recover elemental sulfur.

Gas phase equilibria are established in the DSRP (space velocity over a wide range has little impact on the products of reaction) that can control the composition of the outlet gas for SO_2 content or reduced sulfur compounds by controlling the stoichiometric ratio at the inlet of the reactor.

The conversion to elemental sulfur can be optimized by controlling the stoichiometric balance of gaseous components at the inlet of the reactor.

REFERENCES

Gangwal, S.K., Harkins, S.M., and Dorchak, T.P., June 1988, "Sorbent Based Recovery of Sulfur From Regeneration Tail Gases" Proceedings of the 195th ACS National Meeting, Division of Fuel Chemistry, American Chemical Society, pp. 306-309.

Goar, B.G., June 1986, "Sulfur Recovery Technology," Energy Progress, Vol. 6, No. 2, pp. 71-75.

Grindley, T., May 1988, "Sidestream Zinc Ferrite Regeneration Tests," Proceedings of the Eight Annual Gasification and Gas Stream Cleanup Systems Contractors Review Meeting, Vol. 1, National Technical Information Service, Springfield, Virginia, DOE/METC-88/6092, NTIS/DE88010253, pp. 58-82.

Grindley, T., and Goldsmith, H., November 1987, "Development of Zinc Ferrite Desulfurization Sorbents for Large Scale Testing," Presented at the AIChE Annual Meeting, New York, New York.

Harkins, S.M., and Gangwal, S.K., September 1988, "A Novel Concept for the Ultimate Disposal of Off-Gases From Hot Gas Desulfurization Processes," Proceedings of the AR&TD Direct Utilization, Instrumentation and Diagnostics Contractors Review Meeting, National Technical Information Service, Springfield, Virginia, NTIS/DE89007029, pp. 139-145.

Joseph, T.W., April 1988, Sulfur Emissions Reduction at the Great Plains Coal Gasification Facility: Technical and Economic Evaluations, Chairman, Sulfur Reduction Technical Committee, Report to the U.S. Department of Energy, Office of Fossil Energy, Washington, D.C., National Technical Information Service, Springfield, Virginia, NTIS/DE89000582.

Kowszun, Z., May 1979, Chemically Active Fluid-Bed Process for Sulfur Removal During Gasification of Carbonaceous Fuels, Final Report, Esso Research Centre, Abington, England, U.S. Environmental Protection Agency, Research Triangle Park, North Carolina, EPA/600/7-87/022.

O'Hara, J.B., Chow, J.E., and Findley, J.E., 1987, Sulfur Recovery From Hot Coal Gas Desulfurization Processes, Final Report, National Technical Information Service, Springfield, Virginia, DOE/MC/21097-2338, NTIS/DE87006477.

U.S. Bureau of Mines, November 1988, "Mineral Industry Surveys, Sulfur Monthly."

Table 1. Inlet Gas Composition

COMPONENT	% by Volume
SO ₂	0.85 - 1.9
H ₂ O	1.0 - 25.0
H ₂	0.65 - 1.6
CO	0.85 - 2.1
CO ₂	0.25 - 0.6
N ₂	Balance

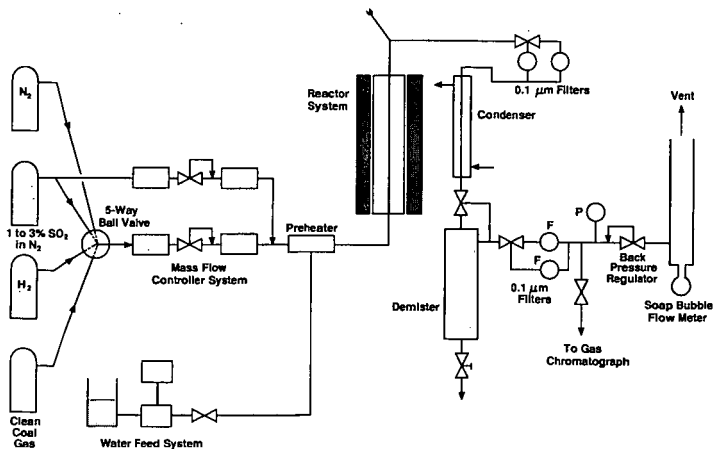


Figure 1. High-Pressure Fixed-Bed Test Apparatus

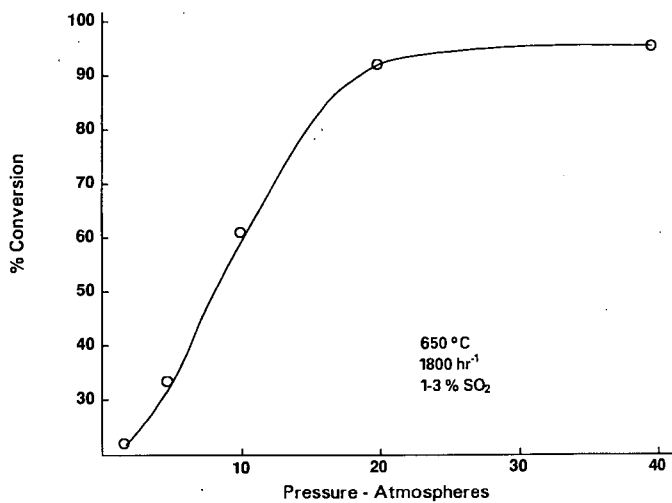


Figure 2. Effect of Pressure on the DSRP

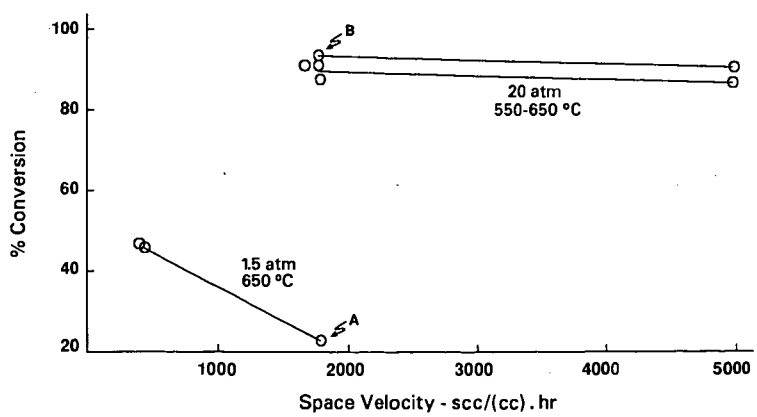


Figure 3. Effect of Space Velocity and Pressure on the DSRP

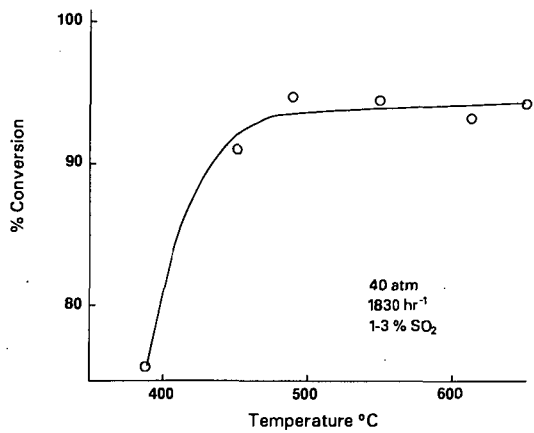


Figure 4. Effect of Temperature on the DSRP

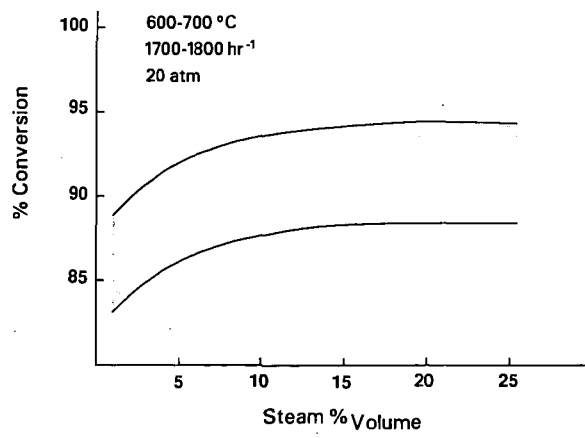


Figure 5. Effect of Steam Content on the DSRP

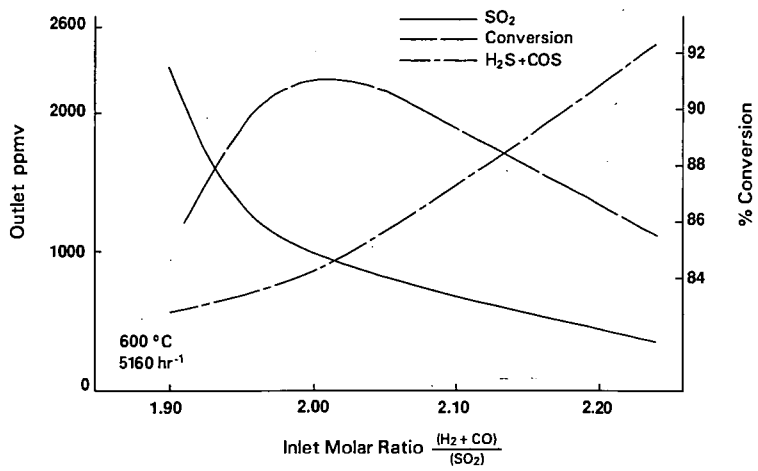


Figure 6. Effect of Stoichiometry on the DSRP